12-11-2009

Analysis and Design of Wood Construction Platforms Using Instrumentation

Martin Feeney Stroble

ANALYSIS AND DESIGN OF WOOD CONSTRUCTION

PLATFORMS USING INSTRUMENTATION

By

Martin Feeney Stroble III

A Thesis
Submitted to the Faculty of
Mississippi State University
in Partial Fulfillment of the Requirements
for the Degree of Master of Science
in Civil Engineering
in the Department of Civil and Environmental Engineering

Mississippi State University

December 2009

ANALYSIS AND DESIGN OF WOOD CONSTRUCTION

PLATFORMS USING INSTRUMENTATION

By

Martin Feeney Stroble III

Approved:

Isaac L. Howard
Assistant Professor of Civil and Environmental Engineering
(Major Professor)

Rubin Shmulsky
Head of Department of Forest Products
(Committee Member)

Philip M. Gullett
Assistant Professor of Civil and Environmental Engineering
(Committee Member)

James L. Martin
Professor and Kelly Gene Cook, Sr. Chair in Civil and Environmental Engineering
Director of Graduate Studies in the Department of Civil and Environmental Engineering

Sarah A. Rajala
Dean of The Bagley College of Engineering

Name: Martin Feeney Stroble III

Date of Degree: December 11, 2009

Institution: Mississippi State University

Major Field: Civil and Environmental Engineering

Major Professor: Isaac L. Howard

Title of Study: ANALYSIS AND DESIGN OF WOOD CONSTRUCTION PLATFORMS USING INSTRUMENTATION

Pages in Study: 178

Candidate for Degree of Master of Science

Wood construction platforms are a common method for inexpensive, temporary soil stabilization under heavy machinery; however, engineering-based platform design is uncommon. Review of literature has shown that only one design method is currently available and is specific to one type of platform configuration. The purpose of this thesis is to develop a design method that is simple, versatile and accurate. The proposed design method allows for designer input in multiple areas of the design. Instrumentation allowed for increased insight into the mechanical behavior of the platforms.

The objective of this research is to use measured strain, load, and deflection in conjunction with fundamental engineering mechanics principles to predict a single platform's mechanical behavior on the ground. Results from this method compare favorably with the only other design guide available and improves the knowledge base by developing design guidance for any type of wood construction platform.

DEDICATION

I would like to dedicate this thesis to my parents, Marty and Madeline Stroble, for their continual love and support.

ACKNOWLEDGMENTS

The author would like to thank the many people without whose help this thesis could not be completed. First of all, sincere thanks are due to Dr. Isaac L. Howard, my graduate advisor, for his leadership, guidance, honesty, and insight in all aspects of my graduate studies. Expressed appreciation is also due to the other members of my graduate committee, namely, Dr. Rubin Shmulsky and Dr. Philip M. Gullett, for their invaluable aid and direction. The author would also like to thank Jon Fiutak of Anthony Hardwood Composites, Inc. for his experience. Finally, the author would like to thank Emily Taylor for her editorial assistance.

TABLE OF CONTENTS

LIST OF TABLES

LIST OF FIGURES

LIST OF SYMBOLS

$A_{\beta z}$	Deflection Periodical Relationship Function
C	Geometric Constant
$C_{\beta z}$	Moment Periodical Relationship Function
CBR	California Bearing Ratio
DAF	Dynamic Amplification Factor
DCDT	Direct Current Displacement Transducers
DCPT	Direct Current Potentiometer Transducers
E, MOE	Modulus of Elasticity
E_C	Composite MOE
E_{CP}	Composite MOE Prediction Value
ERDC	Engineering Research and Development Center
Glulam	Glue-laminated Timber
I	Moment of Inertia
I'	Full-Scale Moment of Inertia
L	Clear Span Length
L'	Scaled Clear Span Length
LSL	Laminated Strand Lumber
LVL	Laminated Veneer Lumber
M	Bending Moment

MOR	Modulus of Rupture
NLSC	Normalized Load-Strain Curve
OSB	Oriented Strand Board
P	Prototype Scale Load
P'	Full-Scale Load
P_{ult}	Prototype Scale Ultimate Load Corresponding to $\varepsilon_{\mathrm{ult\text{-}max}}$
P'_{ult}	Full-Scale Ultimate Load Corresponding to $\varepsilon_{\mathrm{ult\text{-}max}}$
P'_{ED}	Full-Scale Elevated Design Load
P'_{GD}	Full-Scale Ground Design Load
$P_{ult\text{-}min}$	Prototype Scale Minimum Ultimate Load for a Platform Category
$P'_{ult\text{-}min}$	Full-Scale Minimum Ultimate Load for a Platform Category
$\frac{P}{\Delta}$	Slope of Measured Load-Deflection Data
PSL	Parallel Strand Lumber
SCL	Structural Composite Lumber
SF	Safety Factor
USACE	United States Army Corps of Engineers
USDA	United States Department of Agriculture
a_0	First Quadratic Coefficient
a_1	First Quadratic Coefficient for NLSC
b	Base Width, Beam Width
b'	Scaled Base Width
b_0	Second Quadratic Coefficient

b_1	Second Quadratic Coefficient for NLSC
c	Distance from Extreme Fiber to Centroid
c_1	Length Scale Factor
c_2	Base Width Scale Factor
c_3	Height Scale Factor
c_4	Space Scale Factor
h	Height
h'	Scaled Height
k_0	Modulus of Subgrade Reaction
r^2	Correlation Coefficient
s'	Space between Load Heads
z	Distance Along the z-axis
β	Beam-on-Elastic-Foundation Constant
Δ	Deflection
Δ'	Full-Scale Calculated Theoretical Deflection
Δ'_{ED}	Theoretical Full-Scale Elevated Design Deflection
Δ'_{GD}	Full-Scale Ground Design Deflection
ε	Strain
ε_{max}	Allowable Maximum Strain
$\varepsilon_{ult\text{-}max}$	Maximum Ultimate Strain for a Platform Category
σ	Stress
σ_b	Bending Stress

σ_b' Scaled Bending Stress

CHAPTER 1

INTRODUCTION

This thesis discusses the development of design guidance for wood construction platforms as a viable method for soil stabilization. Wood construction platforms can be found on many construction sites, yet they are not typically thought of as an engineered product. Construction platforms can be used for a variety of applications but are most typically used to support heavy machinery (i.e. excavators, pipe layers, oil rigs, loaders, etc.). Figure 1.1 shows wood construction platforms in use. Construction platforms are also necessary on projects in which environmental impact is to be minimized. A prime example of this is installing gas and oil pipelines through environmentally sensitive areas, such as wetlands (Schweitzer and Marinello 1996).

Figure 1.1 Wood Construction Platforms in Use

Platforms can be made of a variety of other materials; however, platforms made of wood are common due to their relatively low cost and efficient strength-density ratio. Another benefit is that wood is a renewable resource. Platforms can also have a variety of geometric configurations, varying by lamination methods, wood orientations, etc.

The purpose of this thesis is to develop a simple design method for a single wood construction platform as it sits on the ground. Using fundamental engineering principles to design platforms can save materials, time, and ultimately money. Consequences of under-designed wood platforms could lead to broken or damaged platforms, as seen in Figure 1.2; while consequences of over-designed platforms could lead to unnecessarily thick platforms supporting small loads. In reality, the goal of this thesis is to develop a method that is somewhere between these two situations.

Figure 1.2 Damaged Wood Construction Platforms

In the overall scheme of large construction projects, the design of construction platforms may not be of significant consequence to the construction industry, or even the timber industry for that matter, as construction platforms account for a relatively small portion of these industries' costs/revenues. However, their design can potentially have a great effect on smaller, related industries such as the composite timber industry or matting systems industry. The design method is not revolutionary, but is a significant and needed advancement. Review of literature has shown wood construction platform design to be scarce. A possible cause is the larger industries of construction and forestry overlooking platform design as advantageous.

This thesis first presents a literature review of wood construction platforms. The literature review begins with broad subjects, such as the timber industry's economic impact, and then switches focus to more specific subjects, such as research on composite wood products. The literature review concludes with a discussion of wood construction platforms. Next, this thesis outlines an experimental program. This differs from most experimental programs because the original data, which was taken for reasons different from this research, had to be reduced and translated into a usable format. After that, the proposed design method is presented, citing all theories, assumptions, and engineering judgment incorporated. This is followed by a discussion of the design method and its implications, as well as a comparison to the only other design method found (***emtek*** 2009). This thesis concludes with a summary and future recommendations.

CHAPTER 2

LITERATURE REVIEW

2.1 Introduction

According to Fridley (2002), wood and wood-based materials are often misconceived as low-tech or second-tier construction materials. In reality, engineered wood products are vastly different from this perception. Wood is a natural and renewable resource that can be used for many construction applications. Of these applications, wood construction platforms are the focus of this research. Wood construction platforms (also known as wood mats or wood matting systems) boast numerous uses, including supporting heavy machinery, such as cranes, over soft soils. They have also been used to construct low-volume, temporary roads in which there is no need or desire for permanent access.

A literature review was conducted that shows the re-emergence of wood, specifically composite wood products, as a competitive construction material. The primary goals of this literature review were to: 1) investigate past research methods and examine the test results for composite wood materials; 2) inspect different methods for modeling composite wood materials, especially pertaining to wood construction platforms; 3) evaluate state-of-the-art wood construction platform analysis, design, and construction; and 4) investigate the use of instrumentation on wood products and, more specifically, wood construction platforms. Secondary goals of this literature review were to assess the importance of composite wood materials from a timber industry standpoint and evaluate the perception of wood as a construction material in relation to competing materials.

The following sections present relevant information obtained during review of literature. First, the potential impact on the timber industry is discussed. Next, current research being performed on composite wood materials is presented and discussed. Finally, the current status of wood construction platforms and the use of instrumented test data in this research are presented.

The review of literature was a major portion of the effort for this thesis. The review extended beyond research literature to include documents and experience from persons currently working in the industry. Additional effort was put into researching design methods for timber construction platforms. This search uncovered little relevant information, illustrating the need for the research conducted.

2.2 Overview of Timber Industry

This section looks at the United States' timber industry and its economic impact, while impacts outside the United States are given secondary consideration. A history of the timber industry is presented to show the development of wood as a construction material. This section ends with a discussion of the perception of wood as a construction material among working professionals.

2.2.1 Timber Industry's Economic Impact

From a global point of view, wood is a vital material. According to Bowyer et al. (2007), 3.5 billion cubic meters of wood were harvested globally in 2005. A little over half was used as fuelwood, with the remainder used for roundwood and industrial roundwood. Fuelwood is used to create energy, while roundwood and industrial roundwood are used in manufacturing an array of wood products. Wood is a popular material because it is a common and renewable resource worldwide. In fact, less energy is required to produce wood materials than all other construction materials. As a result, wood materials are not only readily available, but also relatively inexpensive.

Wood products are most commonly associated with a narrow grouping of conventional products, such as plywood and sawn lumber, while, in reality, they have a variety of other uses. According to Bowyer et al. (2007), "…the weight of wood used every year in the United States exceeds the weight of all metals and all plastics *combined*!" Bowyer et al. (2007) states that this increase is due to the sophistication of wood products.

The timber industry is prevalent in the southern United States. According to Howard (2001) of the United States Department of Agriculture (USDA), in 1999 the South had the largest amount of overall lumber production in the U.S. with 22.1 billion board feet. This suggests that the southern region of the country could benefit from further research into and development of wood products.

2.2.2 Development of Wood as a Construction Material

Wood materials are more common in everyday life than is often perceived. Wood has been used as a construction material for hundreds of years and is still common to most construction sites, whether it is used directly as a structural component or indirectly as a means of soil improvement. Fridley (2002) provides a history of wood as a construction material as well as a discussion of the development and research that is enabling wood to compete with other building materials.

Fridley (2002) discusses the increased use of wood and wood-based products in civil engineering applications. Solid wood, wood-based composites, and hybrid wood composites are all discussed. Wood-based composites, such as timber construction platforms, are the category under investigation in this research. Fridley (2002) attributes increased building efficiency to the introduction of wood-based composites because of their ability to eliminate natural defects and increase the reliability of the structural element. Regarding the future of wood-based materials, Fridley (2002) explains that they must overcome performance issues such as creep, dimensional stability, moisture resistance, fatigue, and biodegradation.

Modern wood-based materials can be broken down into the following categories: glued-laminated (*glulam*) timber, parallel strand lumber (*PSL*), laminated strand lumber (*LSL*), laminated veneer lumber (*LVL*), wood I-joists, and thick oriented strand lumber (*OSL*). Wood-based materials such as plywood, particleboard, and solid-sawn lumber would be considered non-modern wood-based materials. Figure 2.1 shows examples of modern wood-based materials. Each wood-based material was developed to achieve a desired characteristic or to use parts of the tree that were not conventionally used for structural members (Lam 2000). *Glulam* and *LVL* are of specific interest to this paper. *LVL* is similar to *glulam*, except that *LVL*'s intact wood materials are thinner than those used for *glulam*. Typically, *glulam* is made of solid-sawn wood elements glued together, while *LVL* is made of sheathed wood veneer. *Glulam* and *LVL* both have many advantages. They allow for the efficient use of lumber, architectural freedom, and variation of cross-section. They are also considered to be environmentally friendly according to Smulski (1997). Because of their benefits, both products are commonly used. *Glulam* production alone increased 9.1% between 1998 and 1999 (Howard 2001).

Figure 2.1 Examples of Structural Composite Lumber - LVL, OSL, Glulam

2.2.3 Perception of Wood Materials

Because of wood's variability, potential to biodegrade, lack of dimensional stability, and other performance issues, many professionals consider it an inferior construction material. Smith and Stanfill-McMillan (1998) compared the perception of timber bridge performance to the actual present condition of timber bridges in four different states, one of which was Mississippi. Included in this research was a comparison of timber bridges to bridges made of other materials (pre-stressed concrete, reinforced concrete, and steel). Smith and Stanfill-McMillan (1998) found that the bridges in states that had adopted timber design codes were performing better than bridges in states that had no timber design codes. At the time that this research was conducted, Mississippi had not accepted a state-wide timber bridge design philosophy; not coincidentally, Mississippi's timber bridges were rated among the worst in the country. Perceptions of timber bridge performance were also correlated to industry professionals' perceptions of timber as a construction material.

2.3 Composite Wood Product Research

In this section the current status of composite wood materials, specifically *glulam* and *LVL*, is investigated. The aim of this section is to show the obstacles that arise during the development and research of these products. First, a brief overview of the mechanical properties of timber is presented. Next, a review of recent research on these mechanical properties is discussed and the expected research obstacles for this project are presented. The section concludes with a short discussion of instrumentation in the research of timber.

2.3.1 Overview of Mechanical Properties of Timber

Basic mechanical properties of timber are well documented. Chapter 4 of the *Wood Handbook* (1999) discusses these properties extensively for various common wood species. The properties of each wood type are based on “clear” pieces of wood, meaning that no natural defects, such as knots, are present. Wood is a naturally occurring, highly variable material that is orthotropic in nature. Wood has three principal axes: Longitudinal, Radial, and Tangential. Figure 2.2 shows these axes’ orientations with respect to the fiber direction for sawn lumber.

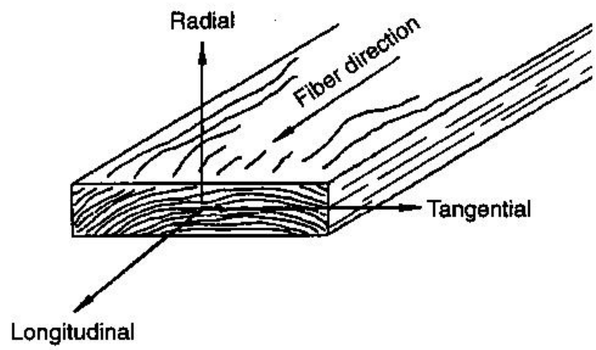

Figure 2.2 Principle Axes of Wood in Respect to Fiber Direction (*Wood Handbook* 1999)

Wood’s mechanical properties depend on the moisture content of the wood. The *Wood Handbook* (1999) reports the strength of wood for two separate moisture conditions: green and 12%. Green wood’s moisture content depends on the wood type. Green wood is weaker, yet more ductile, than air-dried wood.

Wood’s variability presents a problem when designing a structure using the material. Depending on the specific mechanical property, the coefficient of variation for each mechanical property can range from 10-35% for clear wood specimens. Engineered wood products were developed to limit this variation (*Wood Handbook* 1999).

The *Wood Handbook* (1999) explains that engineered wood products, such as *glulam* and *LVL*, use adhesives to overcome wood's variability. The type of adhesive to be used depends on wood type, environment, expected load configurations, and expected jointing configurations. Once the adhesive is chosen, the specimen is prepared, the adhesive is administered, and the member is assembled with the use of pressure. The applied pressure and the adhesive consistency affect the quality of the bonding.

Glulam and *LVL* are discussed extensively in the *Wood Handbook* (1999). However, in order to determine design values of these composite wood products, members must be tested using various ASTM specifications.

2.3.2 Current Status of Wood-Based Composites

Structural composite lumber (*SCL*), such as *glulam* and *LVL*, has been researched extensively in the past decade. *SCL* is any wood-based composite material used for structural components. Because wood is a renewable and abundant material, engineers have endeavored to find multiple applications for every type of wood material. However, before wood can be used for many of these applications some mechanical barriers, mainly bending and shear failure, must be overcome.

Shmulsky and Shi (2008) tested *glulam* beams made of sweet gum lumber, although sweet gum is not typically thought of as a structural grade lumber. Beams were manufactured by gluing together fourteen layers of sweet gum lumber. Great care was taken to eliminate failure due to the manufacturing process (i.e. joint placement). Beams were then tested in three-point bending. Average values of Modulus of Rupture (MOR) and Modulus of Elasticity (MOE) were found to be 49.7 MPa and 10,687 MPa, respectively. The standard deviation of these beams was relatively small. These values were found to be equivalent to a section of solid-sawn red oak lumber twice as deep.

Lam and Craig (2000) tested shear strength in three types of *SCL*: joist-oriented *LVL*, joist-oriented *PSL*, and plank-oriented *PSL*. The *LVL* was made from Douglas fir. Douglas fir and Southern pine were used in both the *PSL* orientations. The joist-oriented specimens were remanufactured into "I" cross-sections to promote longitudinal shear failure. The plank-oriented specimens were kept intact. Both specimen geometries were subjected to center-point bending, five-point bending, and shear block tests. In both cases, lateral support was provided to prevent lateral buckling failures. When tested, most of the specimens failed in shear. Apparent shear strength of the two bending tests and the shear block tests were compared. Specimens tested in five-point bending performed better than shear block tests by factors between 1.03 and 1.39 and better than center-point bending tests by factors of 1.34 and 1.53. This demonstrates the complications with determining shear strengths of *SCL*.

Yoshihara and Kawasaki (2006) observed the failure behavior of spruce wood under combined bending-shear stress fields. To achieve various combined stress fields, grooves were cut at various locations on the wood beams. Beams were tested in three-point bending and asymmetric four-point bending. Bending and shear stresses were calculated using beam theory. Results were then compared to three failure conditions: maximum stress, Hill-type, and Goldenblat-Kopnovs. Goldenblat-Kopnovs captured this behavior most precisely, followed by Hill-type and maximum stress failure conditions.

Joints of *SCL* have also been researched extensively. Jensen and Gustafsson (2004) used glued-in rods to enhance the strength of timber joints. The glued-in rods were meant to transfer load across joints and to increase the shear capacity of the beams. *Glulam* beams were fitted with glued-in rods under various geometric configurations at the center of the beams. Pure shear tests and tensile tests were administered to the beams. These results were then compared to a theoretical model based on beam-on-elastic-foundation theory and quasi-non-linear fracture mechanics. It was found that the theoretical failure shear loads agreed with the test results.

2.3.3 Instrumentation of Timber

Instrumentation does not seem to be commonplace in the research of *SCL*. Most research uses load-deflection data and simple beam theory to estimate failure strains or stresses. Strain gages have been used on small, clear specimens dating back to the mid-1950's. Radcliffe (1955) used bonded wire electric resistance strain gages to determine elastic properties (i.e. Modulus of Elasticity, Modulus of Rigidity, and Poisson's Ratio) of wood specimens at various orientations relative to grain direction.

Loferski et al. (1989) developed a clip-on strain gage transducer for wood. This technology was needed because typical bonded electrical resistance strain gages have problems measuring localized strain due to wood's variability and lack of homogeneity. In addition, transducers are reusable, accurate, lightweight, and relatively cheap to manufacture. The transducer developed as part of the research by Loferski et al. (1989) consists of a thin, flexible spring-steel arch "clipped" onto the surface of the specimen. Four resistance strain gages are bonded to the arch and arranged in a full Wheatstone bridge circuit. The transducer gave accurate results compared to bonded gages and theoretical calculations for various metals and woods under both compression and tension tests.

Fiorelli and Dias (2003) used extensometers to analyze the strength and stiffness of relatively small timber beams reinforced with carbon fiber and glass fiber. These results were then compared to a theoretical model. The carbon fiber and glass fiber could potentially be used in applications where beams have failed due to overload and/or degradation. The carbon fiber and glass fiber were applied to the tension face of the beam. Different thicknesses of glass fibers were tested. Extensometers were placed in the center of the beam between the wood-fiber interface, on the outside of the fiber, on the sides of the beam closest to the tension face, and on the compression face. The results from the bending analysis compared satisfactorily to the theoretical model. The fibers, depending on type and thickness, increased the stiffness of the beam by 15-30%.

Wipf et al. (1996) evaluated the dynamic response of timber bridges. Typically, timber bridges were designed using static loads based on axle and wheel loads. However, timber bridges are commonly used in low-volume forest roads in which a variety of design vehicles may be present. Wipf et al. (1996) dynamically evaluated two types of timber bridge systems: glulam timber girder bridges and stress-laminated (*stress-lam*) deck bridges. *Stress-lam* is the lamination of wood members using a high-strength steel bar and is essentially the same as the bolt-laminated mats to be discussed in the next section. Bridges were instrumented with potentiometer transducers (DCPT) and accelerometers. Bridges were trafficked both at crawl speeds (8 km/hr) and at speeds ranging from 16 km/hr to safe upper limit speeds using a tandem axle dump truck with two vehicle positions: eccentric and concentric. The dynamic amplification factor (DAF) was then calculated. Wipf et al. (1996) were not able to make conclusions about the DAF at the time.

Franklin et al. (1999) set out to compare static vs. dynamic design criteria for portable timber bridge systems. Two bridge types were under investigation: *glulam* bridges for forestry skidder traffic and T-section *glulam* bridges for truck traffic. Bridges were instrumented with displacement transducers (DCDT), and DAFs were calculated for each bridge. The research team found that expected dynamic load could be greater than the static loads, indicating a need to refine design criteria.

2.4 Wood Construction Platforms

This paper has presented a broad overview of ideas related to the timber industry and engineered wood-based products. Thus far, the timber industry, the research of composite wood products, the testing and analysis of timber structural systems, and the modeling of timber structural systems have been discussed. This section attempts to correlate this information with the current status of wood construction platforms. The section begins with a discussion of the history of wood construction mats followed by a review of their development in recent years. Next, an overview of outside research is presented. Finally, a typical construction platform design guide is briefly examined.

2.4.1 History of Wood Construction Platforms

Wood construction platforms have long been used by various construction industries to support large objects, such as cranes, over soft soils. Pipeline construction has utilized wood platforms since the early 1960's. Wood construction platforms are a composite wood product used to improve a soil's strength and stability without having a permanent effect on the environment in which they are used. Wood construction platforms allow for cheap, quick construction and low environmental impact due to pollution or erosion (Mason and Greenfield 1995). They can be made from a variety of wood types with various configurations and methods of lamination.

2.4.2 Research and Development of Wood Construction Platforms

Prior to the past decade or so, research on wood construction platforms has been limited. Most of the research has been conducted by government-affiliated entities, such as the U.S. Army Corps of Engineers (USACE) or the USDA. Industry and practice have had little involvement in this research until recently. In addition, most of this research has been qualitative. Testing platforms to failure and observing the results seems to be a commonplace technique. The rest of this section will examine the different testing configurations and results from current research on wood construction platforms.

Mason and Greenfield (1995) experimentally evaluated five different portable crossing products in Florida (two of which were wood products) based on cost of configuration, ease of placement, weight, and strength. Of the two wood products, the timber mats (i.e. wood construction platforms) are of interest. The platforms were constructed of 10.16 cm by 10.16 cm or 15.24 cm by 15.24 cm posts approximately 1.05 m to 1.83 m long. The posts were then loosely connected to each other by steel cables, which were threaded through the wood at approximately 0.305 m and 1.52 m from each end. The platforms were placed on a geotextile fabric over soft soil, over which a loaded log truck then made 300 passes. Moisture content, cone penetrometer, shear vane, and surface deformation data was collected and compared to a control section. Other portable crossing systems were not as intensely analyzed as the wood platform systems. The control section typically has moisture contents of 5-10% less than that of the test section. The wood construction platforms resulted in minimal environmental impact and a smooth road surface. The control section had deformations ranging from 15.24 cm to 25.40 cm, while the test section had essentially no rutting and a settlement of 12 mm. Also, the 10.16 cm mats were perceived as superior to the 15.24 cm mats. The report concludes by recommending further investigation of all portable crossing configurations, citing no configuration superior to the other.

Schweitzer and Marinello (1996) used wood platforms for utility construction through environmentally sensitive marsh and wetlands in Texas and Louisiana. The platforms used were very similar to those used by Mason and Greenfield (1995). These platforms were also placed upon geotextile fabric to help prevent environmental damage. The cost of the access roads built using the wood construction platforms was 10-15% of the total cost of conventional temporary roads when mitigation is considered.

Hislop (1996) tested and compared rut depth of three different portable crossing surfaces for low-volume roads on two different sites in north central Florida. Wood construction platforms were one of these surfaces. These platforms were similar to those previously discussed in this section. For this research, a control section was compared to a section using the portable crossing surfaces. Before tests were administered, the strength of the soil for each site was evaluated by determining the California Bearing Ratio (CBR) at varying depths. Figure 2.3 shows the CBR values at varying depths for both test sites. From Figure 2.3, one can see that the CBR values were similar for both the control section and the portable crossing section for the two sites. It was found that all three reduced rut depth; however, the most effective portable crossing configuration depends on the project, equipment, funding, and environmental constraints. Hislop (1996) recommends the wood construction platforms as the best overall portable crossing surface for the tests performed.

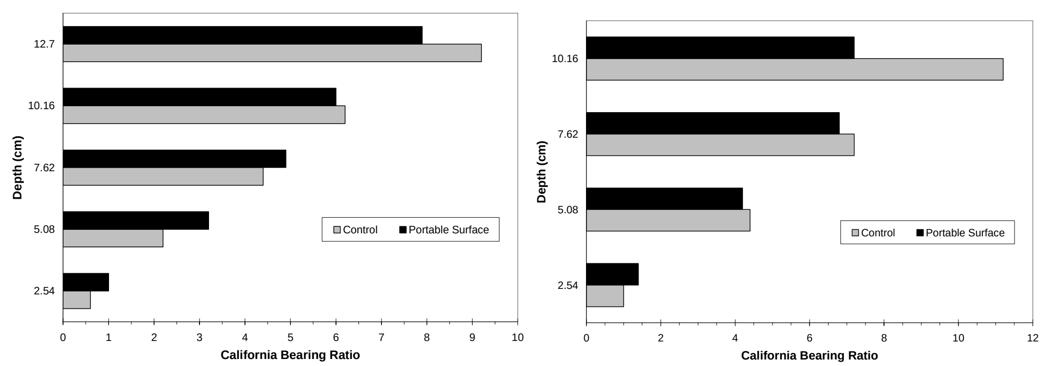

(a) Site 1 *(b) Site 2*

Figure 2.3 Pre-evaluation California Bearing Ratio (Hislop 1996)

Kestler et al. (1999) tested multiple stabilization techniques for vehicle mobility over thawing soils in Wisconsin for the armed forces. Of these stabilization techniques, two were engineered timber products: manufactured oak Unimats (brand-name construction platform) and hand-assembled shipping pallets. The Unimats were 2.44 m by 4.27 m and designed to interlock. Both of these products were tested in the "wooded trail" and "slopes" test sites. Before testing, sites were described based on multiple material characteristics. These characteristics included CBR, moisture content, density, gradation, and general site evaluation. Once the Unimats were put in place, they were trafficked with fifty passes by two different off-road military vehicles. Evaluation of the stabilization techniques was either subjective or empirical. The Unimats were shown to be effective, durable, and able to withstand tank motions. A decision aid was developed for the products and conditions. The decision aid shows all stabilization techniques and their performance on different design criteria, such as overall trafficability, traction, material life expectancy, material availability, material placement, material cost, equipment required for placement, etc. This decision aid is designed to help one choose the best stabilization technique based on which parameters are most important to a particular project.

Santoni et al. (2001) performed research similar to that of Kestler et al. (1999). Like Kestler et al (1999), mobilization of the armed forces was the motivation behind this study. However, the focus of this research was on stabilization techniques over soft soils rather than over thawing soils. SOLOCO (similar to Unimats) manufactured wood construction platforms were tested along with various other stabilization techniques. The platforms were trafficked with 2,000 passes by an off-road military vehicle. Evaluation of the stabilization techniques was subjective. It was found that two layers of SOLOCO wood platforms were capable of sustaining 2,000 passes of military trucks.

<u>2.4.3 Previous Research by Research Team</u>

The previously cited literature on wood construction platforms has not provided evidence that instrumented testing is frequently used for research on timber construction platforms. On the other hand, this paper is the continuation of research on wood construction platforms in which instrumentation is/was extensively used.

Shmulsky et al. (2008) tested twenty-eight mats (i.e. wood construction platforms) and 167 billets in three-point bending. This was a continuation of the work of Shmulsky and Shi (2008). The construction platforms were made of three single billets bolt-laminated together. Each single billet consisted of fourteen planks of sweet gum lumber (≈90%) laminated together using glue, as well as a small amount of mixed hardwoods (≈10%). The primary objective of this research was to compare mechanical properties of the single billets to the composite mechanical properties of the construction platforms using ultimate load and load-deflection data in the elastic range.

For the 167 single billets, data was used to determine the Modulus of Rupture (MOR) and the Modulus of Elasticity (MOE) of the single billets. These values were determined to be 60.4 MPa and 10,551 MPa, respectively. The twenty-eight construction platforms were loaded only on the center billet. A MOR of 113.8 MPa and a MOE of 17,789 MPa was determined for the construction platforms. This shows that the composite action of the construction platforms increases these properties 94% and 68%, respectively. Assuming that the load applied to the center billet is distributed evenly to each side billet and that the side billets are made of the same material as the center billet, each side billet essentially makes the center billet 47% stronger and 34% stiffer. Load-deflection data revealed that the specimens were still in the linear elastic range (i.e. 70-80% of the ultimate load). Subjective examination of the steel rods connecting the billets revealed that load was being carried from the center billet to the side billets through friction and flexure.

As part of the research performed by Shmulsky et al. (2008), Howard et al. (2008) instrumented the construction platforms with foil strain gages in an attempt to give additional insight into the composite behavior of the bolt-laminated platforms. Of the 167 billets previously tested, only thirty were used to compare to the twenty-eight platforms tested. Figure 2.4 shows select strain data from the test program.

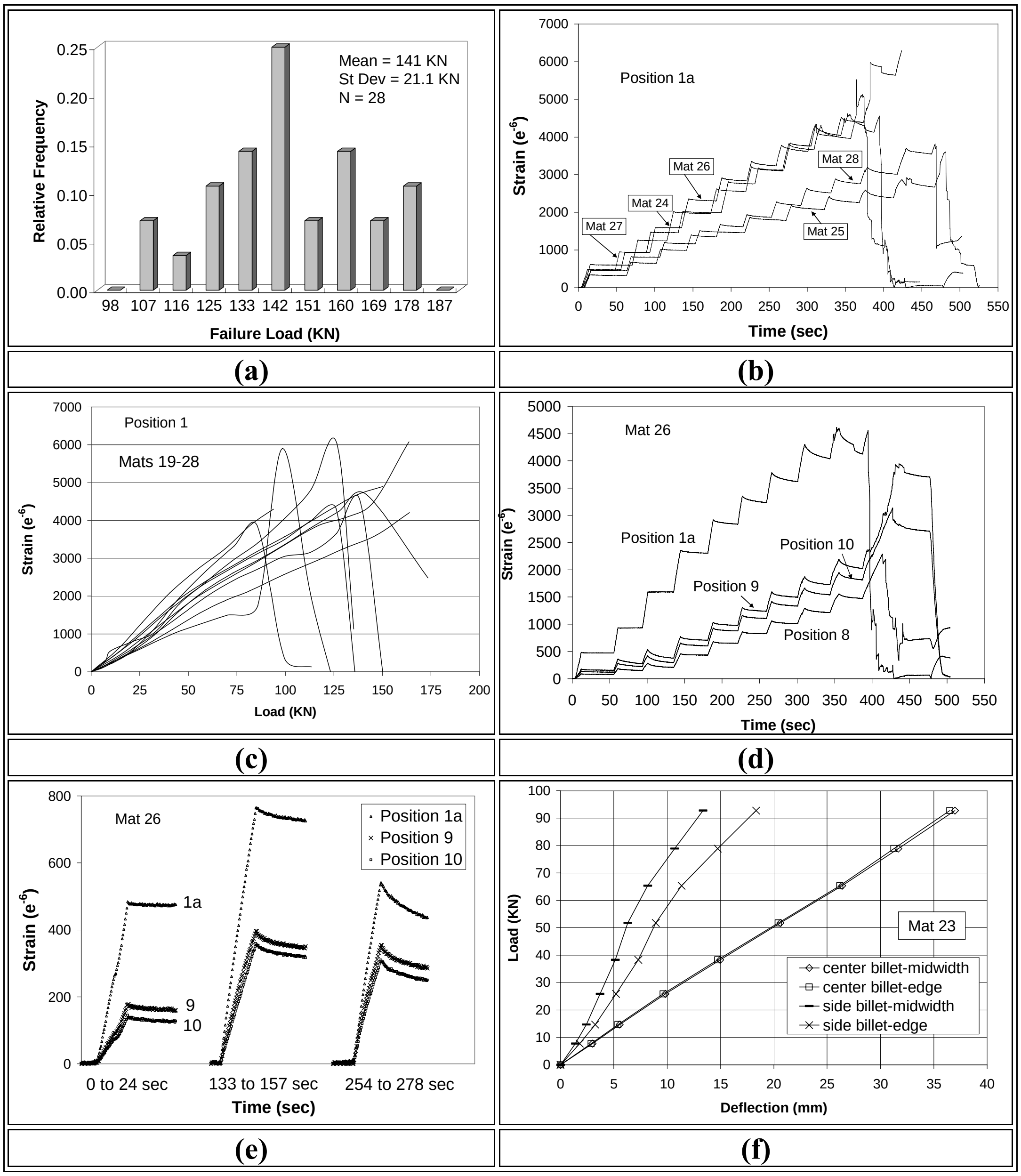

Figure 2.4 Select Test Data (Howard et al. 2008)

Figure 2.4(a) shows the relative frequency of the failure load for the platforms. From this, one can see that the distribution is relatively normal. Figure 2.4(b) shows the strain vs. time in the center billet of the platform. From this figure, one can see that the strains are not repeatable and an envelope of strain would be more representative from a design perspective. Figure 2.4(c) shows the load vs. strain plots, which also support the envelope concept. Figure 2.4(d) shows the efficient load transfer between center and side billets through the rods for a selected platform. Figure 2.4(e) shows isolated portions of Figure 2.4(d) with strains normalized to zero. It can be seen that the slope of the side billet strains approach that of the center billet over time, which implies that the composite action is more significant at higher loads. Figure 2.4(e) also demonstrates excellent relaxation. Figure 2.4(f) shows the load-deflection behavior of a selected platform. This figure illustrates that the center billet deforms in a linear fashion, while the adjacent billets appear to stiffen at intermediate loads.

Other qualitative conclusions were made about the construction platforms tested. The platforms demonstrated good ductility. This is a desirable quality since it allows time for heavy construction equipment to exit the platform before complete loss of stability occurs. The construction platforms also demonstrated excellent relaxation at elevated loading, which is desirable when large equipment will be parked on the platforms.

Howard and Stroble (2008) performed similar research on prototype and full-scale laminated wood platforms. A total of fifty-four prototype and nine full-scale platforms were instrumented and tested. Thirteen prototype geometric configurations and five full-scale geometric configurations were investigated. Platforms were numbered in the order that they were tested. The construction platforms were made of various hardwoods and softwoods. The objectives of this research were to determine the overall quality of the various geometric configurations and wood types and to determine the relaxation behavior of the wood construction platforms. The prototype platforms were tested in three-point bending, while the full-scale platforms were tested in four-point bending. Continuous strain data was acquired at various locations using bonded electrical resistance foil strain gages.

The performance of the platforms was determined based on four criteria: strength-density ratio, deflection, strain, and relaxation. Table 2.1 summarizes the properties of the prototype platforms that were tested with sufficient repetition. Table 2.2 summarizes the performance of the prototype platforms and ranks them from highest to lowest. From these tables, it can be seen that geometries 11 and 12 seemed to have the best performance overall due to their solid wood construction; however, the performance of each platform's geometry is dependent on the application. Based on performance and availability, pine and gum appeared to be the best materials. Failures of the prototype platforms were, in general, observed to occur across a large portion of the transverse direction. This pattern indicates the platforms were carrying load in a relatively uniform fashion and did not fail as a result of an isolated defective area.

For the full-scale platforms, geometry 15 performed the best. This geometry is similar to geometry 12 of the prototype platforms. Full-scale platforms failed either in tension at the center of the platform or due to shear failure at the glue lines.

Table 2.1 Summary of Prototype Mat Properties (Howard and Stroble 2008)

			Mean and/or Representative Values Used						
G[1]	Wood	Mats	Strength kN	Density kN/m^3	*S/D* m^3	Def (Δ)[2] mm	Strain (ε)[2]	ε_R[3]	L_R[4]
7	Pine	27,28,29	10.56	4.85	2.18	11.5	7436	(1) 1.5-9.0	0.0-5.0
8	Pine	4,11,12,13,14	12.77	5.35	2.39	13.0	13294	(2) 1.0-25.0	1.0- 6.3
9	Pine	3,17,18,19,20	10.30	4.91	2.10	14.1	10388	(1) 10-37.0	0.8-10.5
10	Pine	8,24,25,26	13.56	5.24	2.59	13.3	6970	(2) 1.0-4.5	0.8- 4.8
10	Gum	9,52,53,54	14.01	5.32	2.63	15.1	12733	(2) 0.3-2.3	0.3-5.0
11	Pine	6,46,47,48	17.28	6.15	2.81	13.8	12515	(3) 1.3-6.3	0.0-7.8
11	Gum	7,49,50,51	21.15	6.51	3.25	14.8	12406	(2) 1.0-5.0	0.3-7.3
12	Pine	38,39,40,41	17.46	5.91	2.96	13.2	10843	(1) -0.4-0.8	0.0-7.0
12	Gum	30,31,32,33	21.92	6.57	3.33	13.5	13925	(1) -0.3-0.7	0.8-7.0
12	Ash	34,35,36,37	15.75	6.45	2.44	12.2	16586	(1) -0.3-0.5	0.5 -5.0
12	Hickory	42,43,44,45	26.47	7.96	3.32	17.5	17876	(1) -0.2-0.6	0.8-8.0

1: G = Geometry
2: Maximum Strain (ε) and Deflection (Δ) Values Shown.
3: Maximum Relaxation (R) Range for Strain (ε). The Location Used in Shown in Parenthesis.
4: Maximum Relaxation (R) Range for Load (L).

Table 2.2 Summary of Prototype Mat Performance (Howard and Stroble 2008)

			Ranking (1 = Best Ranking)						
G[1]	Wood	Mats	Strength	Density[2]	*S/D*	Deflection (Δ)[3]	Strain (ε)[3]	ε_R[4]	L_R[5]
7	Pine	27, 28, 29	10	1	10	11	10	3	8
8	Pine	4, 11,12, 13, 14	9	5	9	9	4	2	7
9	Pine	3, 17, 18, 19, 20	11	2	11	4	9	1	1
10	Pine	8, 24, 25, 26	8	3	7	7	11	6	11
10	Gum	9, 52, 53, 54	7	4	6	2	5	7	9
11	Pine	6, 46, 47, 48	5	7	5	5	6	4	2
11	Gum	7, 49, 50, 51	3	9	3	3	7	5	4
12	Pine	38, 39, 40, 41	4	6	4	8	8	8	5
12	Gum	30, 31, 32, 33	2	10	1	6	3	9	6
12	Ash	34, 35, 36, 37	6	8	8	10	2	11	10
12	Hickory	42, 43, 44, 45	1	11	2	1	1	10	3

1: G = Geometry
2: Lowest Density Ranked 1
3: Maximum Deflection Ranked 1. Maximum Strain Also Ranked 1
4: Relaxation (R) Ranking for Strain (ε). Table 2.2 Ranges Used for Ranking
5: Relaxation (R) Ranking for Load (L). Table 2.2 Ranges Used for Ranking

Strain-relaxation and load-relaxation plots were also developed to determine relaxation characteristics for the various platforms. Figure 2.5(a) serves as an example of the proper method to determine the first data point in Figure 2.5(b). The relaxation is taken as the difference between the strain before relaxation and the strain after relaxation divided by the ultimate strain. Based on this data, it was determined that platform geometry and glue properties likely have the most effect on relaxation properties of the platforms.

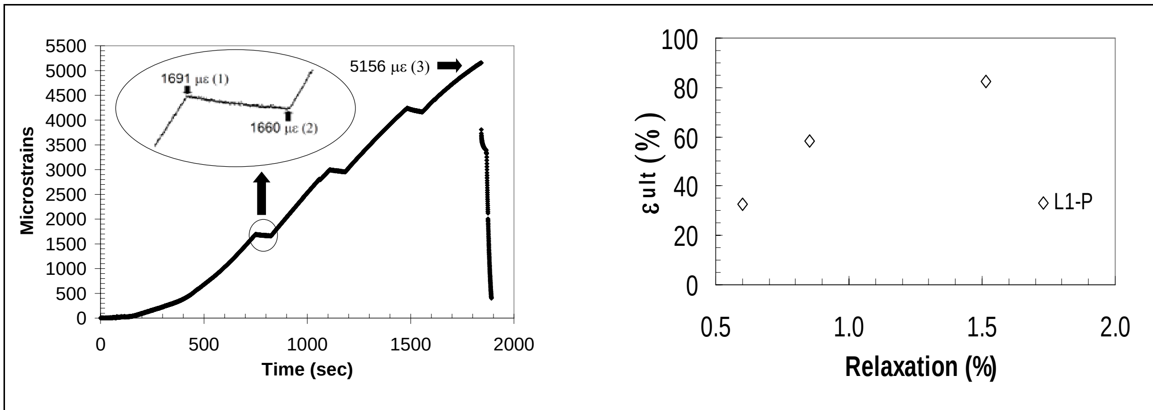

(a) Figure D1(a) Reproduced as Example *(b) Relaxation of Mat 1 from Figure D1(a)*

Figure 2.5 Procedure for Determining Relaxation Values (Howard and Stroble 2008)

2.4.4 Construction Platform Design

Anthony Hardwood Composites of Sheridan, Arkansas, provides a design guide for their **emtek** construction platforms (***emtek*** 2009). The design guide takes into account parameters such as length, boundary conditions, load configurations, and deflections when determining the depth of the platform to be used. There are two different boundary conditions: uniform bearing and end/edge bearing. There are three types of soil conditions ranging from extremely soft to soft. Soils are classified by their modulus of subgrade reaction, k_0. Loading configurations vary based on type of equipment to be used on top of the platforms.

emtek platforms consist of 30.48 cm wide *glulam* beams or billets that are bolt-laminated together to the desired width. Various indigenous Southern hardwoods may be used for **emtek** platforms. The platforms' uniform density ranges from 750 to 850 kg/m^3 depending on moisture content. **emtek** platforms are the type of bolt-laminated platforms tested by Shmulsky et al. (2008).

The ***emtek*** design guide is based on a one-dimensional linear finite element model. This is a simplified subgrade modulus procedure. This method is typically an iterative solution in which the deflection and the subgrade modulus are modified until they converge to a single value for each. For this design guide, an acceptable deflection (as determined by the manufacturer) and an assumed subgrade modulus are used to calculate the depth of the platform rather than an iterative solution.

A strenuous effort was made to acquire alternative design guides for wood construction platforms; however, none were found. Researchers at the USDA Forestry Products Laboratory in Madison, Wisconsin, are not familiar with any alternative design guides. Researchers in the Forestry Products department at Mississippi State University in Starkville, Mississippi, are not familiar with any alternative design guides. However, they were able to pass on contact information for industry professionals at New South Mat, a wood construction platform distributor for North America. Mr. Drew St. John with New South Mat was only familiar with the ***emtek*** design guide discussed earlier. Mr. St. John also expressed a need for alternative design guides for wood construction platforms. Researchers at the USACE Engineering Research and Development Center (ERDC) in Vicksburg, Mississippi, have experience in the testing and design of matting systems for various applications. They recommended additional companies that manufactured matting systems; however, none of these systems were made from timber and were, therefore, irrelevant to the current research. ERDC researchers also indicated that the Army is not typically concerned with the design of timber matting systems as it pertains to optimized dimensions. This is because these stabilization techniques are only used for quick mobilization of troops through rugged terrain. There is often insufficient time to design and install these types of systems.

2.5 Summary of Literature Review

The literature presented has shown that the timber industry has a relatively large impact on the economy. Timber is finding its place in a variety of applications, an advancement that has been aided by the development of composite wood products. Composite wood products reduce the variability of wood, allowing for a more reliable design. Of these wood products, structural composite lumber, specifically *glulam* and *LVL*, is being used in many different applications. Wood construction platforms use this technology for low-impact soil stabilization. However, until recently, research has not demonstrated the use of modern technology, such as instrumentation, in determining the composite mechanical properties of wood construction platforms. The review of literature shows that the design of wood construction platforms would benefit from the use of load-strain and load-deflection data. This data could be easily implemented into the design of composite wood materials and would give the designer insight into the true behavior of the platform, ultimately resulting in improved designs.

The literature review had a large impact on the remainder of this thesis. The literature review found only one design guide for wood construction platforms: a result that suggests a need for alternative design methods. The guide found was based on a finite element model. The design guide proposed in this thesis uses instrumented strain data implemented into beam-on-elastic-foundation theory. This methodology will be presented in Chapter 4. However, before this methodology can be discussed, the data from the previous research efforts must be reduced and compiled into an acceptable format for this analysis. The next chapter will discuss the data reduction process.

CHAPTER 3

EXPERIMENTAL PROGRAM AND DATA REDUCTION

3.1 Introduction

The data used in this research was taken from two research projects where multiple types of wood construction platforms were instrumented and tested. These platforms varied in wood type, geometric configuration, and size. A total of ninety-one platforms (fifty-four prototype, nine adhesive-laminated, twenty-eight bolt-laminated) were instrumented with approximately 220 strain gages. Select data that had adequate test repetition for the needs of this project was compiled from the previous efforts, reduced, and used for analysis. Extraneous data points representing a very small fraction of the total data set were omitted based on engineering judgment and various criteria including: 1) false strain measurements (i.e. broken gages); 2) removal of relaxation pauses (discussed later in this chapter); and 3) insufficient repetition.

The author of this thesis was involved with portions of the two aforementioned research projects. The first project was related to testing of full-scale bolt-laminated construction platforms where the author was involved in instrumentation and testing only. Additional details on this project can be found in Howard et al. (2008), Shmulsky et al. (2008), Shmulsky and Shi (2008), and later in this chapter. The second project was related to testing of prototype and full-scale adhesive-bonded construction platforms where the author was involved in multiple facets and co-authored the report to the sponsor (Howard and Stroble 2008).

Table 3.1 converts the platform designations used in the documents described above to the designations that will be used throughout this report. As seen, seven geometric configurations were chosen from the nineteen available in the four documents from which the data was taken. Designations were numbered in the order in which they were tested for both geometry categories and platforms within a single geometry category. The platforms were also numbered this way for the previous reports. Therefore, the lowest number platform tested will be Platform 1 for the new designation and so on. Each designation begins with the type of platform followed by the material, geometry, and replicate (e.g. **P**rototype **S**cale_**P**ine_**G**eometry**.R**eplicate). Geometric configurations varied based on the placement of joints, the length of spacing between adjacent vertical slats, and the presence of horizontal slats. Refer to Figure 3.1 through Figure 3.7 for all platform geometries, dimensions, and strain gage locations. Table 3.2 summarizes the data utilized in this report by showing the number of platforms tested, total number of strain measurements taken, and number of strain locations for each platform. It should be noted that "mat" and "platform" have the same meaning and may be used interchangeably in this chapter.

Table 3.1 Platform Designation Conversion

Source of Data	Previous Report Wood Type and Geometry Number	New Designation
Howard and Stroble (2008)	Pine - 8	PS_P_G1
	Pine - 9	PS_P_G2
	Pine - 10	PS_P_G3
	Gum - 10	PS_SG_G3
	Pine - 11	PS_P_G4
	Gum - 11	PS_SG_G4
	Pine - 12	PS_P_G5
	Gum - 12	PS_SG_G5
	Ash - 12	PS_A_G5
	Hickory - 12	PS_H_G5
	Pine - 15	FS_P_G6
Howard et al. (2008)	Gum - Bolt-Laminated	FS_SG_G7

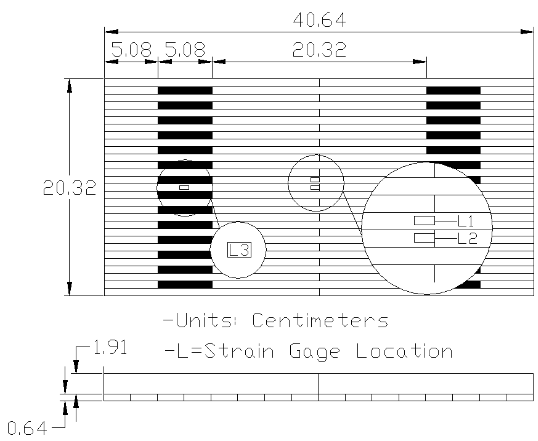

(a) Drawing of G1

(b) Photo of G1

Figure 3.1 Platform Geometry 1 (G1)

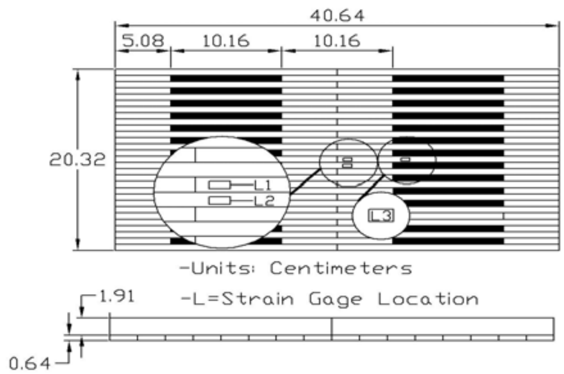

(a) Drawing of G2

(b) Photo of G2

Figure 3.2 Platform Geometry 2 (G2)

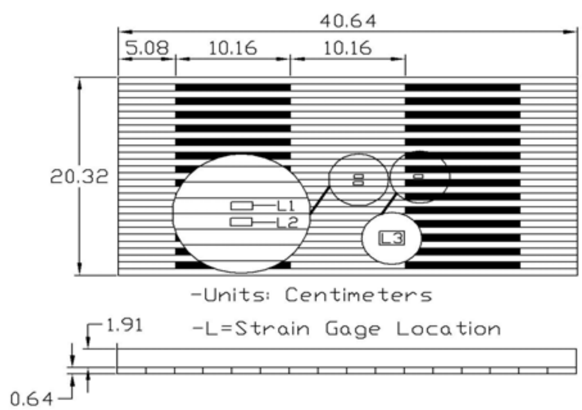

(a) Drawing of G3

(b) Photo of G3

Figure 3.3 Platform Geometry 3 (G3)

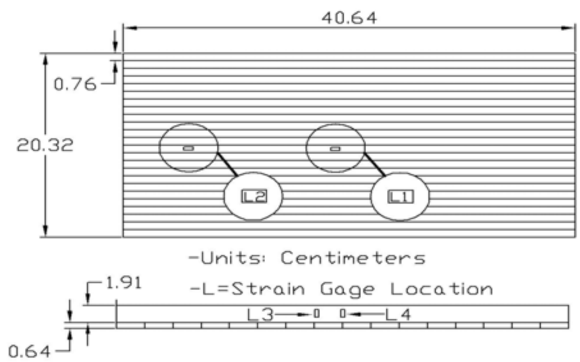

(a) Drawing of G4

(b) Photo of G4

Figure 3.4 Platform Geometry 4 (G4)

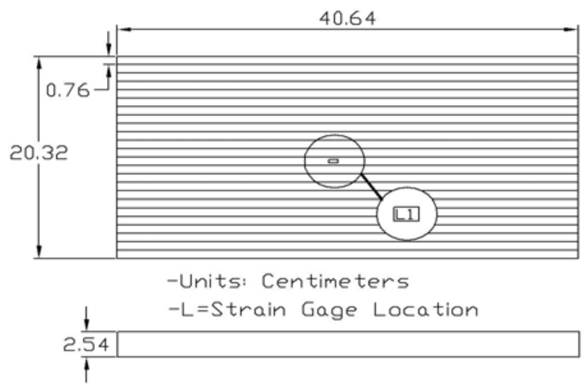

(a) Drawing of G5

(b) Photo of G5

Figure 3.5 Platform Geometry 5 (G5)

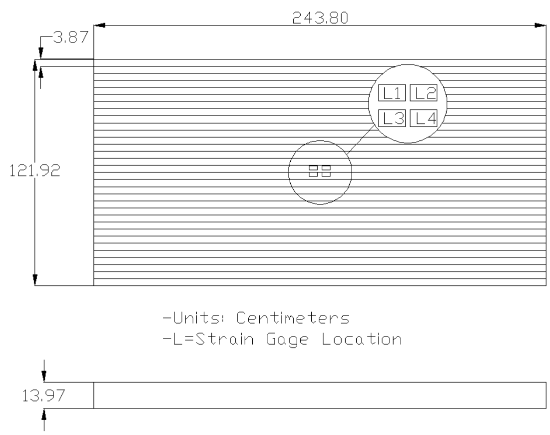

(a) Drawing of G6

(b) Photo of G6

Figure 3.6 Platform Geometry 6 (G6)

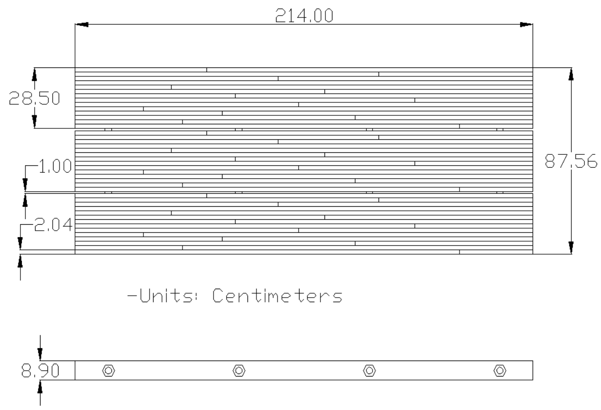

(a) Drawing of G7

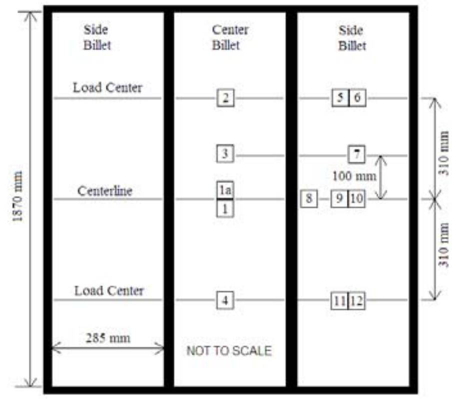

(b) Clear Span Strain Gage Locations

(c) Photo of G7

Figure 3.7 Platform Geometry 7 (G7)

Table 3.2 Summary of Data Utilized

Platform Category	Platforms Instrumented and Tested	Strain Measurements	Strain Locations per Platform
PS_P_G1	5	15	3
PS_P_G2	5	14	3
PS_P_G3	4	12	3
PS_SG_G3	4	11	3
PS_P_G4	4	4	4
PS_SG_G4	4	4	4
PS_P_G5	4	4	1
PS_SG_G5	4	4	1
PS_A_G5	4	4	1
PS_H_G5	4	3	1
FS_P_G6	2	8	4
FS_SG_G7	10	70	13
Total	54	153	---

The next section provides the methodology for the reduction of data, followed by a section showing the extracted load-strain data and another section showing the extracted load-deflection data. The information is presented in two parts: prototype platforms and full-scale platforms.

3.2 Methodology for Data Reduction

A large amount of data was available for each platform. Strain data was originally taken for purposes other than those of the research presented in this paper. Therefore, strain data had to be refined into a consistent format for the needs of this analysis. Using the original data, load vs. strain plots were made for the location of each strain gage in order to develop an envelope of strains for platforms with the same geometry and wood type. The method for developing these plots depended on the data available and the type of platform. Only minor modifications had to be made to the load-deflection data (e.g. formatting and presentation).

3.2.1 Strain Data Reduction of Prototype Platforms

For the prototype platforms, continuous strain data was available for each strain gage location. Strains were measured four times per second for approximately 1,000 seconds depending on the test. The load applied to the platforms was recorded every ten seconds, before each relaxation pause, and after each relaxation pause. Relaxation pauses were approximately 60-second time intervals in which the load was held constant to allow the platforms to relax. It should be noted that the "strain time" and "load time" were not the same. The "strain time" started when the data acquisition system was triggered; shortly thereafter the load began to be applied, beginning the "load time."

In order to develop the load vs. strain plots, two major steps were required to transform the raw data. Refer to Figure 3.8 for this procedure. The first step was to eliminate the relaxation portions of the strain vs. time plots. This was performed by assuming that no redistribution of the load occurred. This is shown in Figure 3.8(a) by the horizontal lines that extend from the load before the relaxation pause to a point above the load after the relaxation pause. Loads that fell below this line were eliminated.

The second step was to equate "strain time" to "load time." "Load time" was assumed to be independent. Loads were held constant for a period on the order of sixty seconds to allow for relaxation to occur, meaning that the load before relaxation was known, as was the time that it occurred. In order to convert "strain time" to "load time," the point in "strain time" immediately before relaxation was recorded and assumed to have occurred at the same time as the load before relaxation. This point was 12.34 kN and 4544 $\mu\varepsilon$ in Figure 3.8. Once this point was known, one could simply step down the strain curve in 10-second intervals and correlate strain to load as seen in Figure 3.8(b). This was performed for each relaxation period, and the results for one segment can be seen in Figure 3.8(c). The measured raw data used to make the load-strain plots is available in Appendix A, and Table 3.3 shows the location of the raw data tables for each platform category in Appendix A.

Table 3.3 Measured Raw Data Location in Appendix A (Prototype Scale)

Platform Category	Raw and Reduced Data
PS_P_G1	Table A.1 through Table A.5
PS_P_G2	Table A.6 through Table A.10
PS_P_G3	Table A.11 through Table A.14
PS_SG_G3	Table A.15 through Table A.18
PS_P_G4	Table A.19 through Table A.22
PS_SG_G4	Table A.23 through Table A.26
PS_P_G5	Table A.27 through Table A.30
PS_SG_G5	Table A.31 through Table A.34
PS_A_G5	Table A.35 through Table A.38
PS_H_G5	Table A.39 through Table A.42

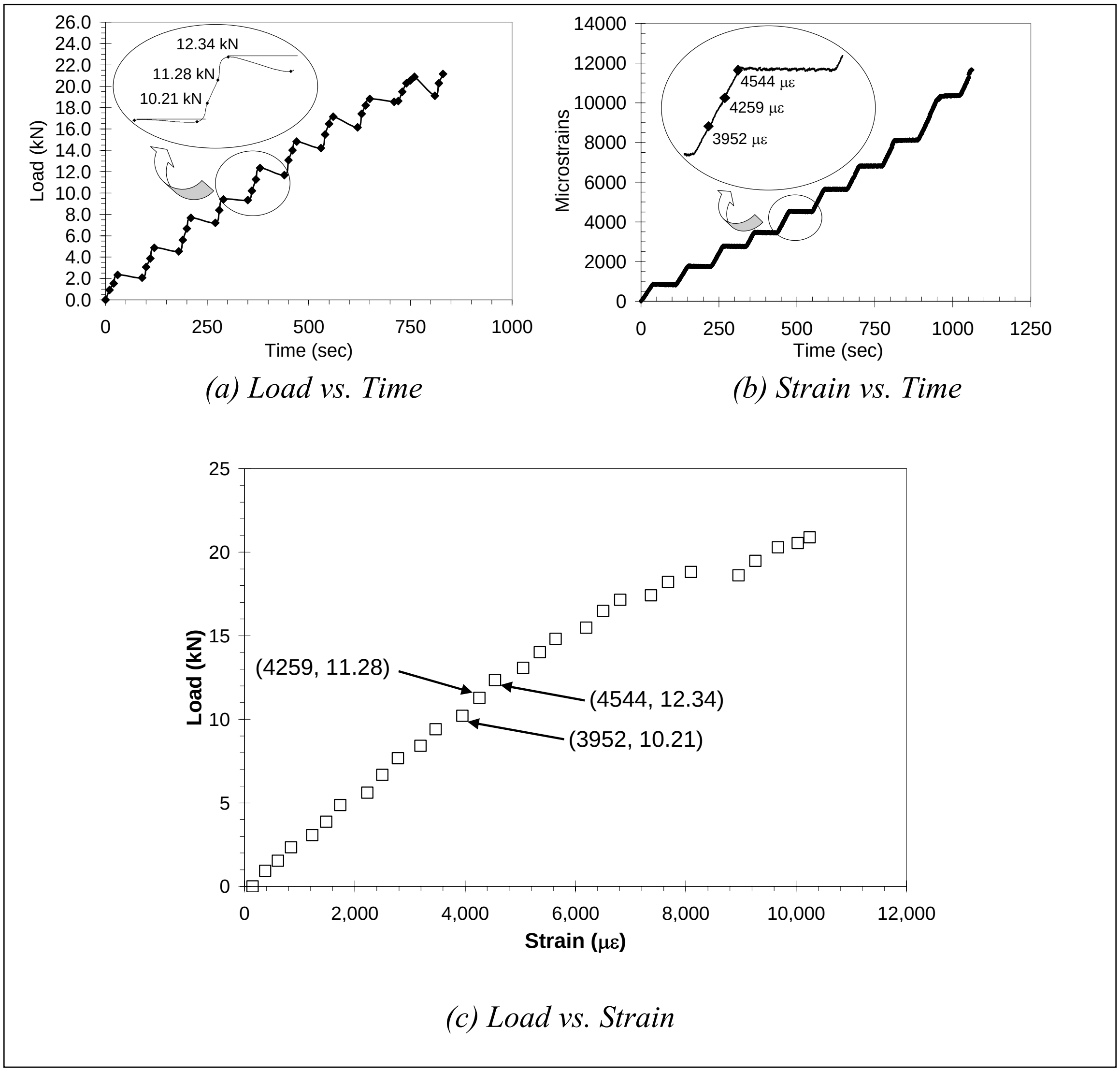

Figure 3.8 Procedures for Developing Load vs. Strain Plots

<u>3.2.2 Strain Data Reduction of Full-Scale Platforms</u>

Geometry 6 (G6) full-scale platforms were tested in a manner similar to that of the G1 through G5 prototype platforms with a few notable differences. First, strain was measured five times per second rather than four times per second. Second, multiple strain gages were placed within a small area of each other to show the reliability and repeatability of the strain measurements. Third, platforms were loaded in a four-point

configuration instead of a three-point configuration. Also, these platforms were only used for a verification of the scaling-up procedure to be discussed in Chapter 4 of this paper, as well as to show the reliability of strain measurements at the center of the platforms. Therefore, no load-strain data is presented for these platforms; rather, strain-time plots are presented later in this chapter.

For Geometry 7 (G7) full-scale bolt-laminated platforms, load vs. strain data was readily available from previous work for each location of each strain gage. As a result, only minor modifications were made to the data (e.g. formatting and presentation). Tables A.43 through Table A.52 of Appendix A contain the data for G7.

3.3 Extracted Strain and Ultimate Load Data

This section presents the extracted strain data for all the platforms. Within each platform category, load-strain behavior for each strain gage location is presented. Load-strain envelopes were determined based on all platforms in which strains were taken for that location. Second-order polynomial regressions were used to develop these envelopes because they provided better correlation to test results than alternative regressions (e.g. linear regressions). Equation 311 shows the second-order polynomial regression equation. All plots show the minimum and maximum ultimate loads for platforms with the same geometric configuration and wood type.

$$P = a_0\varepsilon^2 + b_0\varepsilon \tag{3-1}$$

Where: P = load. (kN)
ε = strain. (με)
a_0 = first quadratic coefficient.
b_0 = second quadratic coefficient.

3.3.1 Strain Data for Prototype Scale Platforms

Load-strain plots for the prototype scale platforms are presented in Figure 3.9 through Figure 3.18. The data available for each plot depends on the platform. Maximum and minimum loads are dependent on the material used and the geometric configuration. Values of the regression coefficients seen in Equation 3-1, as well as correlation coefficients, r^2, are presented in Table 3.4 through Table 3.13. Values in bold denote envelope boundaries (i.e. upper and lower bounds) for a specific wood type, geometry, and strain gage location. Measured raw and reduced data values for each plot are available in the tables in Appendix A. Extraneous data points (very small percentage of the total) were removed from this data set. "Sensor Failure" denotes a location in which the gage failed to record data or in which the data recorded was omitted due to engineering judgment.

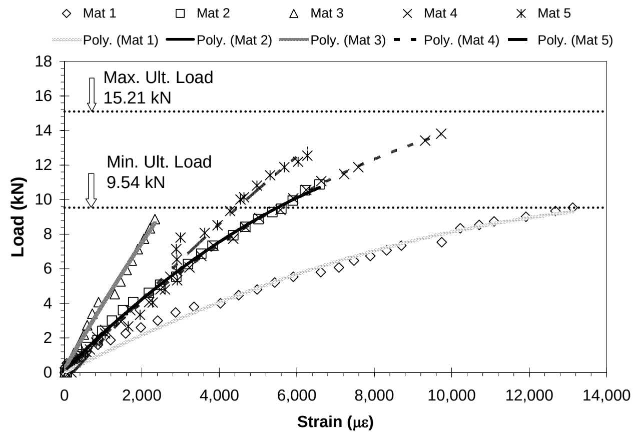

a) Location 1

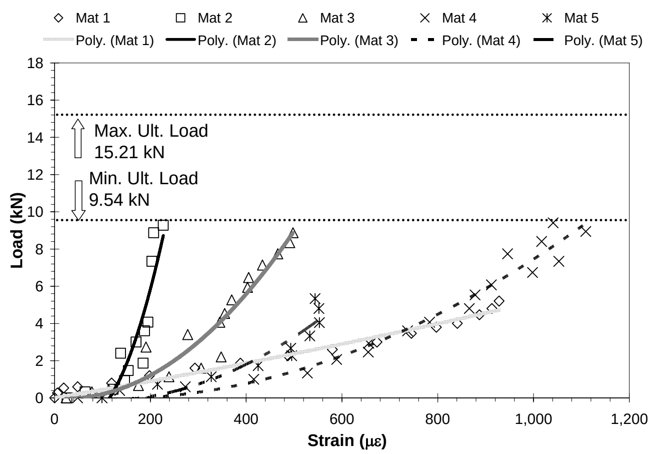

b) Location 2

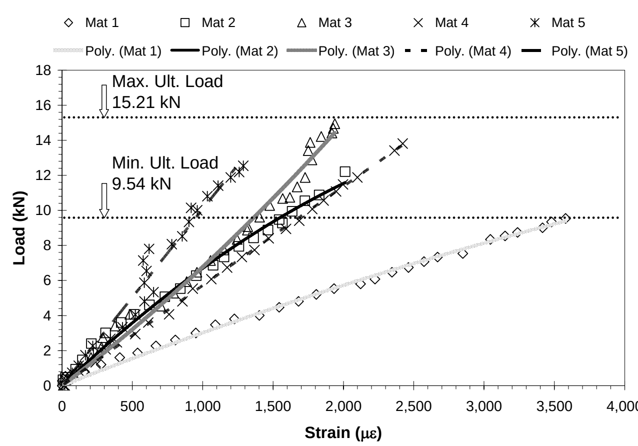

c) Location 3

Figure 3.9 Load vs. Strain for PS_P_G1

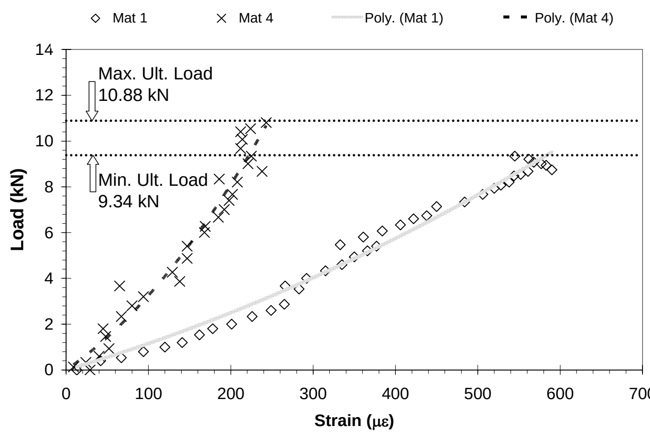

a) Location 1

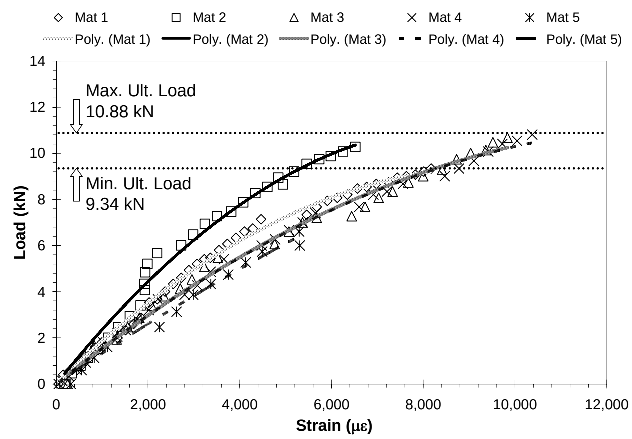

b) Location 2

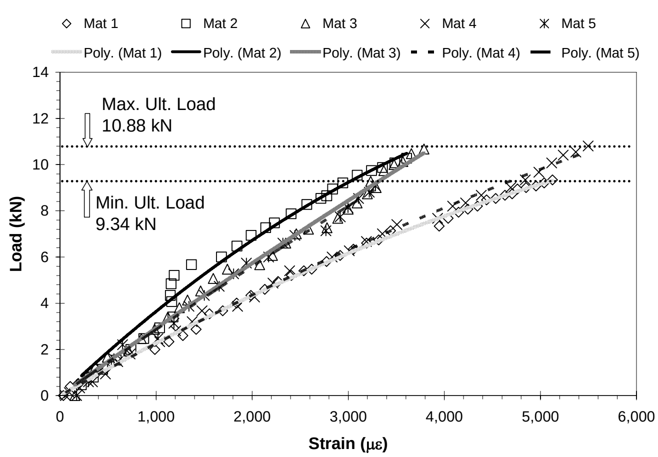

c) Location 3

Figure 3.10 Load vs. Strain for PS_P_G2

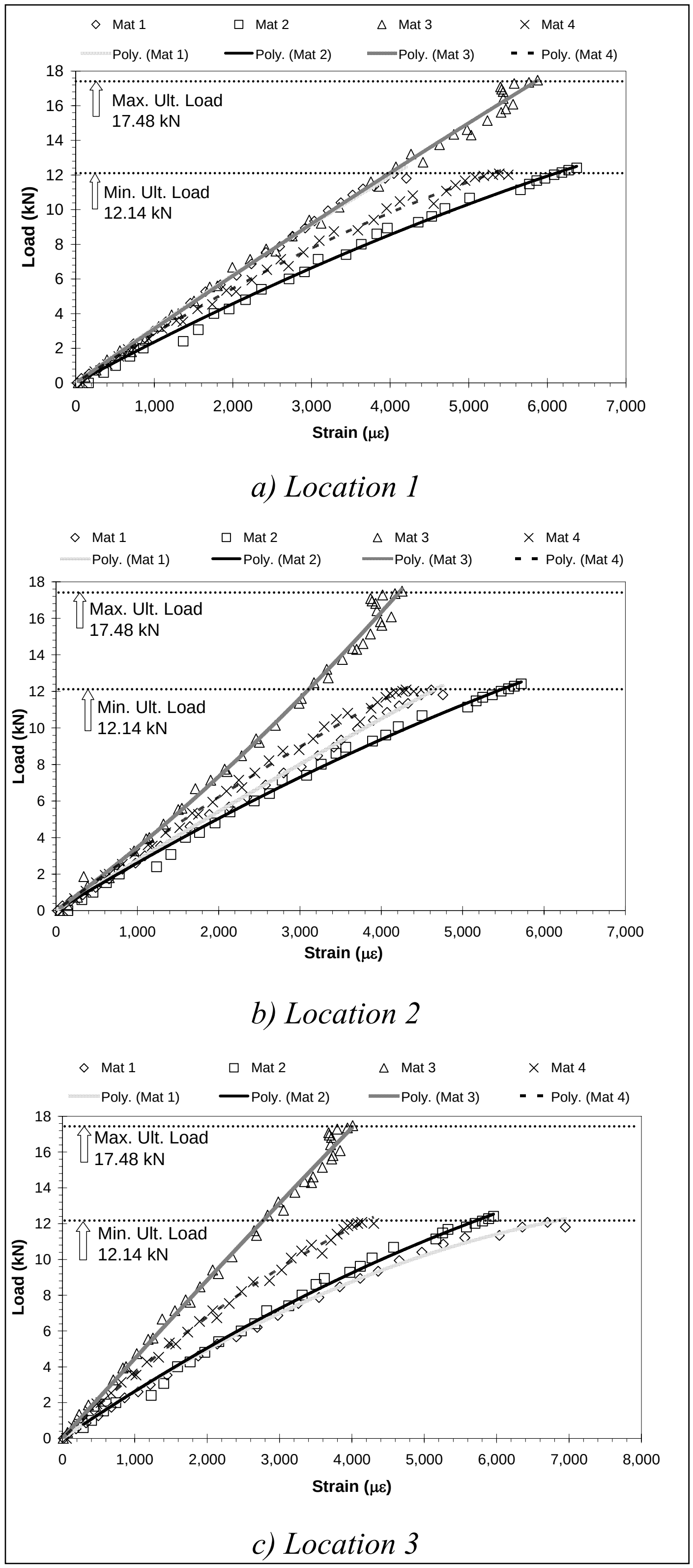

Figure 3.11 Load vs. Strain for PS_P_G3

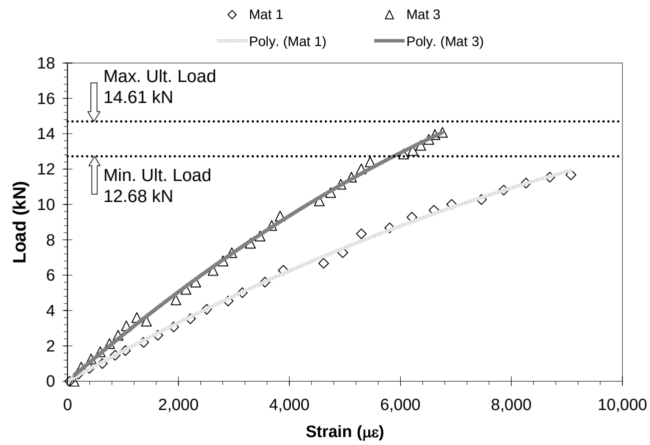

a) Location 1

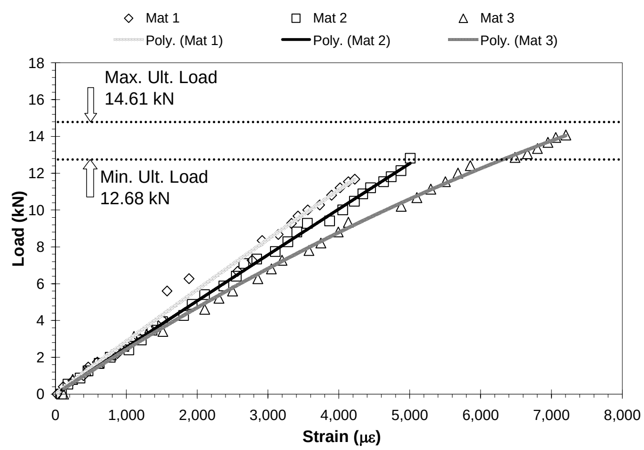

b) Location 2

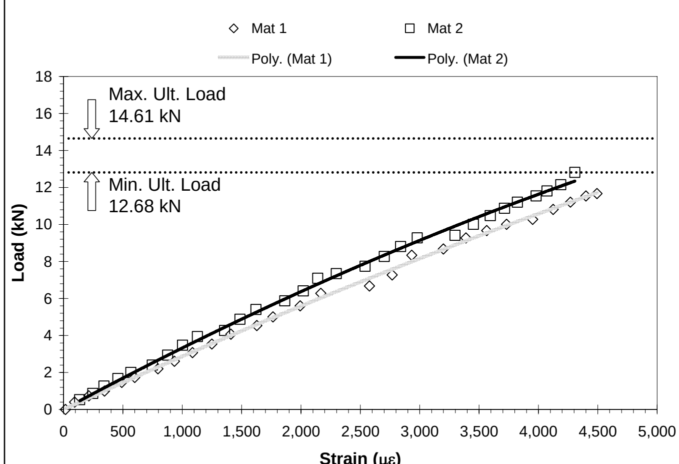

c) Location 3

Figure 3.12 Load vs. Strain for PS_SG_G3

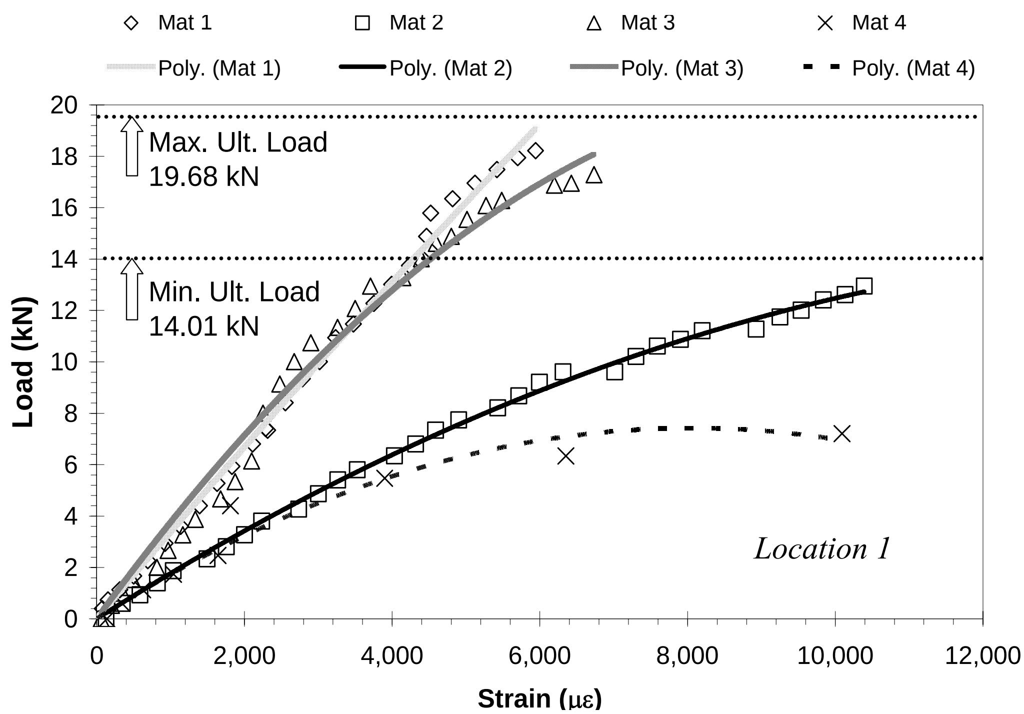

Figure 3.13 Load vs. Strain for PS_P_G4

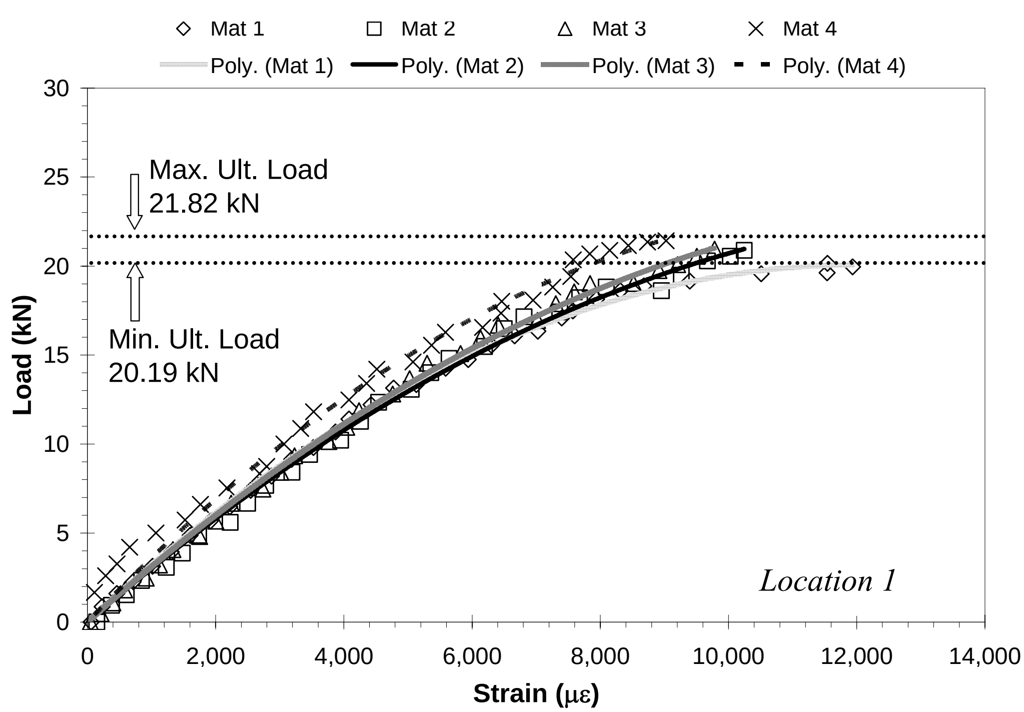

Figure 3.14 Load vs. Strain for PS_SG_G4

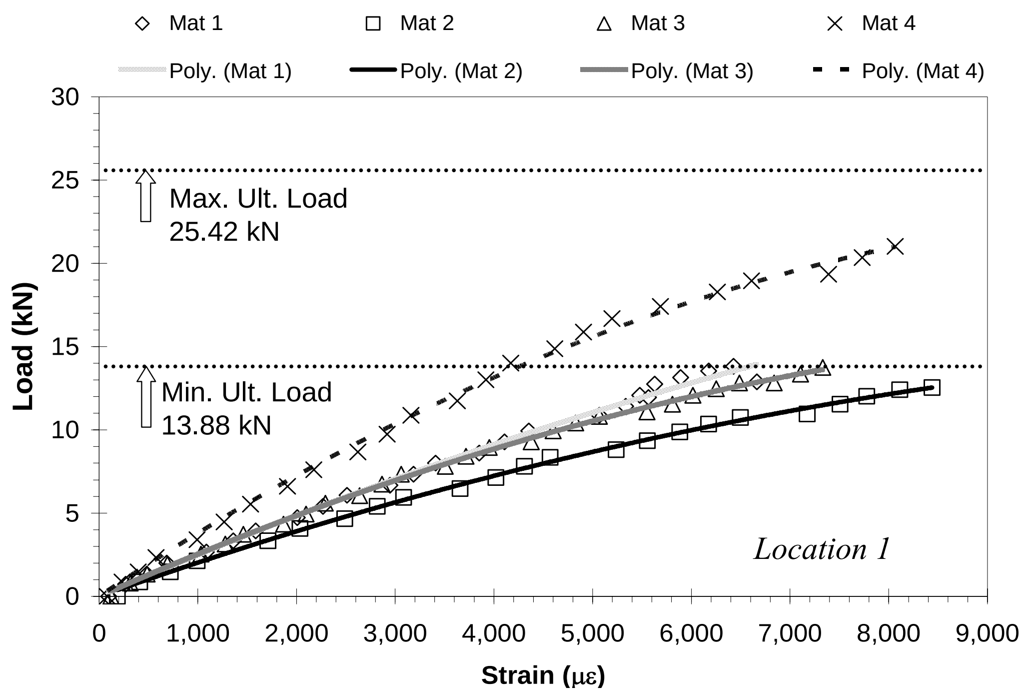

Figure 3.15 Load vs. Strain for PS_P_G5

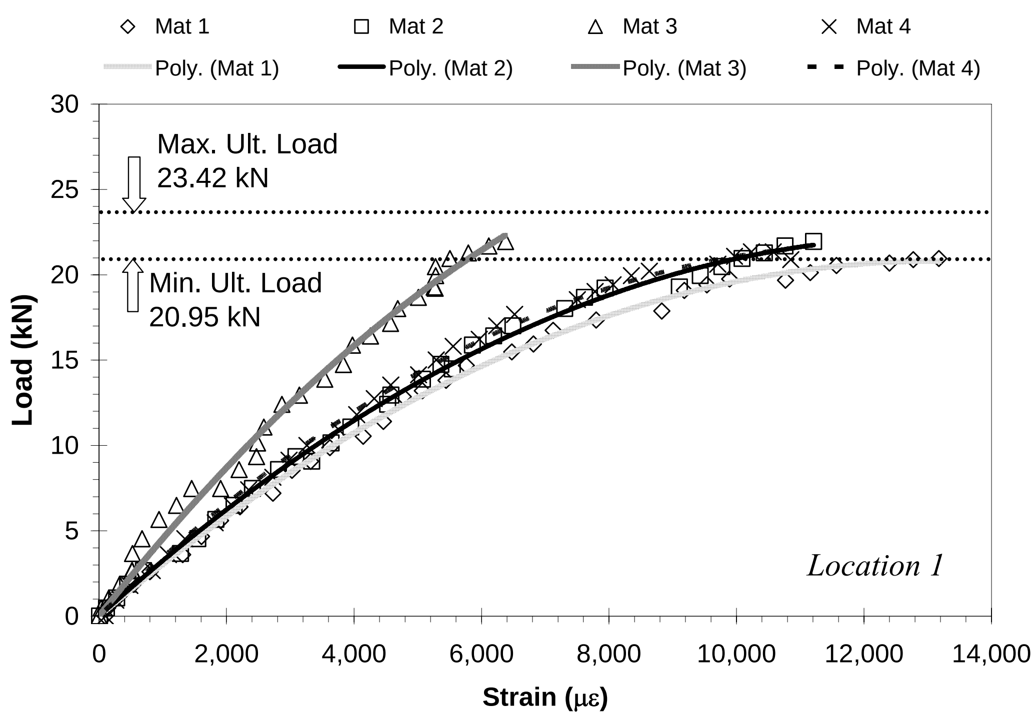

Figure 3.16 Load vs. Strain for PS_SG_G5

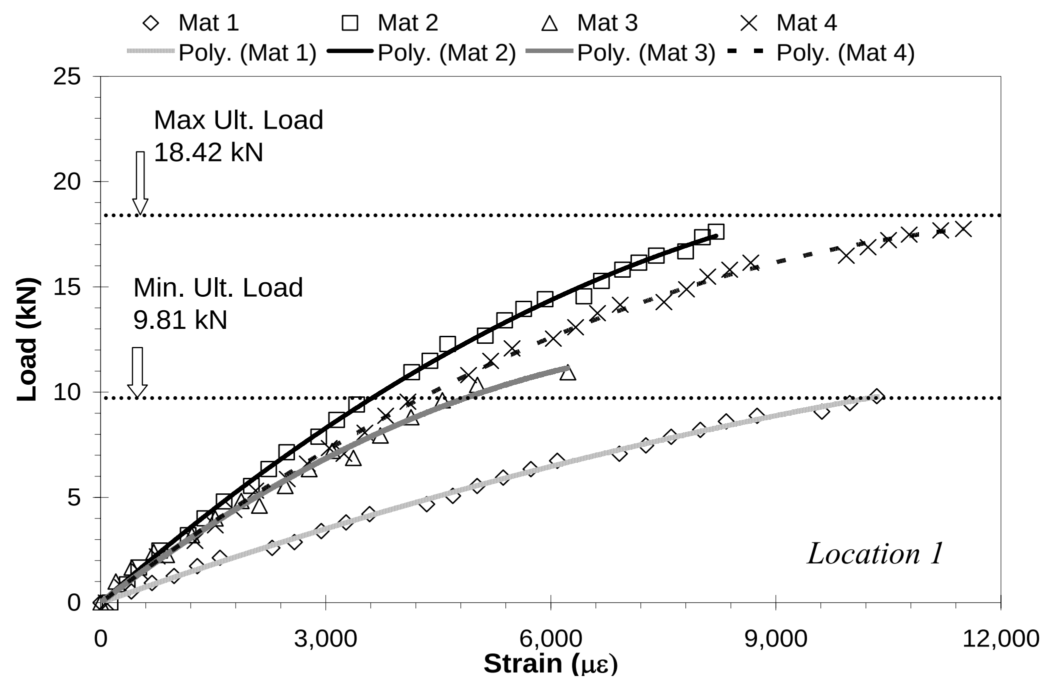

Figure 3.17 Load vs. Strain for PS_A_G5

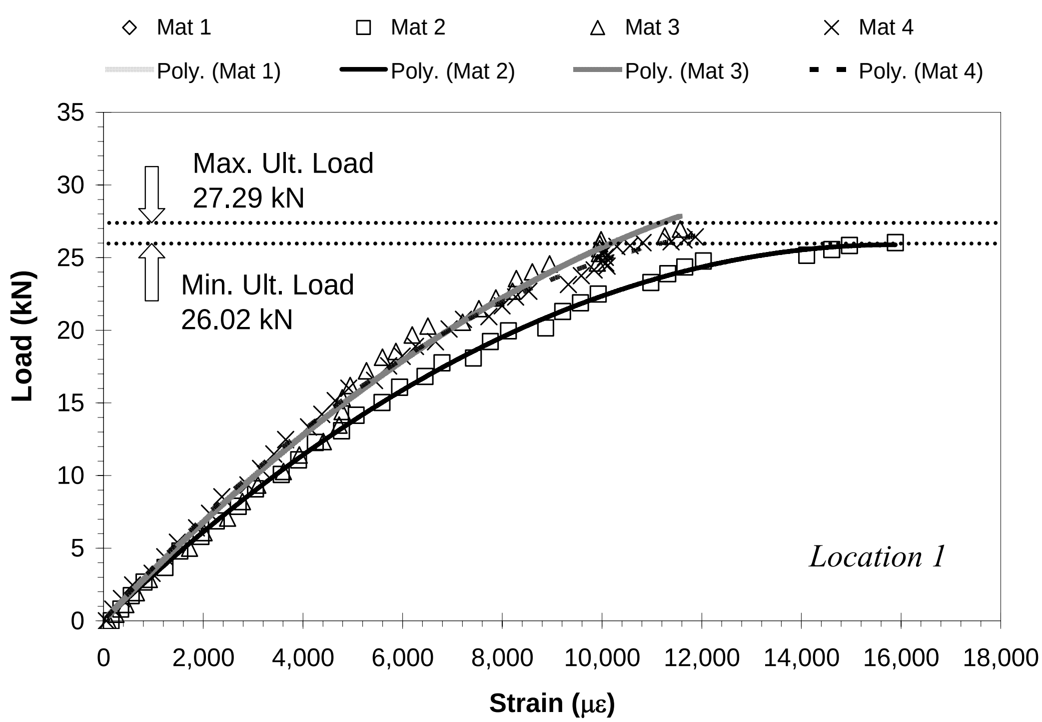

Figure 3.18 Load vs. Strain for PS_H_G5

Table 3.4 Regression Summary for PS_P_G1

Location	Platform	a_0	b_0	r^2
1	1	**-3.34E-08**	**1.15E-03**	**0.988**
	2	-1.08E-07	2.33E-03	0.998
	3	**-2.50E-07**	**4.26E-03**	**0.990**
	4	-7.68E-08	2.16E-03	0.999
	5	-1.29E-08	2.17E-03	0.978
2	1	8.02E-07	4.35E-03	0.975
	2	**3.42E-04**	**-3.93E-02**	**0.822**
	3	3.95E-05	-1.86E-03	0.917
	4	**9.19E-06**	**-1.74E-03**	**0.965**
	5	2.05E-05	-3.69E-03	0.860
3	1	**-1.52E-07**	**3.17E-03**	**0.995**
	2	-9.29E-07	7.63E-03	0.990
	3	7.11E-07	6.06E-03	0.988
	4	-3.38E-08	5.75E-03	0.999
	5	**-1.01E-08**	**1.01E-02**	**0.967**

Table 3.5 Regression Summary for PS_P_G2

Location	Platform	a_0	b_0	r^2
1	1	**9.33E-06**	**1.06E-02**	**0.982**
	2	Sensor Failure		
	3	Sensor Failure		
	4	**7.99E-05**	**2.45E-02**	**0.952**
	5	Sensor Failure		
2	1	-1.01E-07	1.96E-03	0.996
	2	**-1.39E-07**	**2.50E-03**	**0.983**
	3	**-5.69E-08**	**1.60E-03**	**0.990**
	4	-5.65E-08	1.59E-03	0.996
	5	-2.80E-08	1.36E-03	0.984
3	1	**-1.11E-07**	**2.39E-03**	**0.998**
	2	**-2.82E-07**	**3.92E-03**	**0.978**
	3	-5.15E-08	2.97E-03	0.992
	4	-7.22E-08	2.32E-03	0.998
	5	-5.98E-08	2.91E-03	0.993

Table 3.6 Regression Summary for PS_P_G3

Location	Platform	a_0	b_0	r^2
1	1	-6.46E-08	3.24E-03	0.998
	2	**-7.42E-08**	**2.44E-03**	**0.769**
	3	**-3.08E-08**	**3.15E-03**	**0.996**
	4	-1.34E-07	2.99E-03	0.997
2	1	-4.37E-08	2.80E-03	0.999
	2	**-8.99E-08**	**2.70E-03**	**0.769**
	3	**2.08E-07**	**3.25E-03**	**0.993**
	4	-1.20E-07	3.35E-03	0.997
3	1	**-1.43E-07**	**2.76E-03**	**0.999**
	2	-1.06E-07	2.74E-03	0.740
	3	**-3.97E-08**	**4.50E-03**	**0.995**
	4	-2.23E-07	3.83E-03	0.997

Table 3.7 Regression Summary for PS_SG_G3

Location	Platform	a_0	b_0	r^2
1	1	**-4.84E-08**	**1.75E-03**	**0.998**
	2	Sensor Failure		
	3	**-9.34E-08**	**2.71E-03**	**0.998**
	4	Sensor Failure		
2	1	**-3.12E-08**	**2.90E-03**	**0.992**
	2	-8.66E-09	2.55E-03	0.998
	3	**-7.67E-08**	**2.50E-03**	**0.998**
	4	Sensor Failure		
3	1	**-7.51E-08**	**2.94E-03**	**0.998**
	2	**-1.38E-07**	**3.46E-03**	**0.998**
	3	Sensor Failure		
	4	Sensor Failure		

Table 3.8 Regression Summary for PS_P_G4

Location	Platform	a_0	b_0	r^2
1	1	**-3.38E-08**	**3.41E-03**	**0.996**
	2	-5.80E-08	1.83E-03	0.998
	3	-1.87E-07	3.94E-03	0.983
	4	**-1.14E-07**	**1.84E-03**	**0.950**

Table 3.9 Regression Summary for PS_SG_G4

Location	Platform	a_0	b_0	r^2
1	1	**-1.39E-07**	**3.34E-03**	**0.999**
	2	-1.04E-07	3.11E-03	0.996
	3	-1.09E-07	3.22E-03	0.998
	4	**1.51E-07**	**3.74E-03**	**0.987**

Table 3.10 Regression Summary for PS_P_G5

Location	Platform	a_0	b_0	r^2
1	1	-7.09E-08	2.56E-03	0.995
	2	**-7.23E-08**	**2.10E-03**	**0.998**
	3	-1.06E-07	2.64E-03	0.998
	4	**-1.68E-07**	**3.96E-03**	**0.997**

Table 3.11 Regression Summary for PS_SG_G5

Location	Platform	a_0	b_0	r^2
1	1	**-1.20E-07**	**3.16E-03**	**0.999**
	2	-1.28E-07	3.38E-03	0.997
	3	**-1.93E-07**	**4.73E-03**	**0.992**
	4	-1.48E-07	3.58E-03	0.998

Table 3.12 Regression Summary for PS_A_G5

Location	Platform	a_0	b_0	r^2
1	1	**-3.04E-08**	**1.26E-03**	**0.998**
	2	**-1.23E-07**	**3.13E-03**	**0.999**
	3	-1.52E-07	2.74E-03	0.989
	4	-1.01E-07	2.70E-03	0.998

Table 3.13 Regression Summary for PS_H_G5

Location	Platform	a_0	b_0	r^2
1	1	Sensor Failure		
	2	-1.03E-07	3.27E-03	0.999
	3	**-1.03E-07**	**3.60E-03**	**0.990**
	4	**-1.32E-07**	**3.80E-03**	**0.998**

3.3.2 Strain Data for Full-Scale Platforms

For G6 full-scale platforms, strain vs. time plots are presented in Figure 3.19 and Figure 3.20 to show the repeatability of the strain measurements. Ultimate loads are shown on the strain vs. time plots and are taken to occur at the same time as the ultimate strain. This information will be used in Chapter 4 for verification of the scaling procedure, which is also discussed in Chapter 4.

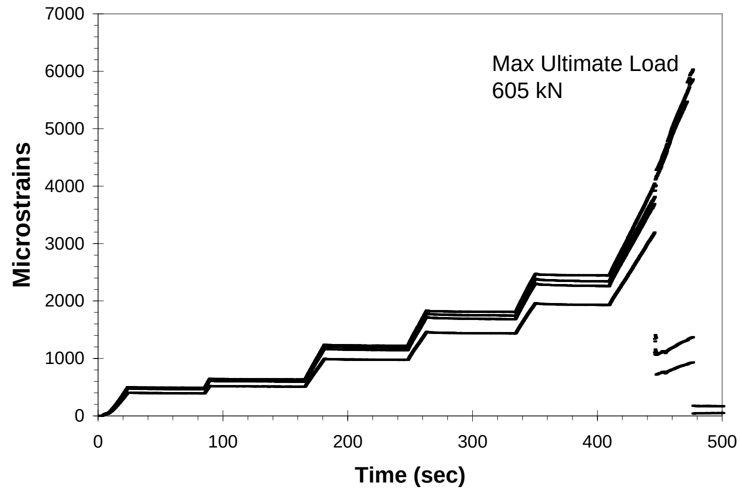

Figure 3.19 Strain Behavior for FS_P_G6.1

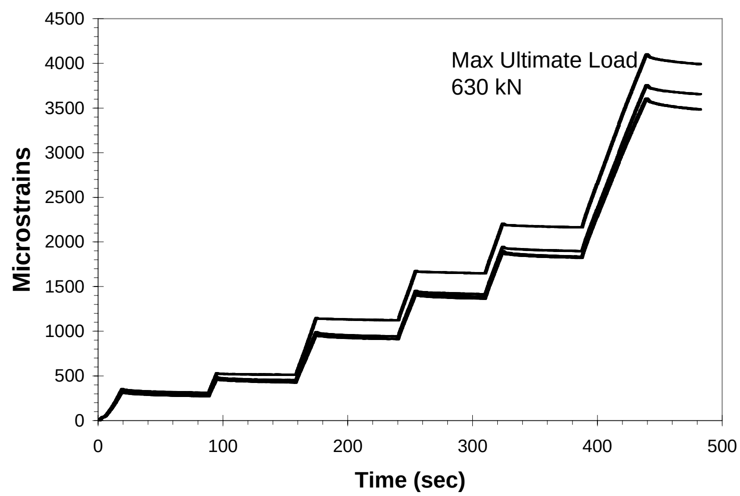

Figure 3.20 Strain Behavior for FS_P_G6.2

Load vs. strain plots for G7 full-scale bolt-laminated mats are presented in Figure 3.21 through Figure 3.28. Locations 1, 2, 4, 5, 6, 10, 11, and 12 all had sufficient repetition to be included in this section (refer to Figure 3.7(b)). Locations 3, 7, 8, and 9 were excluded due to insufficient repetition. The original experimental program used the data for different purposes than the purposes of this paper. Not all locations were instrumented on all platforms. This allowed a large number of locations to be tested on a relatively small number of platforms and measurement channels within the data acquisition system. A maximum ultimate load of 176.6 kN was observed for Mat 9. A minimum ultimate load of 97.7 kN was observed for Mat 6. Table 3.14 shows the regression coefficients from Equation 3.1 as well as the correlation coefficients. Values in bold denote envelope boundaries for a specific strain gage location. Measured raw and reduced data values for each plot are available in Table A.43 through Table A.52 in Appendix A.

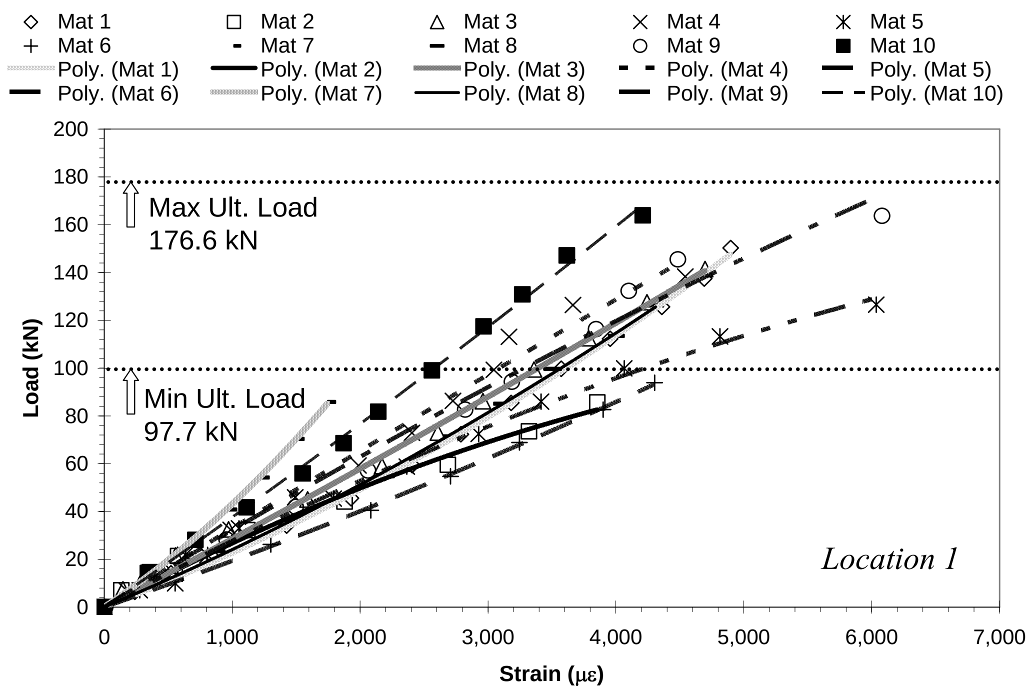

Figure 3.21 Load vs. Strain Plot for FS_SG_G7: Location 1

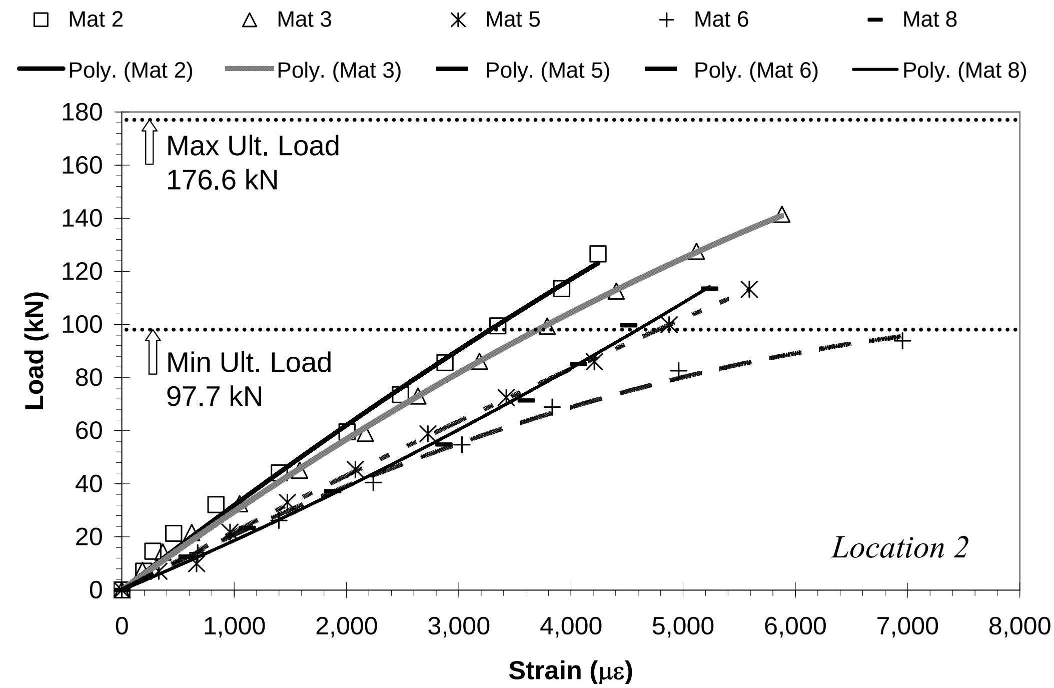

Figure 3.22 Load vs. Strain Plot for FS_SG_G7: Location 2

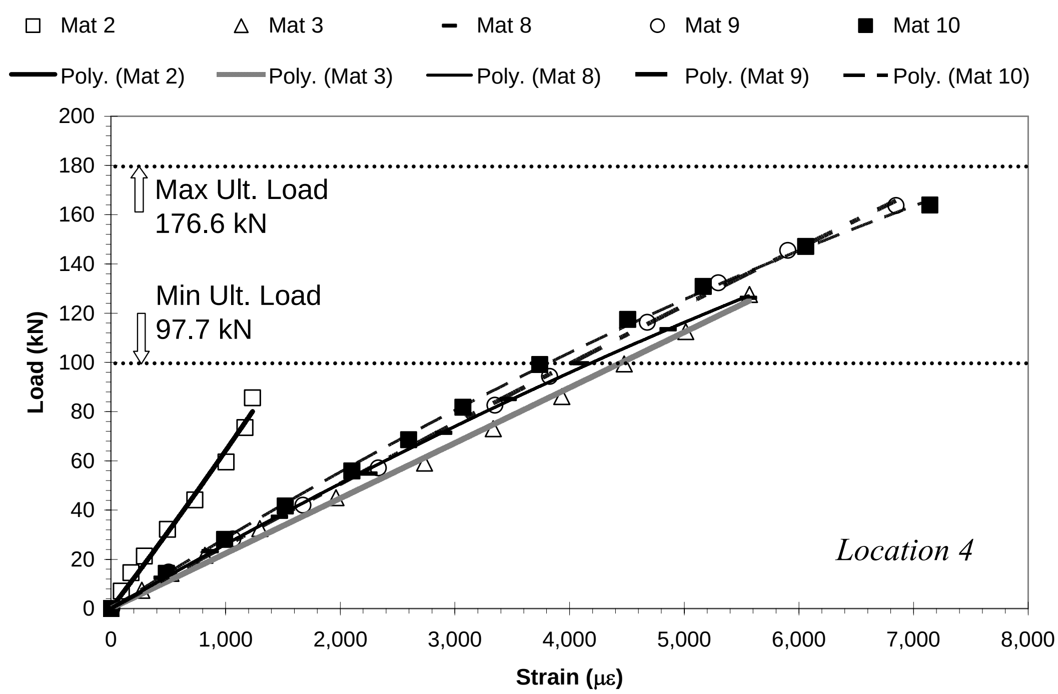

Figure 3.23 Load vs. Strain Plot for FS_SG_G7: Location 4

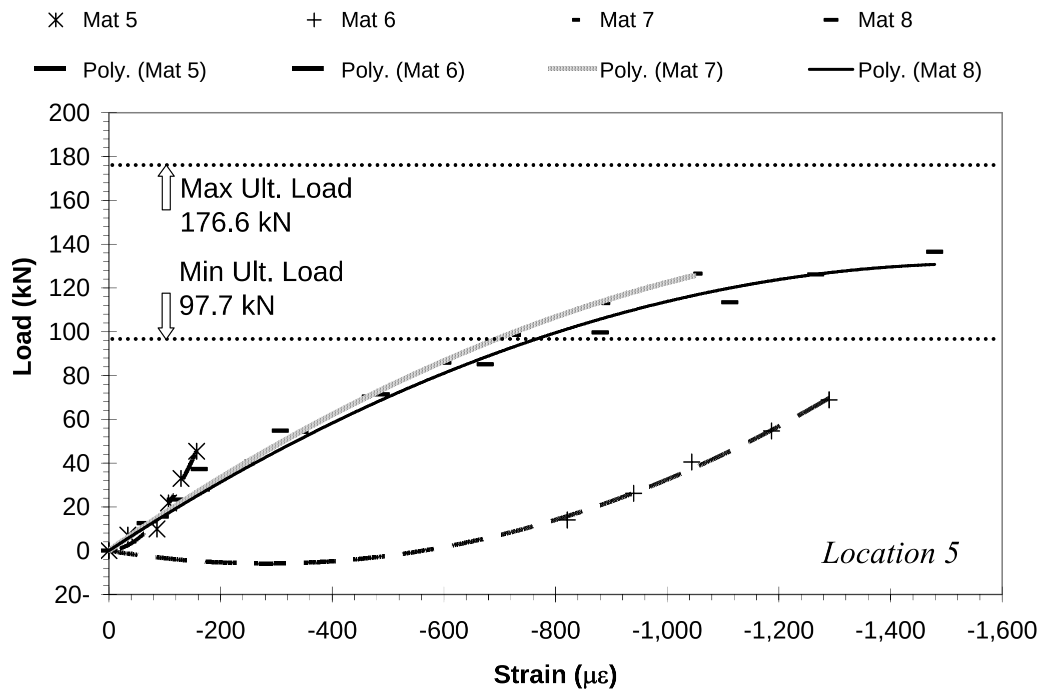

Figure 3.24   Load vs. Strain Plot for FS_SG_G7: Location 5

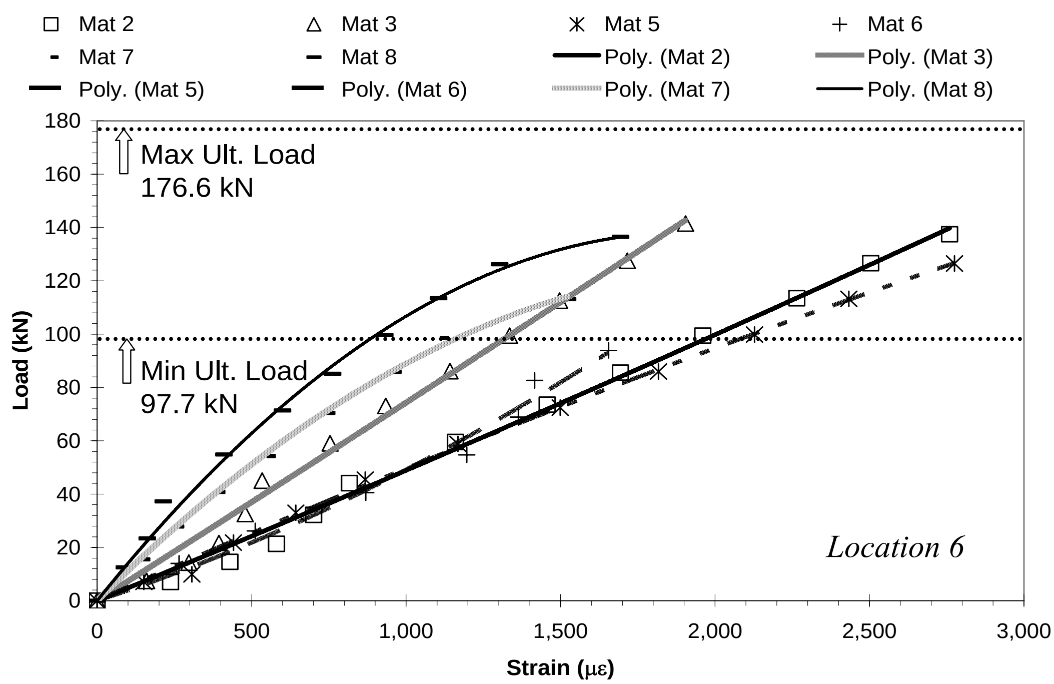

Figure 3.25   Load vs. Strain Plot for FS_SG_G7: Location 6

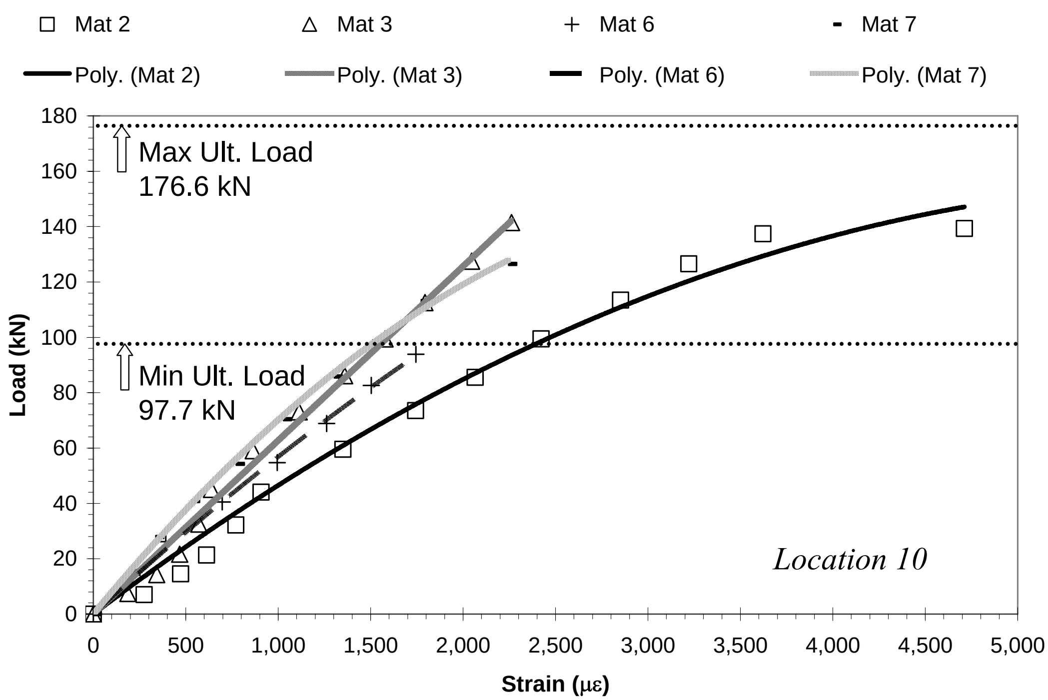

Figure 3.26 Load vs. Strain Plot for FS_SG_G7: Location 10

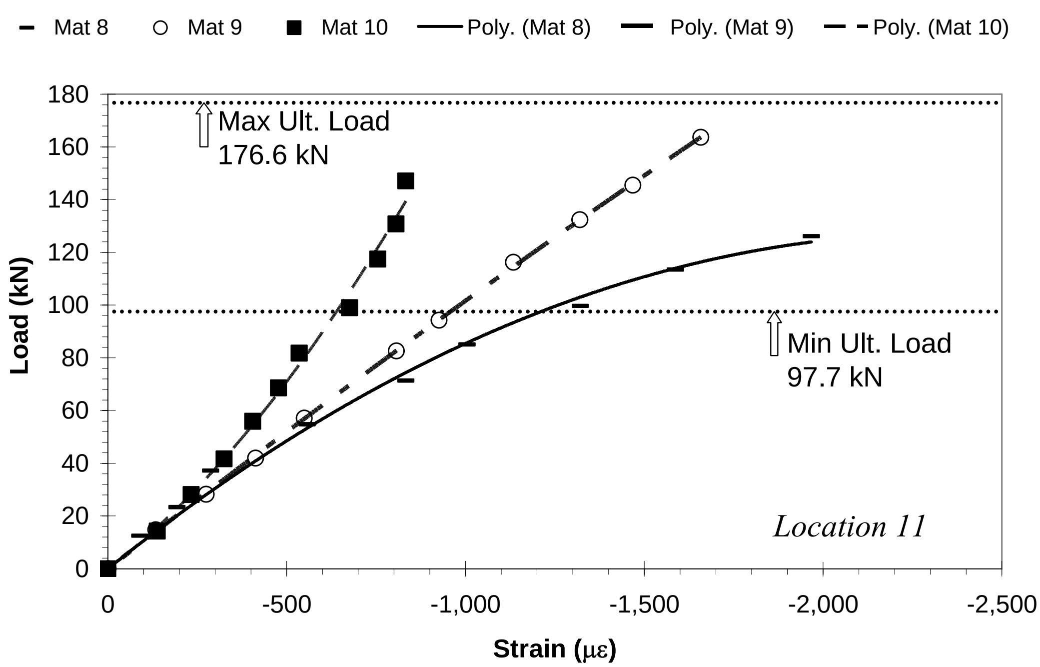

Figure 3.27 Load vs. Strain Plot for FS_SG_G7: Location 11

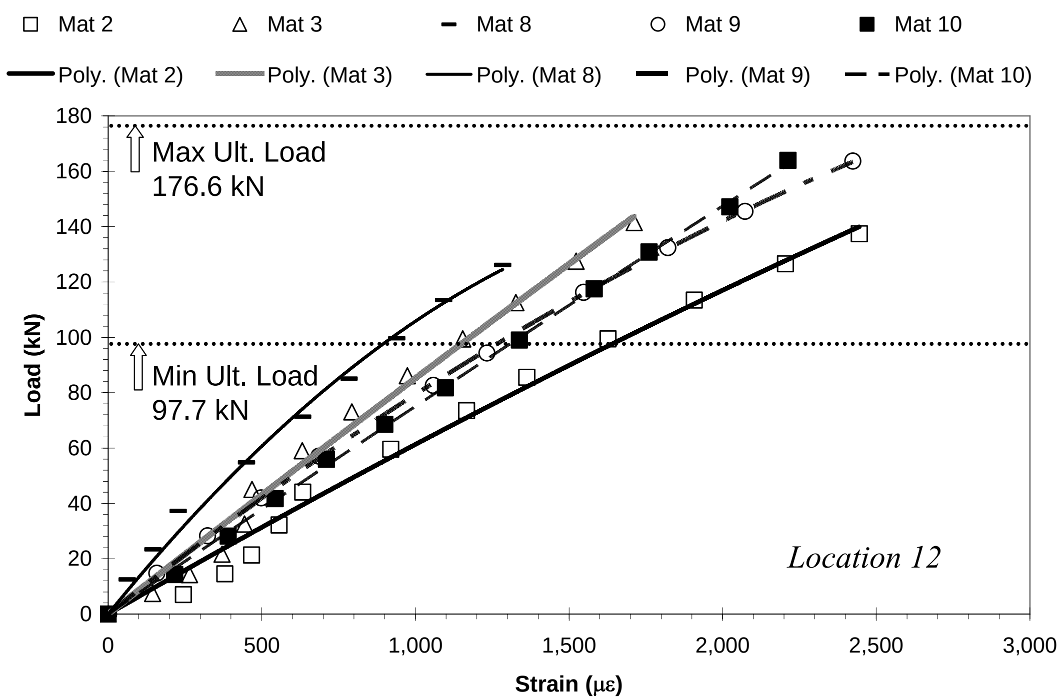

Figure 3.28 Load vs. Strain Plot for FS_SG_G7: Location 12

Table 3.14 Regression Summary for FS_SG_G7

Figure	Platform	a_0	b_0	r^2
3.21	1	1.92E-06	2.07E-02	0.999
	2	-1.85E-06	2.86E-02	0.986
	3	3.91E-07	2.82E-02	0.995
	4	-2.47E-07	3.31E-02	0.988
	5	-1.23E-06	2.89E-02	0.996
	6	**7.10E-07**	**1.86E-02**	**0.999**
	7	**7.65E-06**	**3.54E-02**	**0.999**
	8	1.54E-06	2.25E-02	0.999
	9	-7.41E-07	3.29E-02	0.987
	10	7.58E-07	3.68E-02	0.980
3.22	2	**-8.85E-07**	**3.28E-02**	**0.994**
	3	-1.13E-06	3.07E-02	0.999
	5	-3.68E-07	2.23E-02	0.998
	6	**-1.17E-06**	**2.19E-02**	**0.996**
	8	7.56E-07	1.79E-02	0.997
3.23	2	**3.03E-06**	**6.11E-02**	**0.987**
	3	**1.89E-08**	**2.24E-02**	**0.997**
	8	-7.10E-07	2.68E-02	0.999
	9	-2.28E-07	2.58E-02	0.999
	10	-8.71E-07	2.95E-02	0.999
3.24	5	**1.76E-03**	**-1.43E-02**	**0.971**
	6	**7.43E-05**	**4.18E-02**	**0.996**
	7	-5.46E-05	-1.77E-01	0.999
	8	-5.31E-05	-1.67E-01	0.984
3.25	2	9.87E-07	4.79E-02	0.994
	3	6.97E-07	7.36E-02	0.993
	5	**-2.20E-06**	**5.17E-02**	**0.998**
	6	1.10E-05	3.81E-02	0.984
	7	-2.67E-05	1.16E-01	0.999
	8	**-3.77E-05**	**1.44E-01**	**0.996**
3.26	2	**-4.12E-06**	**5.07E-02**	**0.988**
	3	9.55E-08	6.26E-02	0.993
	6	-4.49E-06	6.13E-02	0.998
	7	**-1.06E-05**	**8.07E-02**	**0.998**
3.27	8	**-2.32E-05**	**-1.09E-01**	**0.994**
	9	-4.45E-06	-1.06E-01	0.999
	10	**7.62E-05**	**-1.04E-01**	**0.994**
3.28	2	**-2.81E-06**	**6.41E-02**	**0.989**
	3	-1.79E-06	8.70E-02	0.988
	8	**-3.11E-05**	**1.37E-01**	**0.993**
	9	-8.38E-06	8.77E-02	0.999
	10	-1.31E-06	7.63E-02	0.999

3.4 Extracted Deflection Data

This section presents the load-deflection data for all the platforms within each category. The platforms are wood-adhesive composites; therefore, a composite modulus of elasticity, E_C, was determined from the load-deflection data and used for the prediction of deflections and beam-on-elastic-foundation analysis in Chapter 4. This is different from the modulus of elasticity for a given wood type; it takes into account the properties of other materials used in the assembly of the platforms (i.e. glue, bolts, etc.). All plots show the minimum and maximum ultimate deflections for platforms with the same geometric configuration and wood type. Linear regressions were used to determine the slope of each load-deflection relationship for each platform. Equation 3-2 is a modified form of general deflection equations and is used to determine E_C. The geometric constant, C, depends on the load configuration as discussed later in this section.

$$E_C = \left(\frac{P}{\Delta}\right) \cdot C \tag{3-2}$$

Where: E_C = composite modulus of elasticity. (GPa)

$\frac{P}{\Delta}$ = slope of measured load-deflection data. (kN/mm)

C = geometric constant. (mm^{-1})

3.4.1 Deflection Data for Prototype Scale Platforms

Load-deflection data was used to determine E_C. Figure 3.29 shows how E_C was calculated for each platform using PS_P_G1 data as an example. First, deflection was limited to 75% of the minimum ultimate deflection of the platform category to ensure that the calculated E_C was based on the linear-elastic behavior of the platforms. All data that fell above this line was eliminated from the calculation of E_C (see Figure 3.30 showing

PS_P_G1 with the aforementioned data removed). Second, prototype platforms were tested in three-point bending. Equation 3-3 shows the general form of this load configuration's deflection equation. From this equation, one can see that the geometric constant, C, for this load configuration is $\frac{L^3}{48I}$ when solved for E_C in the form of Equation 3-2. For prototype scale platforms G1 through G5, all values for clear span length, L, and moment of inertia (at the center of the platform), I, are kept constant for all platforms. For the dimensions of the prototype platforms tested, C is equal to 4.15. P/Δ for Mat 1 was equal to 0.821, which resulted in an E_C of (0.821)*4.15, or 3.41 GPa.

The final step to calculate E_C for use in deflection prediction (to be discussed in Chapter 4) was to determine a representative E_C. If the removal of a single value of E_C resulted in more than a 5% change in the average E_C, then that single value was not used in the calculation of the average value of E_C. With Figure 3.29 data as an example, Mat 1 was excluded from E_C calculation since it resulted in a 7.5% change in average modulus and the average value of E_C used for PS_P_G1 was 5.23 GPa after exclusion of Mat 1. The 7.5% difference was found by determining the average with and without the mat under investigation. For example, Mat 1 was ((5.23 GPa - 4.86 GPa) / 4.86 GPa) * 100, or 7.5%.

$$\Delta = \frac{PL^3}{48E_C I} \tag{3-3}$$

Where: Δ = deflection. (mm)
E_C = composite modulus of elasticity. (GPa)
P = load. (kN)
L = clear span length. (mm)
I = moment of inertia. (mm^4)

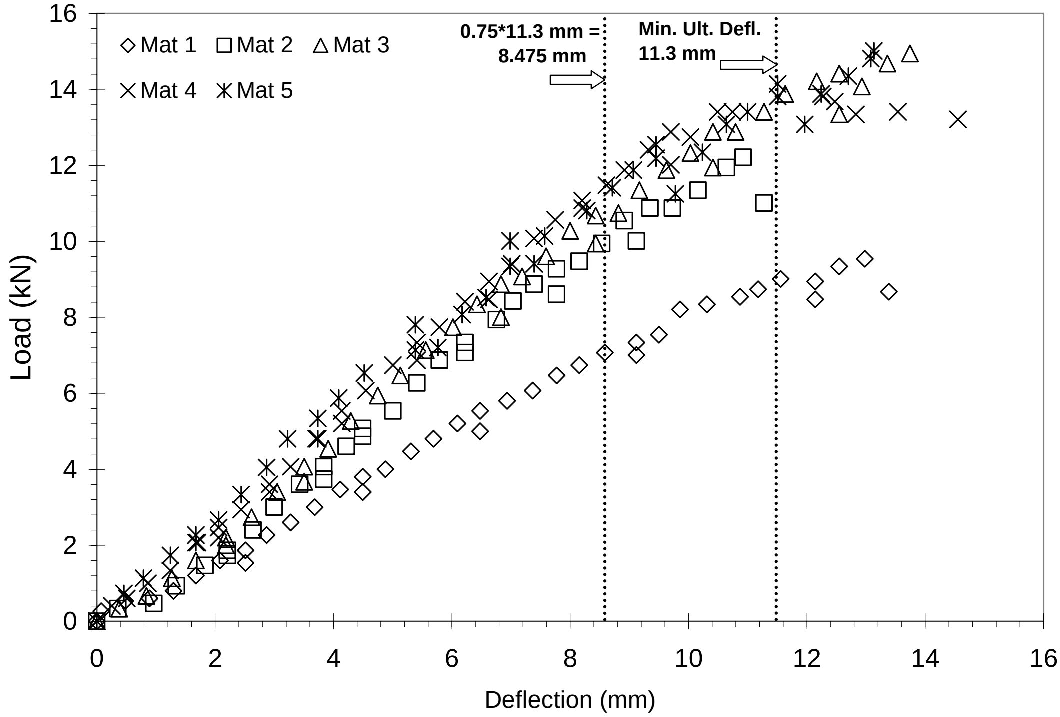

Figure 3.29 Procedure for Determining E_{CP} (PS_P_G1 shown)

Load-deflection plots for prototype scale platforms are presented in Figure 3.30 through Figure 3.39. Maximum and minimum ultimate deflections are presented for each platform category as well as values of E_C for each platform. The average of the platform category's E_C value is rounded to the nearest quarter gigapascal to become the prediction value, E_{CP}, for the platform category. Prediction values for E_{CP} and the platforms used to calculate these values can be seen in Table 3.15. Measured raw and reduced data values for each plot are available in Table A.53 through Table A.62 in Appendix A.

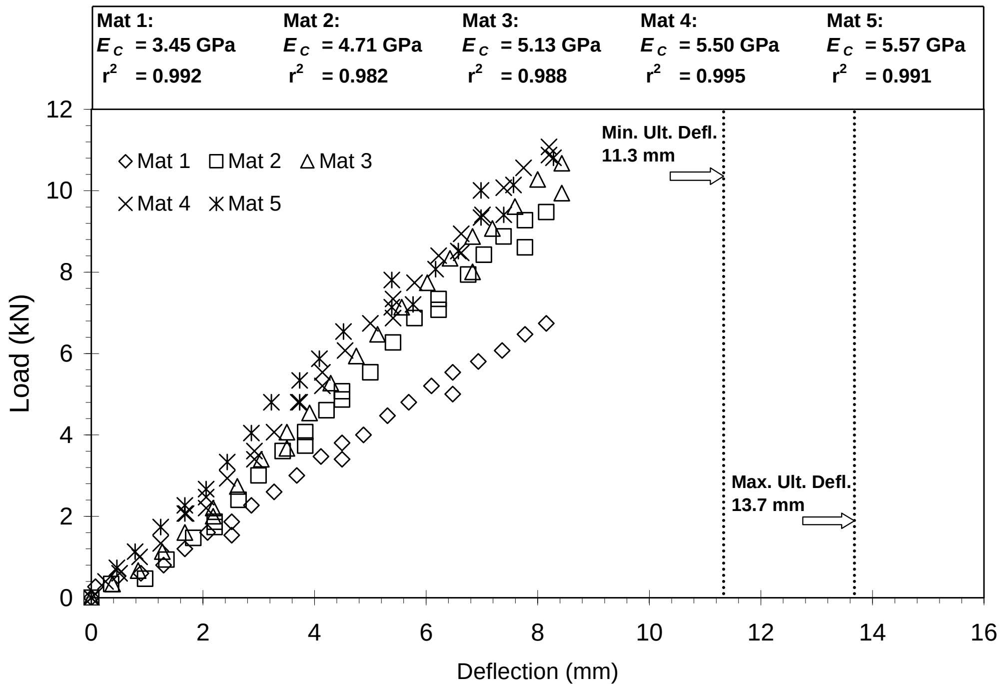

Figure 3.30 Load vs. Deflection Plot for PS_P_G1

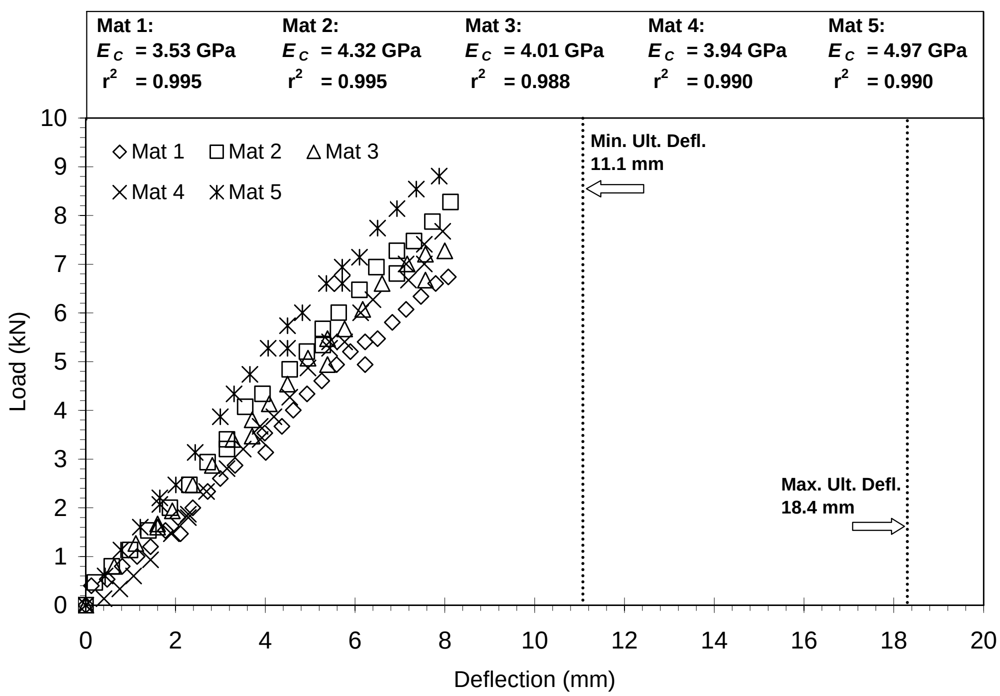

Figure 3.31 Load vs. Deflection Plot for PS_P_G2

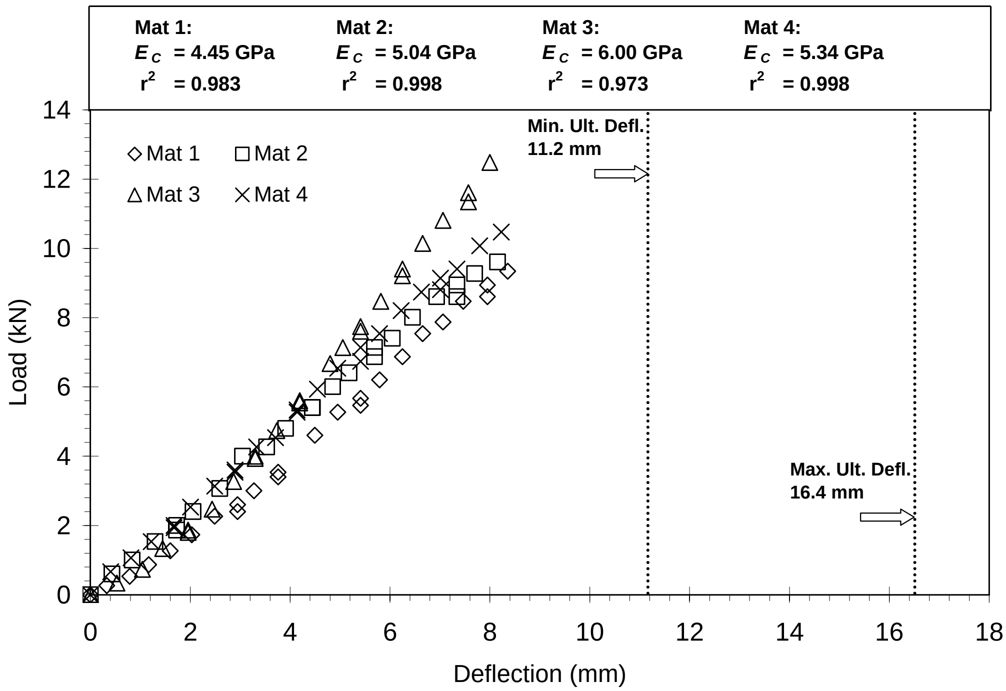

Figure 3.32 Load vs. Deflection Plot for PS_P_G3

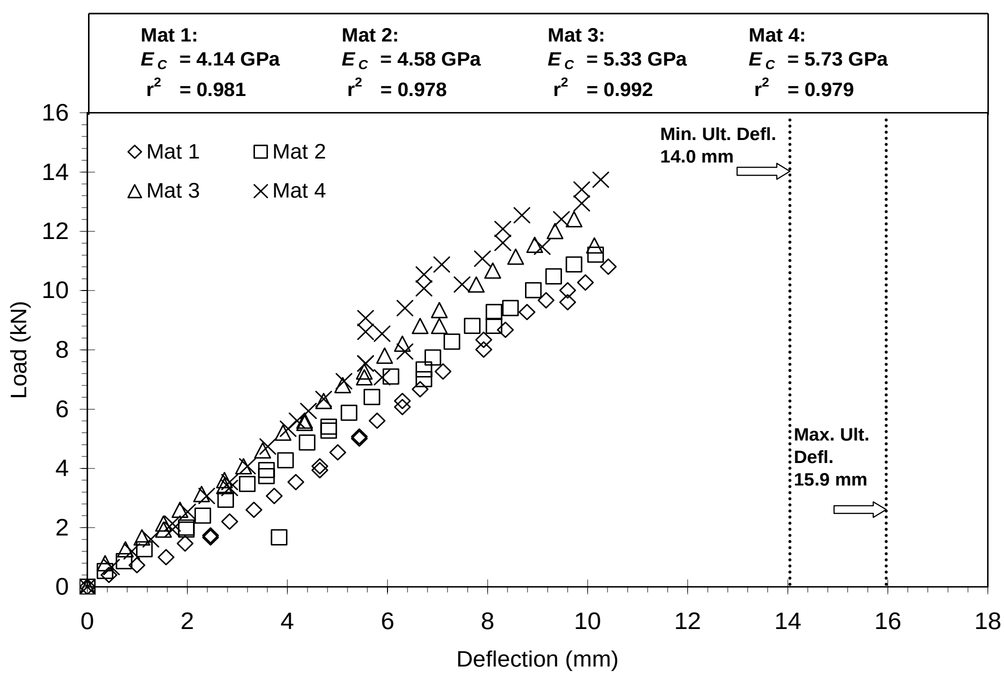

Figure 3.33 Load vs. Deflection Plot for PS_SG_G3

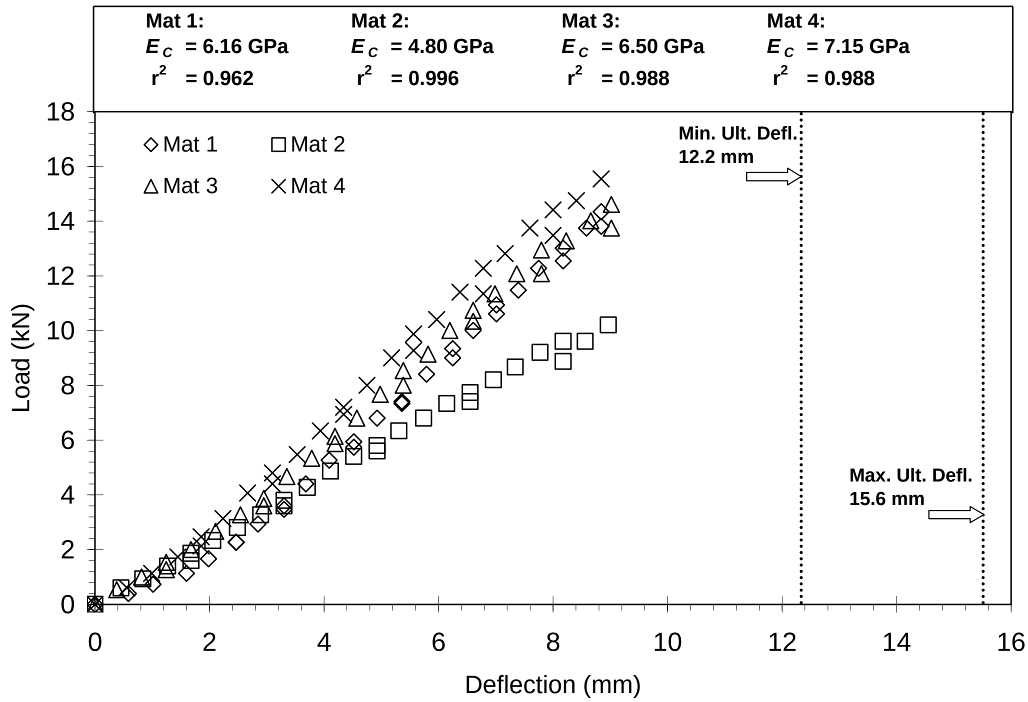

Figure 3.34 Load vs. Deflection Plot for PS_P_G4

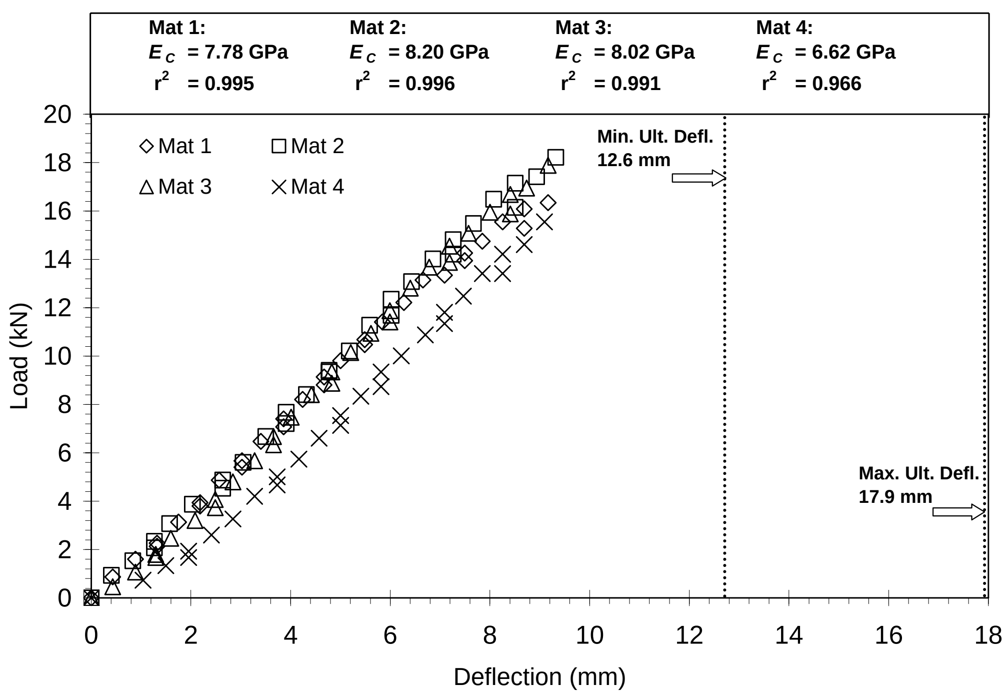

Figure 3.35 Load vs. Deflection Plot for PS_SG_G

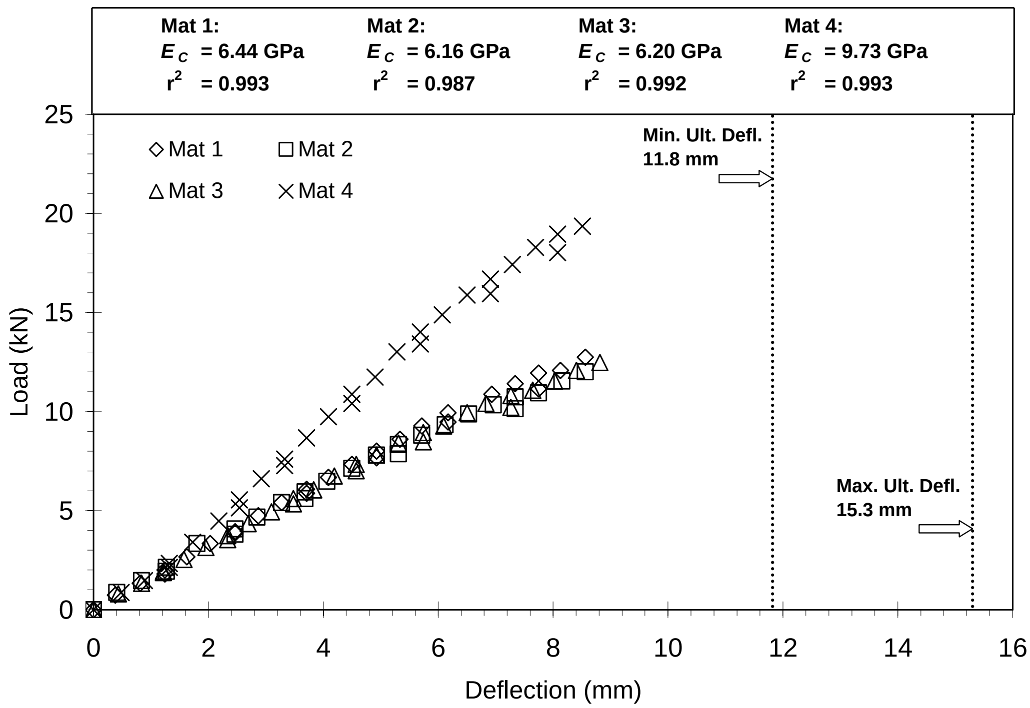

Figure 3.36 Load vs. Deflection Plot for PS_P_G5

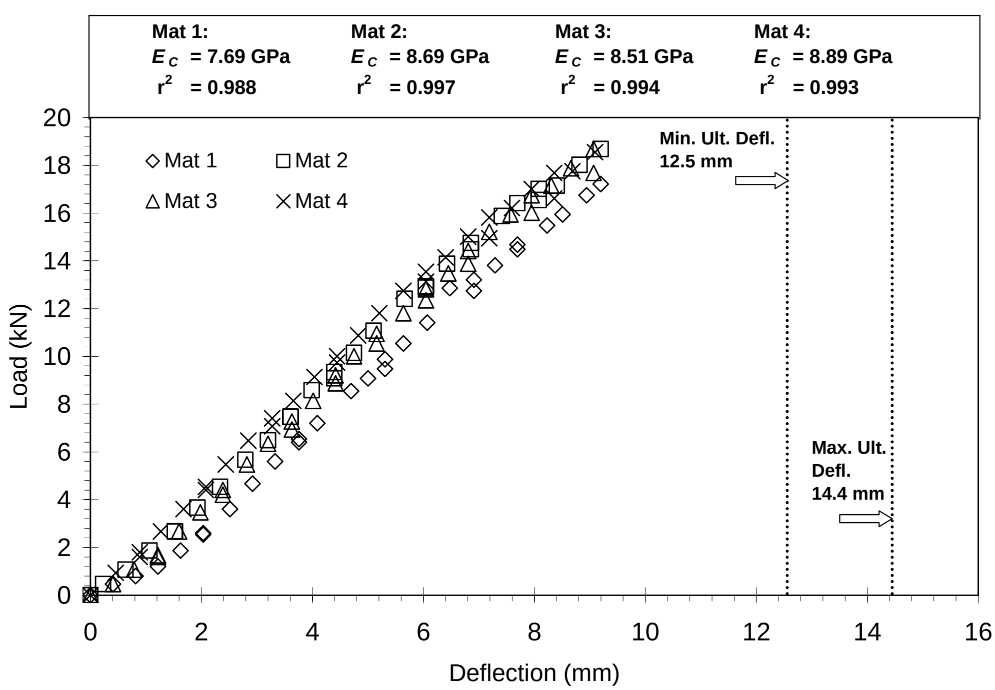

Figure 3.37 Load vs. Deflection Plot for PS_SG_G5

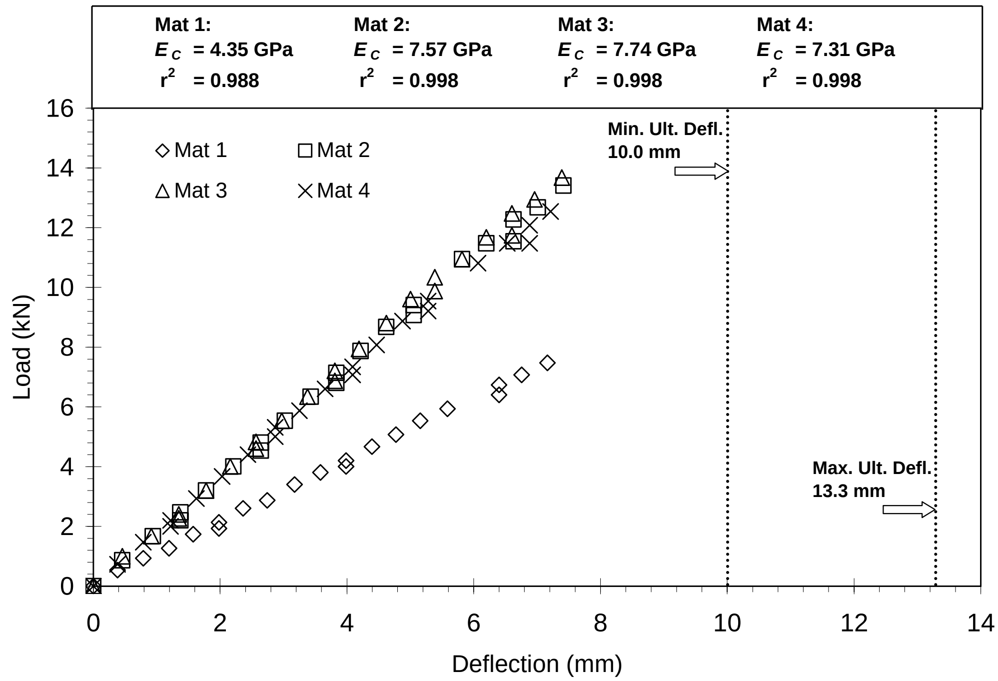

Figure 3.38 Load vs. Deflection Plot for PS_A_G5

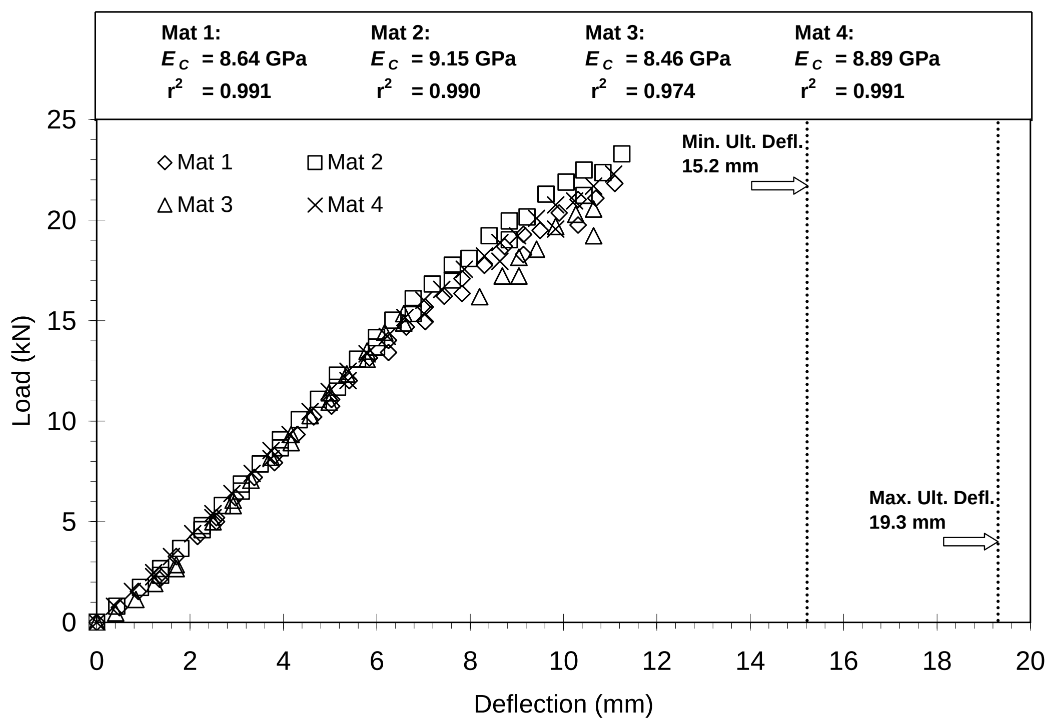

Figure 3.39 Load vs. Deflection Plot for PS_H_G5

Table 3.15 Summary of Deflection Prediction Value E_{CP}

Figure	Mats Used	Avg. E_C (GPa)	E_{CP} (GPa)
3.30	2, 3, 4, 5	5.23	5.25
3.31	1, 2, 3, 4, 5	4.15	4.25
3.32	1, 2, 4	4.94	5.00
3.33	2, 3	4.95	5.00
3.34	1, 3, 4	6.60	6.50
3.35	1, 2, 3, 4	7.66	7.75
3.36	1, 2, 3	6.27	6.25
3.37	1, 2, 3, 4	8.45	8.50
3.38	2, 3, 4	7.54	7.50
3.39	1, 2, 3, 4	8.79	8.75

3.4.2 Deflection Data for Full-Scale Platforms

For G6 full-scale platforms, load-deflection plots are not shown. G6 was only used to verify the scaling procedure to be discussed in Chapter 4 and to show the repeatability of the strain measurement at the center of the platform. Load-deflection data is available in the research by Howard and Stroble (2008).

Deflections were taken at mid-width of the center billet for G7 platforms. A similar analysis was performed for these platforms using Equation 3-2 as for the prototype scale platforms in order to determine E_C; however, a few differences existed. First, deflection data was not recorded to failure. When testing full-scale platforms, recording deflections at failure was not practical due to research team safety using dial gages. Therefore, all load-deflection data was in the linear elastic region; no data had to be eliminated based on the minimum ultimate deflection criteria as in the prototype scale platforms.

Second, the geometric constant, C, was different than that of the prototype scale platforms based on dimensions and load configuration. Full-scale platforms were tested in four-point bending rather than three-point bending. Equation 3-4 shows the general form of this load configuration's deflection equation. From this equation, one can see that the geometric constant for this load configuration is $\frac{(L'-s')(3L'^2-(s'-L')^2)}{96I'}$. For G7 full-scale bolt-laminated platforms, all values for clear span length, L', and moment of inertia (for the single center billet only), I', are the same for all platforms. For the dimensions of full-scale bolt-laminated platforms tested, C is equal to 6.95. Also, no platform's data was eliminated from prediction value, E_{CP}, because this value remained relatively constant even with the removal of extreme slope values. This was due to an increase in the number of platforms tested.

$$\Delta = \frac{P(L'-s')}{96EI'}(3L'^2-(s'-L')^2) \qquad (3\text{-}4)$$

Where: Δ = deflection. (mm)
E = modulus of elasticity. (GPa)
P = load. (kN)
L' = clear span length. (mm)
s' = distance between load heads. (mm)
I' = moment of inertia. (mm^4)

Load-deflection plots for full-scale bolt-laminated platforms are presented in Figure 3.40. Values of E_C and correlation coefficients, r^2, are presented for each platform in Table 3.16. Prediction value, E_{CP}, for G7 platforms is 16.25 GPa. Measured raw and reduced data values for Figure 3.40 are available in Table A.63 in Appendix A. Note these platforms were three billets connected together with metal rods. The E_{CP} value in this load configuration is much higher than the prototype platforms since only the middle billet was loaded and the rods allowed significant composite effects to be realized (Shmulsky et al. 2008). The moment of inertia, I, was taken for one billet, instead of three, since only one billet was loaded. An equivalent approach would be to multiply I by 3 and subsequently divide E_{CP} by 3, which would align the value with the range of prototype E_{CP} values.

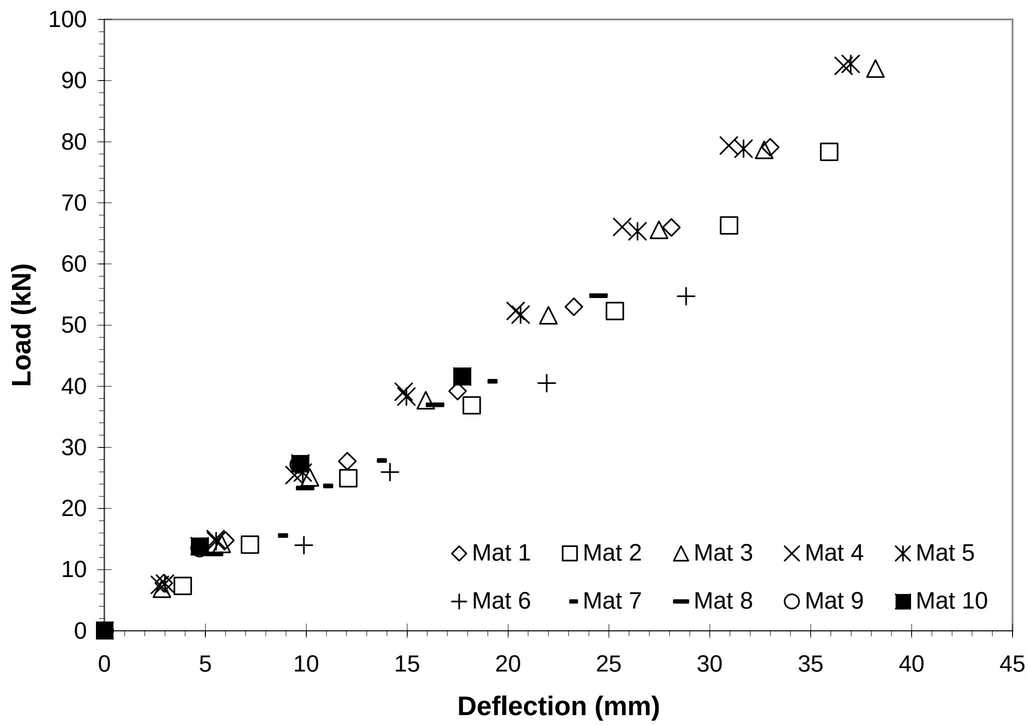

Figure 3.40 Load vs. Deflection Plot for FS_SG_G7

Table 3.16 Summary of Deflection Prediction Values for FS_SG_G7

Platform	E_C (GPa)	r^2
1	16.25	0.998
2	14.73	0.998
3	16.67	0.999
4	17.78	0.999
5	17.37	0.999
6	12.86	0.989
7	14.52	0.991
8	15.69	0.999
9	19.65	0.999
10	17.22	0.978

CHAPTER 4

ANALYSIS AND DESIGN OF WOOD CONSTRUCTION PLATFORMS ON SOIL

4.1 Introduction and Purpose

The purpose of this thesis was to develop a design method for wood construction platforms on ground that utilizes instrumented strain data, load data, and deflection data. A method with these features was not identified in research literature or practice. This chapter uses the data (in an elevated condition) from Chapter 3 to develop a design method for a single full-scale freestanding wood construction platform in uniform bearing subjected to two equal, symmetric loads as illustrated in Figure 4.1. As shown in the literature review in Chapter 2, only one design guide was found for wood construction platforms. The aim of this chapter is to provide a new method for wood construction platform design that is based on test data. This method is not a comprehensive design method, but rather one significant component for the development of future design methods. Creep behaviors, property degradation, and multiple load configurations are needed for a comprehensive design approach.

The methods provided in this chapter are meant to implement the raw extracted data from the previous chapter into a useful design method. Four processes are presented in the flowchart shown in Figure 4.2 and are denoted numerically. The four processes are: 1) Material Assumptions, 2) Scaling of Data, 3) Normalized Load-Strain Curve

(NLSC), and 4) Beam-on-Elastic-Foundation Analysis. Each process includes basic assumptions that require the use of various mechanics theories and the flowchart described in the remainder of this chapter. The processes applied to each platform category depend on the experimental data available. As an example, G7 does not require any load or deflection data to be scaled up because the platforms were tested at full-scale. It should be noted that not all geometries will be used for this design method. G6 is only used to verify a portion of the scaling procedure.

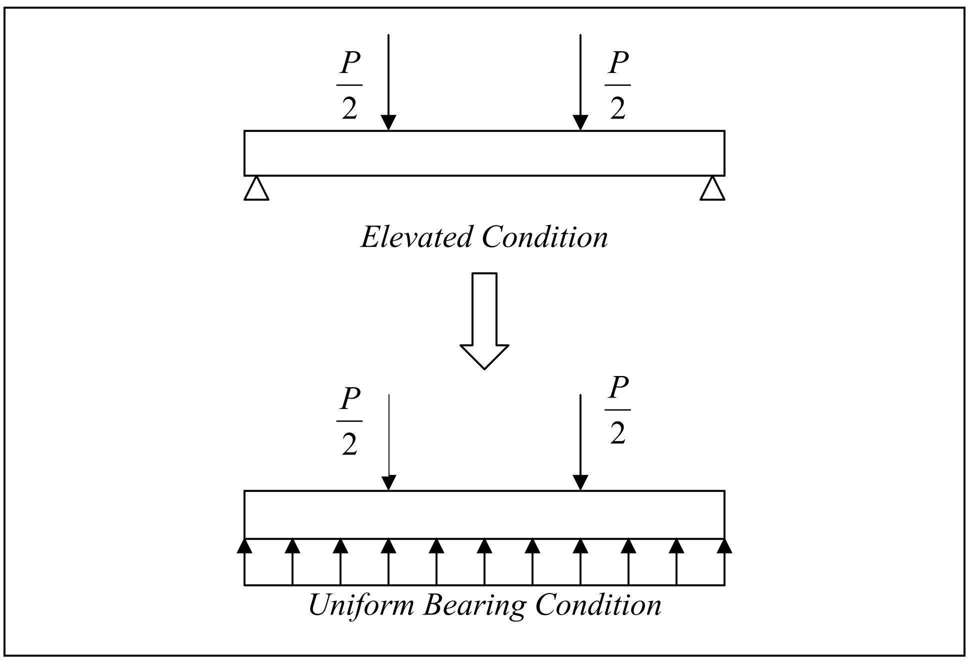

Figure 4.1 Illustration of Design Method's Purpose

The next four sections discuss the processes of this design method, followed by a section that presents the design method results for the adhesive-bonded platforms G1 through G5 and for the bolt-laminated platforms G7.

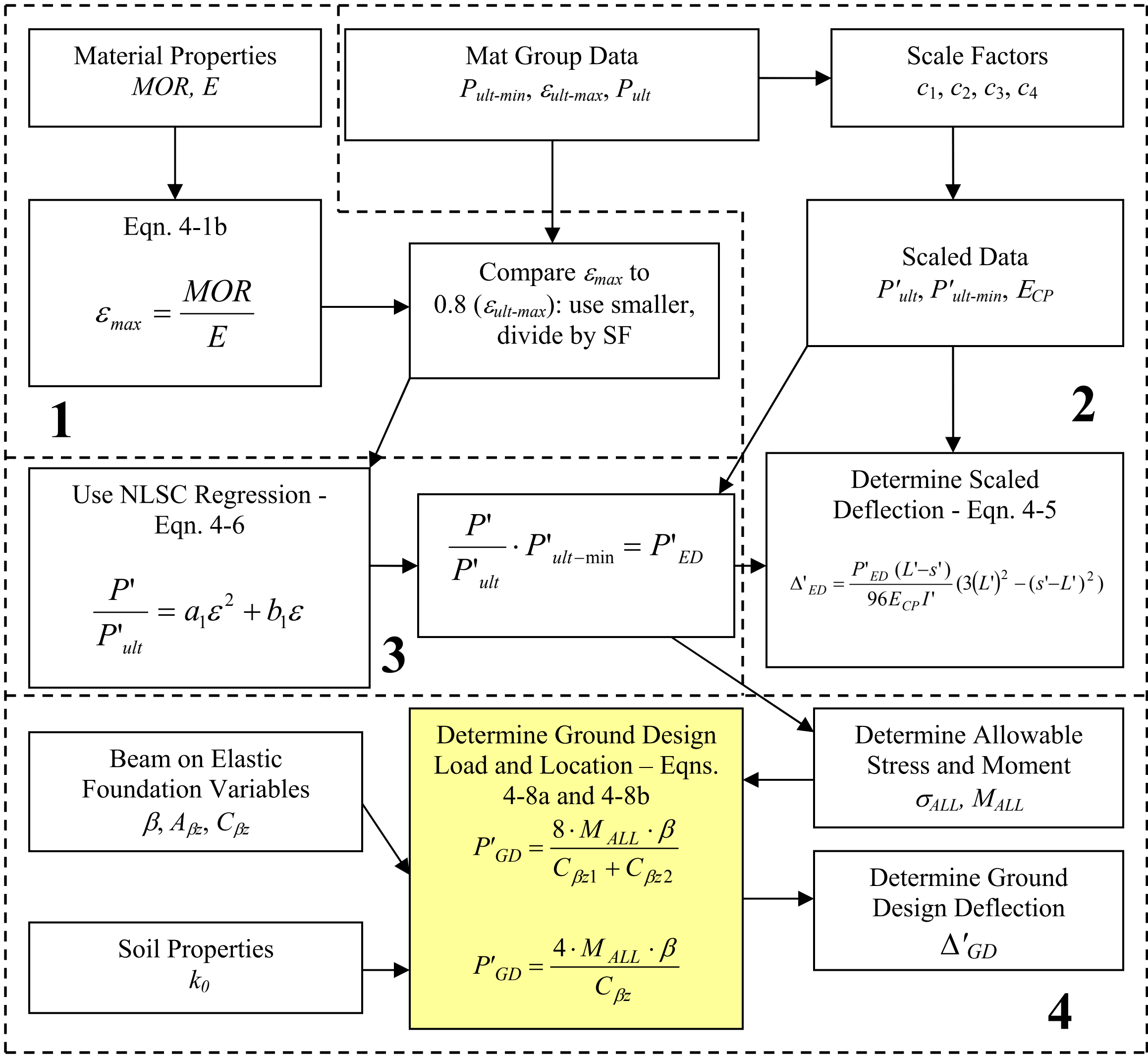

Figure 4.2 Flowchart of Proposed Design Method

4.2 Material Assumptions

This section discusses the first component of the proposed design method. Assumptions about the behavior of the material must be made in order for this design method to be valid. This is denoted in section 1 of Figure 4.2. The first part of this component is to choose a material. In doing this, the designer chooses accepted material properties. Two mechanical properties are relevant to this analysis: Modulus of Rupture

(MOR) and Modulus of Elasticity (MOE). MOR is a strength parameter that represents the maximum bending stress that a given material can withstand. MOE (also denoted by *E*) is a parameter that represents the elastic relationship between stress and strain of the material. In this case, the material is wood. Note the difference in the modulus of wood and the composite modulus of a wood construction platform as seen in Chapter 3. Table 4.1 shows the values for MOR and MOE for the wood types used for the platforms tested.

Table 4.1 Mechanical Properties for Wood Types Used (*Wood Handbook* 1999)

Wood Types	MOR (MPa)	MOE (GPa)	ε_{max}
Ash	103.0	12.0	8,583
Sweet Gum	86.0	11.3	7,611
Hickory	94.0	11.9	7,899
Pine[1]	97.5	13.0	7,500

[1]*Average value of various species of Pine*

The first material assumption is that the material, independent of dimensions and load configuration, fails at the same stress and strain. This allows for the load scaling procedure that will be discussed in the next section as well as the translation from elevated design load to ground design load that will be discussed in following sections represented by E_C.

The second assumption is that the platforms are a homogenous composite material. This allows for the use of Hooke's Law and the Euler-Bernoulli beam equation. These two theories of mechanics are essential to identifying relationships involving stress used herein.

The third assumption of this design method is that failure of the platforms is due to failure of the wood, not of any other material (i.e. glue, bolts, etc.). This assumption is a result of the examination of the failed platforms. Most all failures were due to splitting in the tension face of the platform; members did not appear to delaminate between glued or bolted members. Using this assumption, an allowable maximum strain, ε_{max}, is calculated for the wood platforms and is taken to be the strain at failure. Equation 4-1a shows Hooke's Law which is the basic constitutive relationship between stress, σ, and strain, ε. In order to determine the maximum allowable strain, this equation is adjusted to the form of Equation 4-1b with σ being replaced by MOR. Values for ε_{max} for each wood type can be seen in Table 4.1. Once ε_{max} is determined, it is compared to a percentage (to be determined by the verification using G6 and discussed later in this chapter) of the maximum ultimate strain for the platform category, $\varepsilon_{ult\text{-}max}$. The location and the value of the maximum ultimate strain is determined based on engineering judgment and will be discussed in later sections.

Some measured strains were larger than ε_{max} because the design values for MOR and MOE are determined statistically from many tests. However, wood is highly variable, so it is not unrealistic to measure strains greater than ε_{max} based on typical values. To be conservative, the smaller of these two values is used as the representative failure strain. The representative strain can then be divided by a factor of safety as chosen by the designer.

$$\sigma = E\varepsilon \tag{4-1a}$$

$$\varepsilon_{max} = \frac{MOR}{E} \tag{4-1b}$$

Where: σ = stress. (kPa)
E = modulus of elasticity (MOE). (GPa)
ε = strain. ($\mu\varepsilon$)
ε_{max} = allowable maximum strain. ($\mu\varepsilon$)
MOR = modulus of rupture. (kPa)

4.3 Scaling of Data

Most of the platforms tested were prototype scale with a three-point bending load configuration. In order to make this data useful, it was scaled to represent a full-scale platform in four-point bending. This process is denoted in section 2 of Figure 4.2. The following sections use the assumptions presented in the previous section and basic theories of mechanics to scale up loads and then calculate deflections. There was no need to scale strain because of the first assumption in Section 4.2

4.3.1 Procedure for Scaling Load Data

This section outlines the procedure for scaling of load data. Figure 4.3 shows the two load configurations and the dimensions for the two types of platforms. Figure 4.3(a) shows the prototype scale platform in three-point bending (representative of geometries G1 through G5). Figure 4.3(b) shows the full-scale platform concentrically loaded in four-point bending as well as the scaling factors for each dimension (representative of geometry G6 and G7). It should be noted that length is representative of clear spans between supports. Using the first assumption from Section 4.2 and the scaling factors, the prototype loads can be scaled to full-scale loads. To verify this procedure, the scaled data from geometry PS_P_G5 can be compared to data available for FS_P_G6.

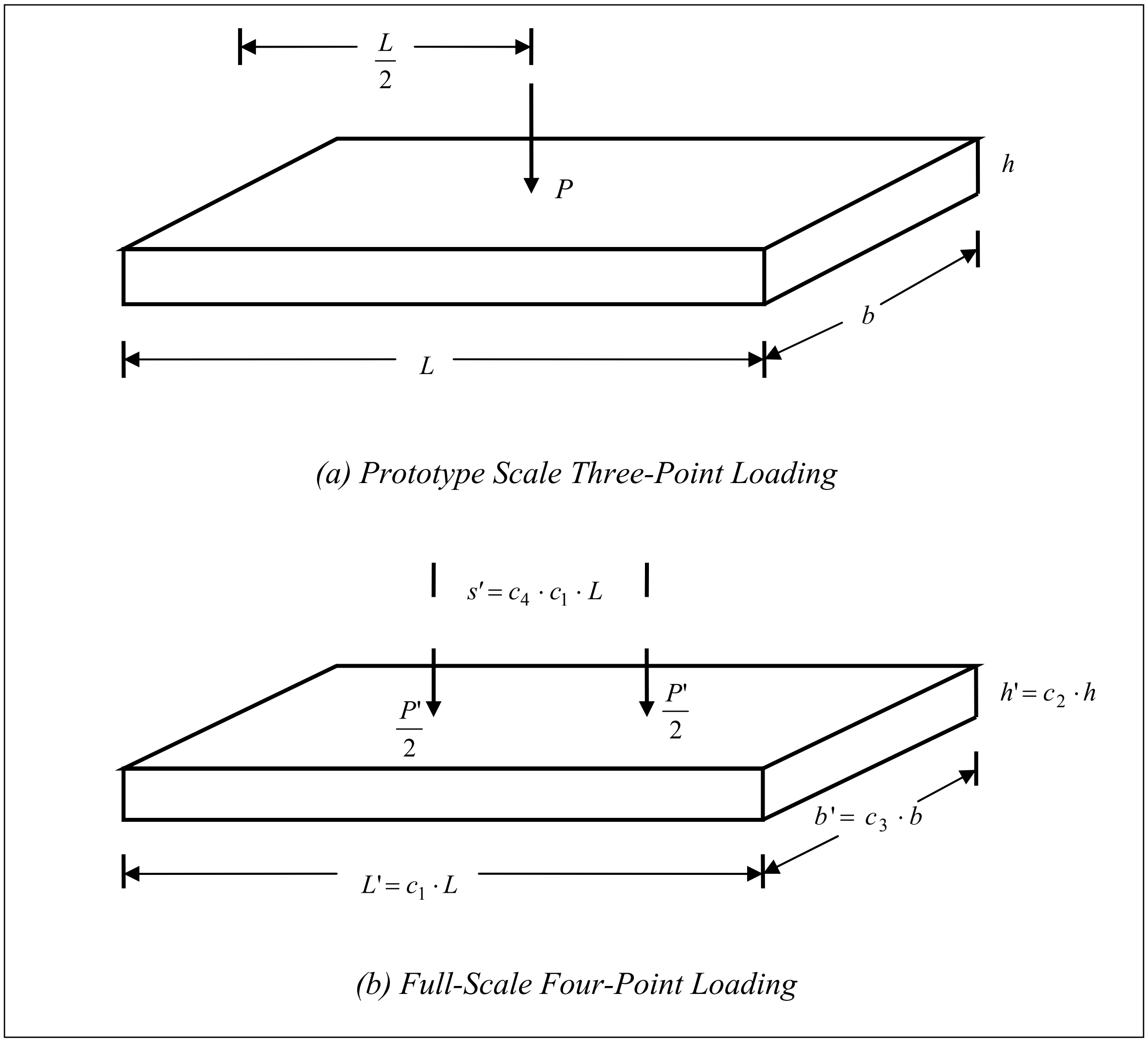

Figure 4.3 Schematic Drawings of Platforms Showing Load Configurations

Note: Dimensions for length represent clear spans, not true dimensions as seen in Chapter 3

The first step of this process was to determine the controlling mechanical design values for each platform category. These measured mechanical design values include: 1) the maximum ultimate strain, $\varepsilon_{ult\text{-}max}$, for the platform category; 2) the ultimate load, P_{ult}, which corresponds to $\varepsilon_{ult\text{-}max}$; and 3) the minimum ultimate load for the platform category, $P_{\text{ult-min}}$. Values were chosen based primarily on conservatism and engineering judgment.

Values that did not seem to be representative of the platform category's mechanical behaviors were not used. As an example, in Figure 3.9(a), "Mat 1" would not be used for $\varepsilon_{ult\text{-}max}$, because this value is nearly double the next highest value.

The second step of this process was to determine the scale factors for each dimension. Each scale factor correlates to a dimension; for example, scale factor c_1 is the length scale factor. In practice, the designer can choose the value for each scale factor to accommodate the desired platform size.

The third step was to use the scale factors to adjust the load. Equation 4-2 shows the Euler-Beroulli beam equation for bending stress, σ_b. It is a function of bending moment, M, moment of inertia, I, and distance from extreme fiber to the centroid, c. These three values depend on the dimensions and the load configuration. Table 4.2 shows the values of M, I, and c symbolically for each scale and load configuration. Using the first assumption in Section 4.2, one can equate the bending stress of the prototype scale platform in three-point bending (σ_b) to the bending stress of the full-scale platform in four-point bending (σ_b') and determine the ratio of full-scale load to prototype load. Equation 4-3a through Equation 4-3c show how this ratio is resolved in terms of the scale factors.

$$\sigma_b = \frac{Mc}{I} \tag{4-2}$$

Where: σ_b = bending stress. (MPa)
M = bending moment. (N-mm)
c = distance from extreme fiber to centroid. (mm)
I = moment of inertia. (mm^4)

Table 4.2 Summary of Values for Equation 4.2

Load Configuration	Prototype Scale in Three-Point Bending	Full-Scale in Four-Point Bending
M	$\frac{PL}{4}$	$\frac{P'}{2}\cdot\left(\frac{c_1\cdot L}{2}-\frac{c_4\cdot c_1\cdot L}{2}\right)$
c	$\frac{h}{2}$	$\frac{c_2\cdot h}{2}$
I	$\frac{bh^3}{12}$	$\frac{(c_3\cdot b)\cdot(c_2\cdot h)^3}{12}$

$$\sigma_b = \sigma_b' \tag{4-3a}$$

$$\frac{3PL}{2bh^2} = \frac{3P'\cdot(c_2\cdot h)\cdot\left(\frac{c_1\cdot L}{2}-\frac{c_4\cdot c_1\cdot L}{2}\right)}{(c_3\cdot b)\cdot(c_2\cdot h)^3} \tag{4-3b}$$

$$\frac{P'}{P} = \frac{-c_2^{\;2}\cdot c_3}{c_1\cdot(c_4-1)} \tag{4-3c}$$

Where: σ_b = bending stress. (MPa)
σ_b' = scaled bending stress. (MPa)
P = load. (N)
P' = scaled load. (N)
L = clear span length. (mm)
c_1 = length scale factor.
b = base width. (mm)
c_2 = base width scale factor.
h = height. (mm)
c_3 = height scale factor.
c_4 = space scale factor.

To verify this procedure, values for scale factors were determined by comparing the dimensions of two geometric configurations that were similar: G5 (381 mm by 203.2 mm by 25.4 mm) and G6 (2261 mm by 1219.2 mm by 139.7 mm). Equation 4-4a through Equation 4-4d show how the scale factors were determined for each dimension. Scale factors for length, width, and height were determined by taking the ratio of the full-scale dimension to the prototype dimension. The scale factor for the space between load heads, *s'*, was determined by taking the ratio of the length of the space to the length of the full-scale platform.

$$c_1 = \frac{L'}{L} = \frac{2261}{381} = 5.93 \tag{4-4a}$$

$$c_2 = \frac{h'}{h} = \frac{139.7}{25.4} = 5.5 \tag{4-4b}$$

$$c_3 = \frac{b'}{b} = \frac{1219.2}{203.2} = 6 \tag{4-4c}$$

$$c_4 = \frac{s'}{L'} = \frac{s'}{c_1 \cdot L} = \frac{596.9}{2261} = 0.264 \tag{4-4d}$$

These values are then substituted into Equation 4-3c to determine the theoretical ratio of *P'* to *P*. The theoretical ratio is approximately 42. This is compared to the ratio of the average value of the load data for FS_P_G6 (618 kN) to the average value of the load data for PS_P_G5 (17.47 kN). This ratio is 35.37, which differs from the predicted value by less than 20%. This is an acceptable difference considering the variability of wood. This difference is incorporated back into the design method by only allowing 80% of the maximum ultimate strain to be used (previously discussed in Section 4.2) to further ensure scaling prototype to full-scale data produces conservative and technically sound designs.

4.3.2 Procedure for Calculating Theoretical Full-Scale Deflections

The fourth and final step of the scaling process was to calculate deflections. Deflections were calculated using Equation 4-5, which is a modified form of the four-point bending deflection equation (see Equation 3-4). This equation uses the scaled load from the previous section and the prediction value E_{CP} from Chapter 3 to calculate theoretical deflections.

$$\Delta' = \frac{P'(L'-s')}{96E_{CP}I'}(3(L')^2-(s'-L')^2) \qquad (4\text{-}5)$$

Where: Δ' = full-scale calculated theoretical deflection. (mm)
P' = full-scale load. (kN)
L' = full-scale clear span length. (mm)
s' = space between load heads. (mm)
E_{CP} = composite MOE prediction value. (GPa)
I' = full-scale moment of inertia. (mm^4)

4.4 Normalized Load-Strain Curve

Once all data has been scaled, it can be used to determine a design load for the full-scale platforms in a simply supported (elevated) boundary condition. This is performed by determining the load that correlates to the failure strain. The next section outlines the process of developing this curve. This process is denoted in section 3 of Figure 4.2.

The Normalized Load-Strain Curve (NLSC) uses the platform that most accurately represents the maximum ultimate strain for the platform category as discussed in Section 4.3.1 to determine a full-scale elevated design load, P'_{ED}. Figure 4.4 shows a typical NLSC for a platform made from pine. On the y-axis, loads are normalized by taking the ratio of an arbitrary load to the ultimate load for that platform. On the x-axis, strain corresponding to each normalized load is presented. Using the scaled test data, a second order polynomial equation is derived in the form of Equation 4.6 (similar to Equation 3.1). Once the coefficients of Equation 4-6 are determined for each platform category, the designer can use the representative strain for the wood type and $P_{\text{ult-min}}$ for the platform category to determine P'_{ED} as shown in Figure 4.4. Once P'_{ED} is determined, it can be substituted into Equation 4-5 to calculate the theoretical full-scale elevated design deflection, Δ'_{ED}.

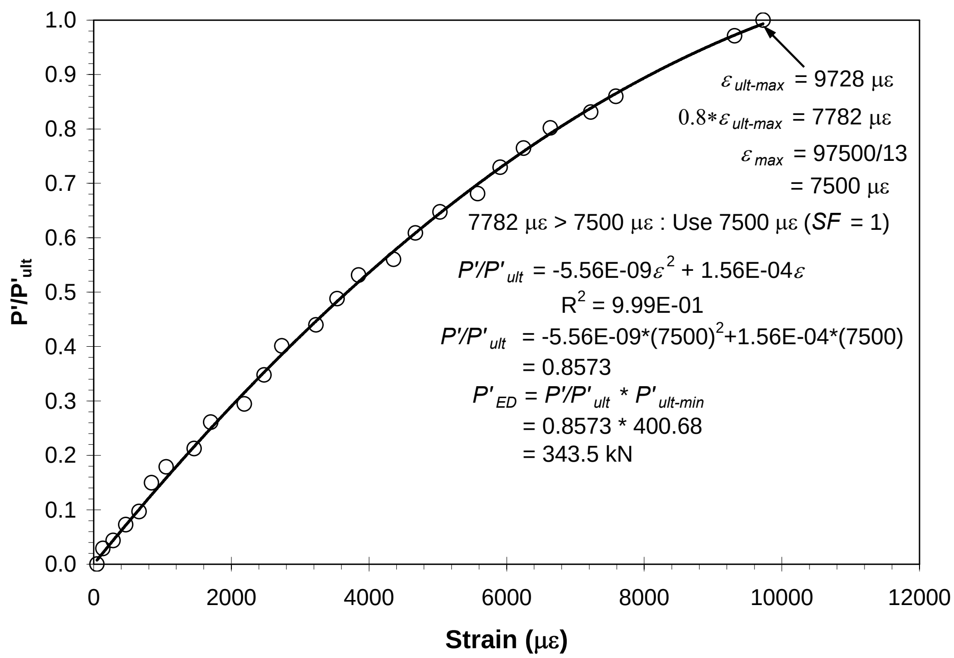

Figure 4.4 Typical Normalized Load-Strain Curve

$$\frac{P'}{P'_{ult}} = a_1\varepsilon^2 + b_1\varepsilon \qquad (4\text{-}6)$$

Where: P' = scaled load. (kN)

P'_{ult} = scaled ultimate load. (kN)

a_1 = first quadratic coefficient for NLSC.

b_1 = second quadratic coefficient for NLSC.

4.5 Beam-on-Elastic-Foundation Analysis

Up to this point, loads and deflections have been representative of a simply supported (elevated) boundary condition. While literature has shown that timber construction platforms have been used for small crossings, the purpose of this design method is to use the elevated design load and design deflection to determine the design load and design deflection of the platform as it sits on the ground in a uniform bearing boundary condition. This is accomplished by implementing beam-on-elastic-foundation analysis. This process is denoted in section 4 of Figure 4.2.

A beam-on-elastic-foundation analysis describes how a beam interacts with a medium, such as soil, in an elastic manner. The soil has an elastic spring constant called the modulus of subgrade reaction, k_0. This value depends on the type of soil. Table 4.3 shows the range of values for various types of soil.

Table 4.3 Values for k_0 for Various Sands and Clays (Boresi and Schmidt 2003)

Soil Type	Range of k_0 (N/mm^3)
Loose Sand	0.005 - 0.016
Medium Sand	0.010 - 0.080
Dense Sand	0.063 - 0.126
Clayey Sand	0.031 - 0.080
Silty Sand	0.024 - 0.048
Clay, q_u<0.2 N/mm^2	0.012 - 0.024
Clay, 0.2 N/mm^2< q_u<0.4 N/mm^2	0.024 - 0.048
Clay, q_u>0.4 N/mm^2	> 0.048

There are multiple beam-on-elastic-foundation analyses that could be used for this design method. However, for simplicity, this design method assumes that the platform is infinitely long, meaning that the concentrated loads are well within the edge boundaries of the platform. Also, this means that no moment or deflection occurs at the edges of the beam. It is also assumed that loads are symmetrically arranged about the center of the platform, meaning that the principle of superposition is applicable. Figure 4.5 shows an infinite beam-on-elastic-foundation. Equation 4-7a through Equation 4-7f show the relationship between load, moment, and deflection for these assumptions and the load configuration seen in Figure 4.5.

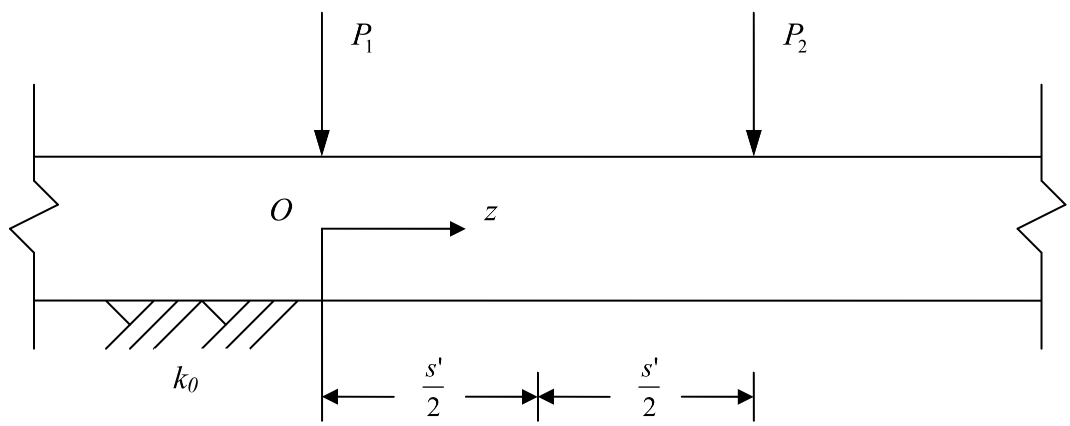

Figure 4.5 Infinite Beam-on-Elastic-Foundation

$$M = \frac{1}{4\beta}\left[P_1 C_{\beta z 1} + P_2 C_{\beta z 2}\right] \tag{4-7a}$$

$$\Delta = \frac{\beta}{2k}\left[P_1 A_{\beta z 1} + P_2 A_{\beta z 2}\right] \tag{4-7b}$$

$$k = b \cdot k_0 \tag{4-7c}$$

$$\beta = \sqrt[4]{\frac{k}{4EI}} \tag{4-7d}$$

$$C_{\beta z} = e^{-\beta z}\left(cos\,\beta z - sin\,\beta z\right) \quad (4\text{-}7e)$$

$$A_{\beta z} = e^{-\beta z}\left(\sin\beta z + \cos\beta z\right) \quad (4\text{-}7f)$$

Where: M = bending moment. (N-mm)
Δ = deflection. (mm)
k_0 = modulus of subgrade reaction. (N/mm^3)
b = beam width. (mm)
P_1, P_2 = load. (N)
E = modulus of elasticity for the beam. (MPa)
I = moment of inertia. (mm^4)
z = distance along the z-axis. (mm)

Using these equations, the designer can translate elevated design load to ground design load. The first step of this process is to determine the allowable bending stress and moment for the beam using P'_{ED}, the Euler-Bernoulli beam equation (Equation 4-2), and the four-point bending moment equation (see Table 4.2). This is validated by the first material assumption, which states that stress in a platform is constant and independent of load configuration and scale. Because the platform has the same dimensions, it will also have the same bending moment.

The second step of this process is to concurrently determine the location of the critical allowable bending moment and the full-scale ground design load, P'_{GD}. The allowable moment can be located either under one of the two loads ($z_1 = 0$ and $z_2 = s'$) or at the center of the platform ($z_1 = z_2 = z = s'/2$). Equation 4-8a and Equation 4-8b show modified forms of Equation 4-7a; one showing the allowable moment under the load and one showing the allowable moment at the center of the platform, respectively. These equations are possible by rearranging Equation 4-7a and equating P_1 and P_2 to one-half of P'_{GD}. The location that gives the most conservative (i.e. the smallest) value for P'_{GD} is used.

$$P'_{GD} = \frac{8 \cdot M \cdot \beta}{C_{\beta z1} + C_{\beta z2}} \tag{4-8a}$$

$$P'_{GD} = \frac{4 \cdot M \cdot \beta}{C_{\beta z}} \tag{4-8b}$$

Where: P'_{GD} = full-scale ground design load. (kN)
M = bending moment. (N-mm)
β = soil-platform interaction constant. (mm^{-1})
$C_{\beta z}$ = moment periodical relationship function.

The final step of this process is to determine the ground design deflection, Δ'_{GD}, that correlates to P'_{GD}. This is done by using Equation 4-9, which is a modified form of Equation 4-7b. For conservatism, this deflection is assumed to occur at the center of the platform. Δ'_{GD} is presented for insight purposes only. Δ'_{GD} is only a local deflection (i.e. no displacement) with respect to the edge of the beam; settlement of the beam (global displacement and deflection) does not occur. This is reasonable considering that the beam is infinite and that this analysis is based on solid mechanics. Figure 4.6 shows a schematic drawing of a platform on the ground.

$$\Delta'_{GD} = \frac{\beta \cdot P'_{GD}}{2 \cdot k} A_{\beta z} \tag{4-9}$$

Where: P'_{GD} = full-scale ground design load. (kN)
k = modulus of subgrade reaction. (N/mm^2)
Δ'_{GD} = full-scale ground design deflection. (mm)
β = soil-platform interaction constant. (mm^{-1})
$A_{\beta z}$ = deflection periodical relationship function.

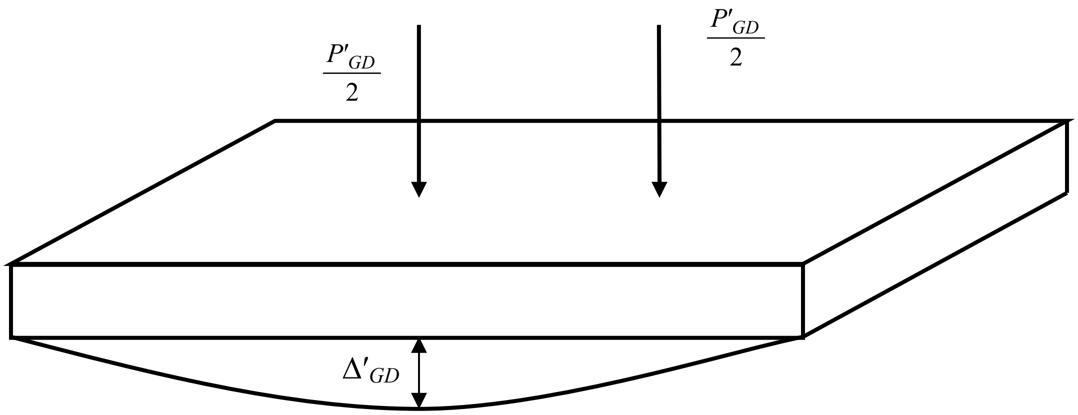

Figure 4.6 Beam-on-Elastic-Foundation Load Configuration

4.6 Design Results

In the previous sections of this chapter, a design method that uses basic material properties, fundamental theories of mechanics, test data, and a beam-on-elastic-foundation analysis has been presented to determine design loads and deflections for wood construction platforms. This section presents the results of this design method for platform geometries G1 through G5 and G7. Results were calculated using Excel spreadsheets in order to automate the process.

Table 4.4 shows the results for the first process in Figure 4.2, Material Assumptions. Data is presented for each platform category. Refer to Section 4.2 for methods and equations necessary to develop this set of data.

Table 4.4 Summary of Material Assumptions

Platform Category	Wood Type	*MOR* (kPa)	*MOE* (GPa)	ε_{max} (με)	$\varepsilon_{ult-max}$ (με)	0.8*$\varepsilon_{ult-max}$ (με)	Design Strain (με)
PS_P_G1	Pine	97,500	13.0	7,500	9,728	7,782	7,500
PS_P_G2	Pine	97,500	13.0	7,500	10,375	8,300	7,500
PS_P_G3	Pine	97,500	13.0	7,500	6,374	5,099	5,099
PS_SG_G3	Sweet Gum	86,000	11.3	7,611	7,205	5,764	5,764
PS_P_G4	Pine	97,500	13.0	7,500	6,732	5,386	5,386
PS_SG_G4	Sweet Gum	86,000	11.3	7,611	11,936	9,549	7,611
PS_P_G5	Pine	97,500	13.0	7,500	8,440	6,752	6,752
PS_SG_G5	Sweet Gum	86,000	11.3	7,611	13,174	10,539	7,611
PS_A_G5	Ash	103,000	12.0	8,583	10,344	8,275	8,275
PS_H_G5	Hickory	94,000	11.9	7,899	15,885	12,708	7,899
FS_SG_G7	Sweet Gum	86,000	11.3	7,611	6,081	4,865	4,865

Table 4.5 shows the results for the second process in Figure 4.2, Scaling of Data. Data is presented for each platform category. Refer to Section 4.3 for methods and equations necessary to develop this data. Scale factors were kept consistent with those chosen for the verification process. Values for E_{CP} were taken from Chapter 3.

Table 4.5 Summary of Scaling of Data

Platform Category	c_1	c_2	c_3	c_4	E_{CP} (MPa)	$P_{ult-min}$ (kN)	$P'_{ult-min}$ (kN)
PS_P_G1	5.93	5.50	6.00	0.264	5,250	9.54	400.68
PS_P_G2	5.93	5.50	6.00	0.264	4,250	9.34	392.28
PS_P_G3	5.93	5.50	6.00	0.264	5,000	12.14	509.88
PS_SG_G3	5.93	5.50	6.00	0.264	5,000	12.68	532.56
PS_P_G4	5.93	5.50	6.00	0.264	6,500	14.01	588.42
PS_SG_G4	5.93	5.50	6.00	0.264	7,750	20.19	847.98
PS_P_G5	5.93	5.50	6.00	0.264	6,250	13.88	582.96
PS_SG_G5	5.93	5.50	6.00	0.264	8,500	20.95	879.90
PS_A_G5	5.93	5.50	6.00	0.264	7,500	9.81	412.02
PS_H_G5	5.93	5.50	6.00	0.264	8,750	26.02	1,092.84
FS_SG_G7	1.00	1.00	1.00	1.00	16,250	---	97.70

Table 4.6 through Table 4.8 show the results for the third process in Figure 4.2, Normalized Load-Strain Curve. Data is presented for each platform category with each table representing a different factor of safety. Refer to Section 4.4 for methods and equations necessary to develop this data. The representative platform and gage location used for each category is presented as well as the coefficients for Equation 4.6 used to determine P'_{ED}.

Table 4.6 Summary of NLSC Data (SF of 1)

Platform Category	Platforms Used	Location Used	a_1	b_1	r^2	P'_{ED} (kN)	Δ'_{ED} (mm)
PS_P_G1	4	1	-5.56E-09	1.56E-04	0.999	343.48	51.34
PS_P_G2	4	2	-5.23E-09	1.47E-04	0.996	317.08	58.54
PS_P_G3	2	1	-5.98E-09	1.96E-04	0.996	430.31	67.53
PS_SG_G3	3	2	-5.45E-09	1.78E-04	0.998	449.97	70.62
PS_P_G4	3	1	-1.08E-08	2.28E-04	0.987	538.21	64.97
PS_SG_G4	1	1	-6.88E-09	1.66E-04	0.999	733.39	74.26
PS_P_G5	2	1	-5.08E-09	1.67E-04	0.999	522.33	65.58
PS_SG_G5	1	1	-5.74E-09	1.51E-04	0.999	718.64	66.34
PS_A_G5	1	1	-3.10E-09	1.28E-04	0.999	348.96	36.51
PS_H_G5	2	1	-3.96E-09	1.25E-04	0.999	809.03	72.55
FS_SG_G7	9	1	-1.34E-08	2.51E-04	0.993	88.31	37.74

Table 4.7 Summary of NLSC Data (SF of 2)

Platform Category	Platforms Used	Location Used	a_1	b_1	r^2	P'_{ED} (kN)	Δ'_{ED} (mm)
PS_P_G1	4	1	-5.56E-09	1.56E-04	0.999	203.07	30.35
PS_P_G2	4	2	-5.23E-09	1.47E-04	0.996	187.39	34.60
PS_P_G3	2	1	-5.98E-09	1.96E-04	0.996	234.98	36.88
PS_SG_G3	3	2	-5.45E-09	1.78E-04	0.998	249.09	39.09
PS_P_G4	3	1	-1.08E-08	2.28E-04	0.987	315.18	38.05
PS_SG_G4	1	1	-6.88E-09	1.66E-04	0.999	451.17	45.68
PS_P_G5	2	1	-5.08E-09	1.67E-04	0.999	294.92	37.03
PS_SG_G5	1	1	-5.74E-09	1.51E-04	0.999	432.46	39.92
PS_A_G5	1	1	-3.10E-09	1.28E-04	0.999	196.34	20.54
PS_H_G5	2	1	-3.96E-09	1.25E-04	0.999	472.02	42.33
FS_SG_G7	9	1	-1.34E-08	2.51E-04	0.993	51.90	22.18

Table 4.8 Summary of NLSC Data (SF of 3)

Platform Category	Platforms Used	Location Used	a_1	b_1	r^2	P'_{ED} (kN)	Δ'_{ED} (mm)
PS_P_G1	4	1	-5.56E-09	1.56E-04	0.999	142.34	21.28
PS_P_G2	4	2	-5.23E-09	1.47E-04	0.996	131.34	24.25
PS_P_G3	2	1	-5.98E-09	1.96E-04	0.996	161.06	25.28
PS_SG_G3	3	2	-5.45E-09	1.78E-04	0.998	171.42	26.90
PS_P_G4	3	1	-1.08E-08	2.28E-04	0.987	220.36	26.60
PS_SG_G4	1	1	-6.88E-09	1.66E-04	0.999	319.56	32.36
PS_P_G5	2	1	-5.08E-09	1.67E-04	0.999	204.11	25.63
PS_SG_G5	1	1	-5.74E-09	1.51E-04	0.999	304.56	28.12
PS_A_G5	1	1	-3.10E-09	1.28E-04	0.999	135.76	14.20
PS_H_G5	2	1	-3.96E-09	1.25E-04	0.999	329.68	29.57
FS_SG_G7	9	1	-1.34E-08	2.51E-04	0.993	36.32	15.52

Table 4.9 through Table 4.13 show the design constants, functions, and results for the fourth process in Figure 4.2, Beam-on-Elastic-Foundation Analysis. Constants, functions, and results are presented for each platform category. Refer to Section 4.5 for

methods and equations necessary to develop this data. For each platform category, three types of soils were used in this analysis to show the variation of the design constants. For k_0, average values were used for each soil type from Table 4.3. For comparison to the ***emtek*** design guide, a very soft clay was chosen as one of the soils (k_0 value taken from ***emtek***). Design results are presented for various factors of safety. Some values in the design results are in bold, which denotes instances when the ratio of P'_{GD} to P'_{ED} is less than one. This is practically impossible; the platform will not hold less on the ground than it did in the air. Therefore, if P'_{GD} is less than P'_{ED}, P'_{ED} will be used as the allowable design load. Also, in this case the calculated theoretical deflection will be calculated using P'_{ED}.

Table 4.9 Summary of Beam-on-Elastic-Foundation Design Constants

Soil Type	Platform Category	k_0 (N/mm^3)	k (N/mm^2)	β (mm^{-1})
Very Soft Clay	PS_P_G1	0.0003	0.33	4.88E-04
	PS_P_G2		0.33	5.15E-04
	PS_P_G3		0.33	4.94E-04
	PS_SG_G3		0.33	4.94E-04
	PS_P_G4		0.33	4.63E-04
	PS_SG_G4		0.33	4.43E-04
	PS_P_G5		0.33	4.67E-04
	PS_SG_G5		0.33	4.33E-04
	PS_A_G5		0.33	4.47E-04
	PS_H_G5		0.33	4.30E-04
	FS_SG_G7		0.08	5.16E-04
Medium Sand	PS_P_G1	0.0450	54.86	1.75E-03
	PS_P_G2		54.86	1.85E-03
	PS_P_G3		54.86	1.77E-03
	PS_SG_G3		54.86	1.77E-03
	PS_P_G4		54.86	1.66E-03
	PS_SG_G4		54.86	1.59E-03
	PS_P_G5		54.86	1.68E-03
	PS_SG_G5		54.86	1.55E-03
	PS_A_G5		54.86	1.60E-03
	PS_H_G5		54.86	1.54E-03
	FS_SG_G7		12.83	1.85E-03
Clayey Sand	PS_P_G1	0.0555	67.67	1.85E-03
	PS_P_G2		67.67	1.95E-03
	PS_P_G3		67.67	1.87E-03
	PS_SG_G3		67.67	1.87E-03
	PS_P_G4		67.67	1.75E-03
	PS_SG_G4		67.67	1.68E-03
	PS_P_G5		67.67	1.77E-03
	PS_SG_G5		67.67	1.64E-03
	PS_A_G5		67.67	1.69E-03
	PS_H_G5		67.67	1.63E-03
	FS_SG_G7		15.82	1.95E-03

Table 4.10 Summary of Beam-on-Elastic-Foundation Design Periodical Functions

Soil Type	Platform Category	$A_{\beta z}$	$C_{\beta z}$	$C_{\beta z1}$	$C_{\beta z2}$
Very Soft Clay	PS_P_G1	0.981	0.730	1.000	0.501
	PS_P_G2	0.979	0.717	1.000	0.479
	PS_P_G3	0.980	0.727	1.000	0.496
	PS_SG_G3	0.980	0.727	1.000	0.496
	PS_P_G4	0.983	0.743	1.000	0.523
	PS_SG_G4	0.984	0.753	1.000	0.541
	PS_P_G5	0.982	0.741	1.000	0.519
	PS_SG_G5	0.985	0.758	1.000	0.550
	PS_A_G5	0.984	0.751	1.000	0.538
	PS_H_G5	0.985	0.760	1.000	0.552
	FS_SG_G7	0.977	0.706	1.000	0.461
Medium Sand	PS_P_G1	0.810	0.218	1.000	-0.128
	PS_P_G2	0.793	0.189	1.000	-0.146
	PS_P_G3	0.806	0.211	1.000	-0.132
	PS_SG_G3	0.806	0.211	1.000	-0.132
	PS_P_G4	0.826	0.246	1.000	-0.107
	PS_SG_G4	0.838	0.270	1.000	-0.089
	PS_P_G5	0.823	0.241	1.000	-0.111
	PS_SG_G5	0.844	0.282	1.000	-0.079
	PS_A_G5	0.836	0.265	1.000	-0.092
	PS_H_G5	0.846	0.285	1.000	-0.076
	FS_SG_G7	0.779	0.167	1.000	-0.159
Clayey Sand	PS_P_G1	0.793	0.190	1.000	-0.146
	PS_P_G2	0.775	0.161	1.000	-0.163
	PS_P_G3	0.789	0.183	1.000	-0.150
	PS_SG_G3	0.789	0.183	1.000	-0.150
	PS_P_G4	0.810	0.218	1.000	-0.127
	PS_SG_G4	0.823	0.242	1.000	-0.111
	PS_P_G5	0.807	0.213	1.000	-0.131
	PS_SG_G5	0.830	0.254	1.000	-0.101
	PS_A_G5	0.821	0.237	1.000	-0.114
	PS_H_G5	0.832	0.258	1.000	-0.098
	FS_SG_G7	0.760	0.138	1.000	-0.174

Table 4.11 Summary of Beam-on-Elastic-Foundation Design Results (SF of 1)

Soil Type	Platform Category	P'_{ED} (kN)	Δ'_{ED} (mm)	σ_{ALL} (MPa)	M_{ALL} (N-mm)	P'_{GD} (kN)	Δ'_{GD} (mm)	P'_{GD}/P'_{ED}
Very Soft Clay	PS_P_G1	343.48	51.34	35.65	1.41E+08	367.78	266.49	1.07
	PS_P_G2	317.08	58.54	32.91	1.31E+08	363.35	276.99	1.15
	PS_P_G3	430.31	67.53	44.66	1.77E+08	468.00	343.11	1.09
	PS_SG_G3	449.97	70.62	46.70	1.85E+08	489.38	358.78	1.09
	PS_P_G4	538.21	64.97	55.86	2.22E+08	538.46	370.58	1.00
	PS_SG_G4	**733.39**	**74.26**	**76.12**	**3.02E+08**	**694.21**	**483.70**	**0.95**
	PS_P_G5	522.33	65.58	54.21	2.15E+08	529.10	367.60	1.01
	PS_SG_G5	**718.64**	**66.34**	**74.59**	**2.96E+08**	**660.87**	**463.48**	**0.92**
	PS_A_G5	**348.96**	**36.51**	**36.22**	**1.44E+08**	**333.73**	**231.99**	**0.96**
	PS_H_G5	**809.03**	**72.55**	**83.97**	**3.33E+08**	**737.30**	**518.12**	**0.91**
	FS_SG_G7	**88.31**	**37.74**	**24.45**	**9.20E+06**	**26.00**	**288.31**	**0.29**
Medium Sand	PS_P_G1	343.48	51.34	35.65	1.41E+08	2,272.53	29.39	6.62
	PS_P_G2	317.08	58.54	32.91	1.31E+08	2,259.60	30.17	7.13
	PS_P_G3	430.31	67.53	44.66	1.77E+08	2,896.72	37.75	6.73
	PS_SG_G3	449.97	70.62	46.70	1.85E+08	3,029.05	39.47	6.73
	PS_P_G4	538.21	64.97	55.86	2.22E+08	3,297.72	41.23	6.13
	PS_SG_G4	733.39	74.26	76.12	3.02E+08	4,213.97	51.16	5.75
	PS_P_G5	522.33	65.58	54.21	2.15E+08	3,246.21	40.84	6.21
	PS_SG_G5	718.64	66.34	74.59	2.96E+08	3,991.03	47.70	5.55
	PS_A_G5	348.96	36.51	36.22	1.44E+08	2,029.36	24.78	5.82
	PS_H_G5	809.03	72.55	83.97	3.33E+08	4,445.10	52.86	5.49
	FS_SG_G7	88.31	37.74	24.45	9.20E+06	162.21	9.12	1.84
Clayey Sand	PS_P_G1	343.48	51.34	35.65	1.41E+08	2,446.37	26.47	7.12
	PS_P_G2	317.08	58.54	32.91	1.31E+08	2,427.52	27.06	7.66
	PS_P_G3	430.31	67.53	44.66	1.77E+08	3,116.95	33.97	7.24
	PS_SG_G3	449.97	70.62	46.70	1.85E+08	3,259.34	35.52	7.24
	PS_P_G4	538.21	64.97	55.86	2.22E+08	3,555.97	37.27	6.61
	PS_SG_G4	733.39	74.26	76.12	3.02E+08	4,549.06	46.37	6.20
	PS_P_G5	522.33	65.58	54.21	2.15E+08	3,499.44	36.90	6.70
	PS_SG_G5	718.64	66.34	74.59	2.96E+08	4,310.53	43.28	6.00
	PS_A_G5	348.96	36.51	36.22	1.44E+08	2,190.31	22.44	6.28
	PS_H_G5	809.03	72.55	83.97	3.33E+08	4,801.63	47.98	5.94
	FS_SG_G7	88.31	37.74	24.45	9.20E+06	173.94	8.15	1.97

Note: $P'_{GD} / P'_{ED} < 1$ is taken as 1.

Table 4.12 Summary of Beam-on-Elastic-Foundation Design Results (SF of 2)

Soil Type	Platform Category	P'_{ED} (kN)	Δ'_{ED} (mm)	σ_{ALL} (MPa)	M_{ALL} (N-mm)	P'_{GD} (kN)	Δ'_{GD} (mm)	P'_{GD}/P'_{ED}
Very Soft Clay	PS_P_G1	203.07	30.35	21.08	8.36E+07	217.43	157.55	1.07
	PS_P_G2	187.39	34.60	19.45	7.71E+07	214.73	163.70	1.15
	PS_P_G3	234.98	36.88	24.39	9.67E+07	255.55	187.36	1.09
	PS_SG_G3	249.09	39.09	25.85	1.03E+08	270.91	198.61	1.09
	PS_P_G4	315.18	38.05	32.71	1.30E+08	315.33	217.02	1.00
	PS_SG_G4	**451.17**	**45.68**	**46.83**	**1.86E+08**	**427.07**	**297.57**	**0.95**
	PS_P_G5	294.92	37.03	30.61	1.21E+08	298.74	207.55	1.01
	PS_SG_G5	**432.46**	**39.92**	**44.89**	**1.78E+08**	**397.69**	**278.91**	**0.92**
	PS_A_G5	**196.34**	**20.54**	**20.38**	**8.08E+07**	**187.78**	**130.53**	**0.96**
	PS_H_G5	**472.02**	**42.33**	**48.99**	**1.94E+08**	**430.17**	**302.29**	**0.91**
	FS_SG_G7	**51.90**	**22.18**	**14.37**	**5.41E+06**	**15.28**	**169.44**	**0.29**
Medium Sand	PS_P_G1	203.07	30.35	21.08	8.36E+07	1,343.53	17.38	6.62
	PS_P_G2	187.39	34.60	19.45	7.71E+07	1,335.40	17.83	7.13
	PS_P_G3	234.98	36.88	24.39	9.67E+07	1,581.79	20.61	6.73
	PS_SG_G3	249.09	39.09	25.85	1.03E+08	1,676.81	21.85	6.73
	PS_P_G4	315.18	38.05	32.71	1.30E+08	1,931.21	24.14	6.13
	PS_SG_G4	451.17	45.68	46.83	1.86E+08	2,592.40	31.48	5.75
	PS_P_G5	294.92	37.03	30.61	1.21E+08	1,832.88	23.06	6.21
	PS_SG_G5	432.46	39.92	44.89	1.78E+08	2,401.68	28.70	5.55
	PS_A_G5	196.34	20.54	20.38	8.08E+07	1,141.84	13.94	5.82
	PS_H_G5	472.02	42.33	48.99	1.94E+08	2,593.46	30.84	5.49
	FS_SG_G7	51.90	22.18	14.37	5.41E+06	95.33	5.36	1.84
Clayey Sand	PS_P_G1	203.07	30.35	21.08	8.36E+07	1,446.31	15.65	7.12
	PS_P_G2	187.39	34.60	19.45	7.71E+07	1,434.64	15.99	7.66
	PS_P_G3	234.98	36.88	24.39	9.67E+07	1,702.04	18.55	7.24
	PS_SG_G3	249.09	39.09	25.85	1.03E+08	1,804.29	19.66	7.24
	PS_P_G4	315.18	38.05	32.71	1.30E+08	2,082.44	21.83	6.61
	PS_SG_G4	451.17	45.68	46.83	1.86E+08	2,798.54	28.52	6.20
	PS_P_G5	294.92	37.03	30.61	1.21E+08	1,975.85	20.83	6.70
	PS_SG_G5	432.46	39.92	44.89	1.78E+08	2,593.94	26.04	6.00
	PS_A_G5	196.34	20.54	20.38	8.08E+07	1,232.40	12.63	6.28
	PS_H_G5	472.02	42.33	48.99	1.94E+08	2,801.47	27.99	5.94
	FS_SG_G7	51.90	22.18	14.37	5.41E+06	102.23	4.79	1.97

Note: $P'_{GD} / P'_{ED} < 1$ *is taken as 1.*

Table 4.13 Summary of Beam-on-Elastic-Foundation Design Results (SF of 3)

Soil Type	Platform Category	P'_{ED} (kN)	Δ'_{ED} (mm)	σ_{ALL} (MPa)	M_{ALL} (N-mm)	P'_{GD} (kN)	Δ'_{GD} (mm)	P'_{GD}/P'_{ED}
Very Soft Clay	PS_P_G1	142.34	21.28	14.77	5.86E+07	152.41	110.43	1.07
	PS_P_G2	131.34	24.25	13.63	5.41E+07	150.50	114.73	1.15
	PS_P_G3	161.06	25.28	16.72	6.63E+07	175.16	128.42	1.09
	PS_SG_G3	171.42	26.90	17.79	7.06E+07	186.43	136.68	1.09
	PS_P_G4	220.36	26.60	22.87	9.07E+07	220.47	151.73	1.00
	PS_SG_G4	**319.56**	**32.36**	**33.17**	**1.32E+08**	**302.48**	**210.76**	**0.95**
	PS_P_G5	204.11	25.63	21.19	8.40E+07	206.76	143.65	1.01
	PS_SG_G5	**304.56**	**28.12**	**31.61**	**1.25E+08**	**280.07**	**196.42**	**0.92**
	PS_A_G5	**135.76**	**14.20**	**14.09**	**5.59E+07**	**129.83**	**90.25**	**0.96**
	PS_H_G5	**329.68**	**29.57**	**34.22**	**1.36E+08**	**300.45**	**211.14**	**0.91**
	FS_SG_G7	**36.32**	**15.52**	**10.06**	**3.78E+06**	**10.69**	**118.58**	**0.29**
Medium Sand	PS_P_G1	142.34	21.28	14.77	5.86E+07	941.75	12.18	6.62
	PS_P_G2	131.34	24.25	13.63	5.41E+07	935.95	12.49	7.13
	PS_P_G3	161.06	25.28	16.72	6.63E+07	1,084.17	14.13	6.73
	PS_SG_G3	171.42	26.90	17.79	7.06E+07	1,153.94	15.04	6.73
	PS_P_G4	220.36	26.60	22.87	9.07E+07	1,350.22	16.88	6.13
	PS_SG_G4	319.56	32.36	33.17	1.32E+08	1,836.14	22.29	5.75
	PS_P_G5	204.11	25.63	21.19	8.40E+07	1,268.53	15.96	6.21
	PS_SG_G5	304.56	28.12	31.61	1.25E+08	1,691.38	20.21	5.55
	PS_A_G5	135.76	14.20	14.09	5.59E+07	789.49	9.64	5.82
	PS_H_G5	329.68	29.57	34.22	1.36E+08	1,811.40	21.54	5.49
	FS_SG_G7	36.32	15.52	10.06	3.78E+06	66.72	3.75	1.84
Clayey Sand	PS_P_G1	142.34	21.28	14.77	5.86E+07	1,013.79	10.97	7.12
	PS_P_G2	131.34	24.25	13.63	5.41E+07	1,005.51	11.21	7.66
	PS_P_G3	161.06	25.28	16.72	6.63E+07	1,166.60	12.71	7.24
	PS_SG_G3	171.42	26.90	17.79	7.06E+07	1,241.67	13.53	7.24
	PS_P_G4	220.36	26.60	22.87	9.07E+07	1,455.95	15.26	6.61
	PS_SG_G4	319.56	32.36	33.17	1.32E+08	1,982.14	20.20	6.20
	PS_P_G5	204.11	25.63	21.19	8.40E+07	1,367.49	14.42	6.70
	PS_SG_G5	304.56	28.12	31.61	1.25E+08	1,826.77	18.34	6.00
	PS_A_G5	135.76	14.20	14.09	5.59E+07	852.10	8.73	6.28
	PS_H_G5	329.68	29.57	34.22	1.36E+08	1,956.68	19.55	5.94
	FS_SG_G7	36.32	15.52	10.06	3.78E+06	71.54	3.35	1.97

Note: $P'_{GD} / P'_{ED} < 1$ *is taken as 1.*

4.7 Summary of Design Method

In summary, a design method that implements instrumented strain data, load data, and deflection data was presented. Within this chapter, the theories, assumptions, and equations used to develop and validate this design method were also presented. The design results for each platform category were then calculated using the aforementioned theories, assumptions, and equations, as well as the extracted raw data from Chapter 3. The next chapter will both discuss the implications of this design method and compare this method with the only design guide—***emtek***—found in the review of literature.

CHAPTER 5

DISCUSSION AND DESIGN IMPLICATIONS

5.1 Overview

The previous chapter presented a method for designing a single full-scale wood construction platform that sits on the ground using test data from prototype scale lab tests. This method was then used to calculate the design results for various geometric configurations, wood types, and design parameters. The purpose of this chapter is to discuss the proposed design method, the results from the proposed design method, and the implications of the proposed design method. The next section evaluates important qualities of the proposed design method. The following section compares the theory and design results of the bolt-laminated (G7) platforms to the ***emtek*** design guide found in the review of literature. The final section discusses the various implications of the design method.

5.2 Discussion of Design Method

The proposed design method has many advantages, as well as a few disadvantages. This section discusses both the advantages and disadvantages of the proposed design method. Certain qualities of the proposed design method will be discussed as well as the associated advantages and/or disadvantages for each. The qualities of the proposed design method that will be discussed in this chapter are: 1) Ease of Use; 2) Versatility; and 3) Accuracy. These qualities are related to each other as well; the next three sections look at these qualities and their relationships.

5.2.1 Ease of Use

The biggest advantage of the proposed design method is its ease of use. The method uses fundamental assumptions and theories of mechanics to give fairly accurate results that can be calculated quickly and easily. If, for example, on the job site an anticipated load changes, the new results can be calculated immediately. This method could be easily replicated by anyone with a moderate knowledge of the subject in a matter of days (in absence of obtaining test data). The cost of such replication could be inexpensive as well. In order to replicate this method, the interested party would need to test a sufficient amount of platforms, collect strain data, load data, and deflection data for each platform tested. The platforms could either be tested at prototype scale (more cost efficient) or full-scale (more accurate), depending on monetary or test site restrictions. Also, platforms could be made from a variety of materials and platform configurations.

With simplicity comes lack of accuracy. This could be a disadvantage if design values start to converge with failure values. A Safety Factor (SF) was implemented to reduce this disadvantage and can be chosen by the designer based on his or her experience. This method leads to fairly accurate test results; however, the results might not be as accurate as the results by other, more complicated methods. As an example, a finite element method could lead to refined uses of the test data. However, finite element procedures can be complicated and should only be used by personnel with finite element experience. A finite element method would not easily lend itself to onsite changes.

5.2.2 Versatility

Another important quality of the design method is its versatility. The design method was intentionally developed to allow for variation of materials, configurations (geometric and load), dimensions, and acceptable risk as dictated by the designer. The dimension factors are a good example. Versatility allows for this method to be used in a wide range of situations. Also, versatility and simplicity are related; in order for this method to be versatile, it must be simple enough to account for all basic mechanical phenomena. On the other hand, versatility, like simplicity, can lead to less accurate results, which can be a disadvantage. As an example, the proposed design method does not take into account advanced failure mechanisms such as creep. For the method proposed, failure modes such as creep were out of the scope of work.

5.2.3 Accuracy

Simplicity and versatility have been discussed in the context of accuracy; however, no speculation has been made to the degree of accuracy for this method. This method is acceptably accurate considering its simplicity and versatility. After discussions with experienced personnel at Anthony Hardwood Composites in Sheridan, Arkansas, values for P'_{GD} were deemed reasonable; the maximum value of P'_{GD} found was the total load capacity for PS_H_G5. This value was thought to be unlikely, but not impossible considering platform materials and soil conditions.

Obviously, there is some loss in accuracy from the data extraction and scaling procedures. This was unavoidable considering the research was performed for reasons other than this design method. The best way to determine the true accuracy of this method would be to set up a test in which full-scale platforms are loaded in uniform bearing under a massive loading frame. However, this could be an expensive project once costs for materials, testing equipment (i.e. actuators, framing, etc.), and personnel are considered. On the other hand, the proposed method could be compared to a more computationally intensive method to determine its accuracy. The ***emtek*** design guide is based on a finite element model and lends itself well to comparison with the results from the FS_SG_G7 bolt-laminated platforms as discussed in the next section.

5.3 Comparison to Existing Method

emtek (2009) was the only design guide found during review of literature. Similar to the proposed design method of this thesis, it is based on a beam-on-elastic-foundation analysis. For the ***emtek*** design guide, Anthony Hardwood Composites contracted out a local engineering company. The company divided a platform into a series of discrete springs 30.48 cm (1 ft.) apart and calculated results using a one-dimensional linear finite element model. A one-dimensional finite element model allows for each element to have two nodes, one at each end. Each element interacts with adjacent elements at adjoining nodes as well as with the soil below it. The interaction between the element and the soil is often described by a spring representing the soil's Modulus of Subgrade Reaction. Governing equations describe the load-deflection behavior at the nodes in between elements and between soil and each element. While a one-dimensional linear finite element model is the simplest of finite element models, the equations and necessary math to complete these models can be complicated.

The next two sections compare the proposed method to the ***emtek*** (2009) guide. The first section will compare the two methods from a theoretical point of view. The second section will compare the results from the two methods.

5.3.1 Theoretical Comparison

The design method proposed by this thesis treats the platform as an infinite beam, directly solving the closed form equations from the beam-on-elastic-foundation analysis. This allows a few fundamental equations to describe the load-deflection behavior of the platforms. The limitation of this method is that some impractical results can be calculated. An example is the results from the FS_SG_G7 platforms on the very soft clay. As values for k approach zero, the governing equations start to reach their limits. Also, as the depth (i.e. inertia) of the platform decreases, the platform starts to act more as a membrane rather than an infinite beam. This is why P'_{GD} / P'_{ED} must be greater than or equal to 1 in the proposed method; it is practically impossible that a platform would fail at a lower load on the ground than in the air. For this method, engineering judgment and experience should not be sacrificed in any situation. Also, the proposed method accounts for the composite behavior of the platforms; load transfer through steel bolts between adjacent billets was taken into consideration. This is represented by an E_{CP} value of 16,250 MPa (2350 ksi). The ***emtek*** design guide does not take this into account per the manufacturer's recommendation. ***emtek*** uses a value of 11,032 MPa (1600 ksi).

Allowable deflection is an interesting parameter for theoretical comparison between the two methods. ***emtek*** deflections depend on the soil and loads, and represent a settlement (global displacement) rather than a deflection (local displacement with respect to the edge of the platform). The proposed method allows for relatively large deflections because the deflection is based on an infinite beam; therefore, on a soft soil, the beam can develop a relatively large deflection over an infinitely large length. On the other hand, for stiffer soils, the proposed design method allows for very reasonable deflections. As a result, the deflections for each design method are not comparable because they portray separate mechanical phenomena. Both methods' deflections results can be deceiving; engineering judgment and experience should be used when determining an allowable deflection. Allowable deflection is often a serviceability criterion and is out of the scope of this project.

Another interesting parameter for comparison is the allowable bending stress. ***emtek*** reports a value of 28.43 MPa (4100 psi). This value includes a load duration factor of 1.33. For the same construction platform, allowable bending stress in the proposed design method reports a value of 24.45 MPa (3550 psi) when an SF of 1 is used. These values are very similar and allow a reasonable comparison between the two methods.

emtek also reports an allowable shear stress of 2.61 MPa. The proposed design method does not report an allowable shear stress for two reasons. First, platforms were not evaluated for shear failures; no short, deep beams were tested (see ASTM D 5456 – 05 for acceptable length-depth ratio for testing pure bending in beams). Second, no shear failures were observed during testing.

5.3.2 Design Results Comparison

To compare the results of these two methods, a platform of similar size and load configuration was designed using each method. A 365.76 cm by 91.44 cm by 8.89 cm (12 ft. by 3 ft. by 3.5 in.) size platform was chosen for comparison between these two methods. The load configuration used was "Load Case 1" in the ***emtek*** design guide which uses two equal, concentric loads placed 182.88 cm (6 ft.) apart from each other as seen in Figure 5.1(a). In addition, the soil chosen for comparison was ***emtek***'s Type A (SGM-1), which is the same as the very soft clay used in Chapter 4. An excerpt from the ***emtek*** design results table that corresponds to these design criteria is shown in Figure 5.2(b). The comparable values are outlined by bold lines. ***emtek*** results are based on a width of 30.48 cm (1 ft.). To determine the load for a 91.44 cm (3 ft.) wide platform, simply multiply the design load by 3. Therefore, the ground design load, P'_{GD}, from the ***emtek*** design procedure is calculated in Equation 5-1.

$$P'_{GD} = 3ft. \cdot (2 \cdot 1.6kip / ft.) \cdot 4.45kN / kip = 42.72kN \qquad (5\text{-}1)$$

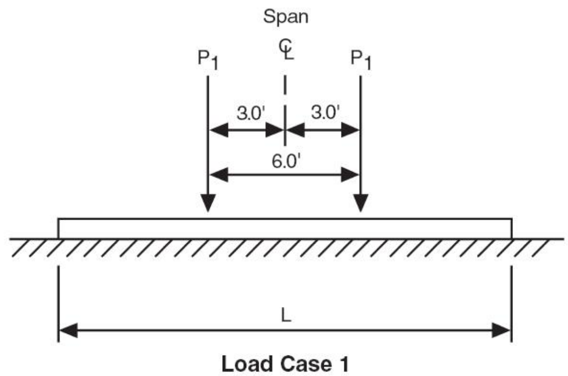

(a) Load Configuration

Length	Thickness	Load Case 1		
Feet	Inches	P Load Kips	Defl. Inches	Bearing PSI
24	2.75	1.7	2.0	2.1
	3.5	1.9	2.0	2.1
	4.5	2.1	2.0	2.1
	5.5	2.4	2.0	2.1
	6.5	2.6	2.0	2.1
	7.5	2.8	2.0	2.1
20	2.75	1.7	2.0	2.1
	3.5	1.8	2.0	2.1
	4.5	2.0	2.0	2.1
	5.5	2.2	2.0	2.1
	6.5	2.4	2.0	2.1
	7.5	2.5	2.0	2.1
16	2.75	1.7	2.0	2.1
	3.5	1.8	2.0	2.1
	4.5	2.0	2.0	2.1
	5.5	2.1	2.0	2.1
	6.5	2.1	2.0	2.1
	7.5	2.2	2.0	2.1
12	2.75	1.5	2.0	2.1
	3.5	1.6	2.0	2.1
	4.5	1.7	2.0	2.1
	5.5	1.7	2.0	2.1
	6.5	1.7	2.0	2.1
	7.5	1.7	2.0	2.1

(b) Design Table

Figure 5.1 Excerpt From ***emtek*** Design Guide

To calculate results from the proposed method, one simply starts with the allowable bending stress of 24.45 MPa that corresponds to an SF of 1. Using a modified form of Equation 4-2 and appropriate dimensions, the allowable moment is calculated for the dimensions and load configuration as seen in Equation 5-2a. Next, the value for β (corresponding to FS_SG_G7 and the very soft clay) is taken from Table 4.9 and multiplied by the values of z_1 = 0 mm and z_2 = 1828.8mm. Equation 5-2b and Equation 5-2c show the periodical relationship function $C_{\beta z}$ (Equation 4-7e) calculated using $\beta z1$ = 0 and $\beta z2$ = 0.9436. Finally, Equation 5-2d shows the calculation for P'_{GD} using Equation 4-8a.

$$M = \frac{\sigma I}{c} = \frac{24.45 \cdot \left(1.67 \times 10^{7}\right)}{\left(44.5\right)} = 9.18 \times 10^{6}\, N - mm \tag{5-2a}$$

$$C_{\beta z1} = e^{-\beta z1}\left(cos\, \beta z1 - sin\, \beta z1\right) = e^{-(0)}\left(cos\, 0 - sin\, 0\right) = 1 \tag{5-2b}$$

$$C_{\beta z2} = e^{-(0.9436)}\left(cos\, 0.9436 - sin\, 0.9436\right) = -0.5813 \tag{5-2c}$$

$$P'_{GD} = \frac{8 \cdot M \cdot \beta}{C_{\beta z1} + C_{\beta z2}} = \frac{8 \cdot \left(9.18 \times 10^{6}\right) \cdot \left(5.16 \times 10^{-4}\right)}{1000 \cdot \left(1 - .5813\right)} = 90.51 kN \tag{5-2d}$$

At first glance, one might think there is an error in the proposed method because it gives a ground design load of just over twice the ***emtek*** method's ground design load. However, some increase in strength is expected because the proposed method takes the composite behavior of the platform into consideration. In the research by Shmulsky et al. (2008), a three-billet platform was found to be 1.94 times stronger than the single billet. The increase in strength was attributed to the composite behavior. Therefore, it is no surprise that the proposed method allows for twice the design ground load that ***emtek*** design method allows. This comparison shows that the results calculated by the proposed design method are reasonable. Table 5.1 summarizes a comparison of the results for each method.

Table 5.1 Comparison of Design Results

Design Value	Proposed Design Method	***emtek*** Design Guide
E (MPa)	16250 (composite)	11032
σ_{ALL} (MPa)	24.45 (SF of 1) 14.37 (SF of 2) 10.06 (SF of 3)	28.43
P'_{GD} (kN)	90.51 (SF of 1) 52.34 (SF of 2) 37.27 (SF of 3)	42.72

Also, it is interesting to see the range of values for P'_{GD} depending on the factor of safety chosen. When compared to the value from the ***emtek*** (2009) guide, one can see this value falls within the range of values for P'_{GD} from the proposed method. This implies not only a good comparison, but also that designer input and experience can compensate for the use of the composite modulus of elasticity.

5.4 Implications of Design Method

The proposed method was shown to be simple, versatile, and accurate. Hence, the proposed method of this thesis will have implications on various elements of the wood construction platform industry including material retention, freight costs, and safety. The method could also have smaller implications on large industries; however, these implications are not investigated in this thesis. An effort was made to explore the implications of this design method in detail; however, information was limited due to company confidentiality. Therefore, the implications of the proposed method are discussed in a broad, hypothetical sense. The author recommends these implications be evaluated in more detail by interested personnel.

Material retention is one of the larger implications of the proposed design method. The proposed design method allows for an accurate design, as well as a conservative design. It is anticipated that a better design will help to retain wood construction platforms, implying that less material will be wasted on poorly designed platforms. This is not to say that a severely overly-designed platform (one that will never fail) is acceptable, but rather that a more conscious design will extend the life of construction platforms. This would be advantageous to a company that rents or leases wood construction platforms or a company that uses wood construction platforms regularly on various types of construction projects. Hypothetically, for a platform with no design, a company might average five uses per platform at a rental cost of $800 per platform, meaning the platform's expected life income is $4,000. If a design method could be used to increase the average number of uses per platform to eight uses, an extra $2,400 of income could be generated. Also, if a designed platform leads to a longer lasting platform, a company might be able to rent platforms for cheaper than its competitor, giving that company an obvious advantage.

Freight costs are another implication of the proposed design method. Freight costs change daily and could be a gray area when bidding a job using wood construction platforms. Any way to reduce this cost would be beneficial. Information on freight costs for wood constructions platforms was extremely difficult to find; however, the implications associated with freight costs are easy to understand without specific information. From a practical standpoint, one can understand an efficiently designed platform will lead to a more efficient use of material. A more efficient use of material will lead to less unnecessary material shipped to the construction site, ultimately saving money on freight costs. A simple comparison between the strength-density ratios of designed platforms versus undesigned platforms would be an indicator of how much money could be saved on freight costs.

Safety is the third and final design implication to be discussed in this thesis. Safety should be (and usually is) considered paramount on all construction sites. Any action or practice that realistically improves a construction site's safety is valuable. Safer construction leads to increased bonding, which in turn leads to the ability to do larger projects. There are two design criteria associated with safety: strength and serviceability. For these design criteria, the goal is not necessarily a stronger platform with less deflection, but rather the ability to define the risk and safety associated with the strength and deflection of the platform.

From a strength point of view, safety is associated with, not only strong platforms, but also, platforms that fail gracefully. Howard et al. (2008) demonstrated that the platforms exhibited good ductility. Ductility allows for the platforms to fail, but not fail violently. Used with adequate inspection, ductility would allow for damaged or failed platforms to be identified before any catastrophic failure would occur. This is quite valuable considering heavy equipment, such as cranes, are typically supported by wood construction platforms.

From a serviceability point of view, excessive deflection and/or settlement of the platform could lead to tipping of heavy machinery. This can be costly when considering operator injury, machinery damage and repairs, construction site damage, lost time, etc. Serviceability is very hard to predict using either of the methods available, implying the need for a risk evaluation of deflection and settlement.

CHAPTER 6

SUMMARY, CONCLUSIONS, AND RECOMMENDATIONS

6.1 Summary and Conclusions

A wood construction platform design method was developed in this thesis. A review of literature demonstrated the need for an easy to use, yet accurate design method. This method differs in theory from the only other available design method, but still leads to relatively accurate results. The results from the proposed design method correspond favorably with those from the ***emtek*** design guide. The proposed method also makes use of modern instrumentation technology.

The proposed method does have a few limitations when dealing with "thin" platforms or extremely soft soils; however, when used in conjunction with engineering judgment and experience, these limitations are insignificant. The implications of this design method cover a wide array of subjects, but are mostly associated with material retention, freight costs, and safety.

In conclusion, eleven platform categories were tested with seven different geometric configurations and four different wood types. In air load-deflection and load-strain data was used in conjunction with fundamental theories of mechanics to develop a design method for a single platform on the ground. The method was shown to be easy to use, versatile, and accurate, which implies its usefulness in various related industries.

6.2 Recommendations

The proposed design method is one of platform design for all needed variables. This leaves the door open for various research projects related to platform design. A full-scale load test on soil with proper instrumentation would prove extremely valuable, though, expensive once costs for materials, testing equipment, and personnel are considered. An evaluation of load transfer between platforms (placed side by side or one on top of another) would also prove valuable considering single platforms are seldom used in practice. Shear failure should be evaluated for short, deep platforms as well. Alternative load configurations should also be evaluated. Most importantly, a strenuous statistical analysis should be performed to accurately describe the risk and reliability associated with wood platform design. This type of analysis would help determine acceptable values for platform design.

A variety of complex mechanical phenomena should also be tested and implemented into this design procedure. Time-dependent behavior (i.e. creep and relaxation) should be investigated when considering long-duration loading of platforms. Wood platforms are also subject to the effects of biodegradation and moisture cycles. Both of these behaviors would involve long-term research on the order of years.

Aside from research related to engineering mechanics, various other research could be conducted that would prove valuable to the industry. A full economic analysis should be performed to show the cost-benefit of superiorly designed platforms. Also, a Life Cycle Assessment should be performed to determine the true environmental impact of wood platforms compared to various other soil stabilization techniques.

REFERENCES

Boresi, A.P. and Schmidt, R.J. (2003). *Advanced mechanics of materials*. John Wiley and Sons, Inc., Hoboken, NJ.

Bowyer, J.L., Shmulsky, R., Haygreen, J.G. (2007). *Forest products & wood science: an introduction*. Blackwell Publishing, Ames, IA.

emtek*: heavy equipment mat design guide*. (2009). Anthony Hardwood Composites, Sheridan, AR.

Fiorelli, J. and Dias, A.A. (2003). "Analysis of the strength and stiffness of timber beams reinforced with carbon fiber and glass fiber." *International Journal of Materials Research*, 6(2), 193-202.

Franklin, J.M., Taylor, S.E., Morgan, P.A., and Ritter, M.A. (1999). "Design criteria for portable timber bridge systems: static versus dynamic loads." *Paper No. 99-4208,* ASAE, July 18-21, Toronto, Canada, 21.

Fridley, K.J. (2002). "Wood and wood-based materials: current status and future of a structural material." *Journal of Materials in Civil Engineering*, 14(2), 91-96.

Hislop, L.E. (1996). *Improving access and environmental sensitivity with portable surfaces on low volume roads*. 9624 1211-SDTDC, United States Department of Agriculture (USDA), Madison, WI.

Howard, J.L. (2001). *U.S. timber production, trade, consumption and price statistics 1965 -1999*. FPL-RP-595, USDA, Madison, WI.

Howard, I.L., Saucier, C.L., Shmulsky, R. (2008). "Testing of instrumented construction mats and billets." *Proceedings of Geo Congress 2008,* Characterization, Monitoring, and Modeling of GeoSystems-Geotechnical Special Publication No. 179, ASCE, Mar 9-12, New Orleans, LA, 340-347.

Howard I.L. and Stroble, M.F. (2008). *Prototype and full scale instrumented testing of wood construction platforms*. Final Report CMRC-08-01. Mississippi State University (MSU), Starkville, MS.

Jensen, J.L. and Gustafsson, P.J. (2004). "Shear strength of beam splice joints with glued-in rods." *Journal of Wood Science*, 50, 123-129.

Kestler, M.A., Shoop, S.A., Henry, K.S., Stark, J.A., and Affleck, R.T. (1999). *Rapid stabilization of thawing soils for enhanced vehicle mobility: a field demonstration project.* CRREL Report 99-3, US Army Corps of Engineers (USACE), Hanover, NH.

Lam, F. and Craig, A.C. (2000). "Shear strength in structural composite lumber." *Journal of Materials in Civil Engineering*, 12(3), 196-204.

Loferski, J.R., Davalos, J.F., Yadama, V. (1989). "A laboratory-built clip-on strain gauge transducer for testing wood." *Forest Products Journal,* 39(9), 45-48.

Mason, L.E., and Greenfield, P.H. (1995). "Portable crossings for weak soil areas and streams." *Transportation Research Record: Journal of the Transportation Research Board,* 1504, 118-124.

Radcliffe, B. M. (1955). "A method for determining the elastic constants for wood by means of electric resistance strain gages." *Forest Products Journal,* 5(2), 77-80.

Santoni, R.L., Smith, C.J., Tingle, J.S., and Webster, L.W. (2001). "Expedient road construction over soft soils." Report TR-01-7, USACE ERDC Geotechnical and Structures Lab, Vicksburg, MS.

Schweitzer, L., and Marinello, S. (1996). "Do heavy construction in fragile wetland with hardwood mat systems." *Electrical World*, 210(12.3).

Shmulsky, R., Saucier, C.L., and Howard, I.L. (2008). "Composite effect of bolt-laminated sweetgum and mixed hardwood billets." *Journal of Bridge Engineering*, 13(5), 547-549.

Shmulsky, R., and Shi, S. (2008). "Development of novel industrial laminated planks from sweetgum lumber." *Journal of Bridge Engineering*, 13(1), 64-66.

Smith, R.L., and Stanfill-McMillan, K. (1998). "Comparison of perception versus reality in timber bridge performance." *Journal of Materials in Civil Engineering*, 10(4), 238-243.

Smulski, S. (1997). *Engineered wood products: a guide for specifiers, designers and users*. PFS Research Foundation, Madison, WI.

Wipf, T.J., Ritter, M.A., and Wood, D.L. (1996). "Dynamic evaluation of timber bridges." *National Conference on Wood Transportation Structures,* Oct 23-25, USDA, Madison, WI, 114-121.

Wood handbook: wood as an engineering material. (1999). General Technical Report 113, USDA, Madison, WI.

Yoshihara, H., and Kawasaki, T. (2006). "Failure behavior of spruce wood under bending-shear combined stress field." *Journal of Materials in Civil Engineering*, 18(1), 93-98.

APPENDIX A

RAW AND REDUCED DATA

Table A.1 Raw and Reduced Strain Data of *PS_P_G1.1*

Strain Time (sec)	Load Time (sec)	Load (kN)	Microstrains		
			L1	L2	L3
3	0	0.00	0	0	0
13	10	0.26	13	6	2
23	20	0.53	58	19	24
33	30	0.60	144	48	61
43	40	0.80	342	119	158
53	50	1.20	578	198	277
63	60	1.60	867	293	410
73	70	1.86	1191	388	537
147	140	2.26	1581	487	667
157	150	2.60	1972	580	806
167	160	3.00	2410	673	951
177	170	3.46	2870	745	1090
187	180	3.80	3348	797	1225
266	250	4.00	4028	841	1402
276	260	4.47	4500	887	1543
286	270	4.80	4975	913	1681
296	280	5.20	5429	928	1807
306	290	5.53	5910	801	1933
383	360	5.80	6620	691	2122
393	370	6.07	7087	572	2224
403	380	6.47	7479	520	2346
413	390	6.73	7900	440	2462
423	400	7.07	8320	408	2573
433	410	7.33	8701	391	2669
509	480	7.53	9742	401	2849
529	500	8.34	10224	372	3045
539	510	8.54	10708	407	3149
549	520	8.74	11092	403	3238
569	540	9.00	11916	399	3416
648	620	9.34	12677	331	3480
658	630	9.54	13125	334	3580

Table A.2 Raw and Reduced Strain Data of *PS_P_G1.2*

Strain Time (sec)	Load Time (sec)	Load (kN)	Microstrains		
			L1	L2	L3
10	0	0.00	28	26	-6
20	10	0.33	90	64	7
30	20	0.46	209	122	24
40	30	0.93	419	146	97
50	40	1.46	566	154	145
60	50	1.86	859	185	257
141	120	2.40	982	138	208
151	130	3.00	1230	170	310
161	140	3.60	1515	188	421
171	150	4.07	1778	195	512
258	220	4.60	2183	137	621
268	230	5.07	2474	181	731
356	300	5.53	2889	143	841
366	310	6.27	3194	172	954
376	320	6.87	3535	195	1074
386	330	7.33	3828	203	1152
477	400	7.94	4360	164	1257
487	410	8.42	4671	188	1362
497	420	8.87	5014	207	1464
507	430	9.27	5368	227	1566
589	500	9.47	5601	151	1544
599	510	9.94	5896	181	1636
609	520	10.54	6211	196	1726
619	530	10.87	6586	216	1828
762	630	12.21	1730	90	2013

Table A.3 Raw and Reduced Strain Data of *PS_P_G1.3*

Strain Time (sec)	Load Time (sec)	Load (kN)	Microstrains		
			L1	L2	L3
10	0	0.00	8	24	8
20	10	0.33	50	78	28
30	20	0.66	151	175	82
40	30	1.13	247	239	132
50	40	1.60	371	306	206
60	50	2.20	501	348	280
140	120	2.73	589	191	290
150	130	3.40	719	278	377
160	140	4.07	881	345	482
260	210	4.53	1301	355	702
270	220	5.27	1451	370	794
280	230	5.93	1607	403	886
290	240	6.47	1741	405	958
300	250	7.13	1897	434	1055
310	260	7.73	2057	466	1151
320	270	8.34	2208	491	1245
330	280	8.87	2338	498	1317
417	350	9.07	275	313	1320
427	360	9.60	279	351	1405
437	370	10.27	259	334	1476
447	380	10.67	281	363	1568
538	450	10.74	221	227	1620
548	460	11.34	232	42	1671
558	470	11.87	219	5	1728
642	560	12.87	171	-23	1776
652	570	13.41	151	-47	1750
662	580	13.87	167	-30	1764
672	590	14.21	183	-2	1842
682	600	14.41	194	3	1918
708	680	14.67	193	104	1928
718	690	14.94	212	126	1939

Table A.4 Raw and Reduced Strain Data of *PS_P_G1.4*

Strain Time (sec)	Load Time (sec)	Load (kN)	Microstrains		
			L1	L2	L3
8	0	0.00	46	48	13
18	10	0.40	134	136	40
28	20	0.60	283	273	94
38	30	1.00	466	416	161
48	40	1.33	659	528	239
58	50	2.06	840	589	310
68	60	2.46	1053	655	390
159	130	2.93	1459	656	520
169	140	3.60	1701	737	613
257	160	4.07	2189	783	761
267	170	4.80	2477	866	856
277	180	5.53	2735	878	929
362	200	6.07	3231	912	1061
372	210	6.73	3537	998	1173
382	220	7.33	3850	1053	1278
469	240	7.73	4358	946	1368
479	250	8.40	4675	1017	1469
489	260	8.94	5031	1109	1592
577	280	9.40	5580	1041	1686
587	290	10.07	5908	1104	1779
597	300	10.56	6246	1132	1859
607	310	11.07	6635	1191	1948
697	330	11.47	7224	1069	1997
707	340	11.87	7588	1148	2100
824	390	13.41	9314	1167	2363
834	400	13.81	9728	1213	2421

Table A.5 Raw and Reduced Strain Data of *PS_P_G1.5*

Strain Time (sec)	Load Time (sec)	Load (kN)	Microstrains		
			L1	L2	L3
12	0	0.00	186	99	20
22	10	0.73	379	215	72
32	20	1.13	593	327	118
42	30	1.73	819	425	166
52	40	2.26	1052	495	218
152	110	2.66	1649	493	343
162	120	3.33	1956	533	430
172	130	4.04	2278	553	521
182	140	4.80	2599	552	586
192	150	5.33	2912	544	651
241	220	5.87	2901	348	585
251	230	6.53	2905	350	601
261	240	7.13	2887	322	577
271	250	7.80	3000	370	619
291	270	8.07	3623	479	780
301	280	8.51	3954	487	854
311	290	9.34	4278	469	902
321	300	10.01	4544	447	961
397	320	10.14	4637	297	917
407	330	10.80	4972	359	1033
417	340	11.40	5309	354	1109
427	350	11.87	5679	N/A	1199
437	360	12.18	6032	N/A	1259
447	370	12.54	6271	N/A	1288

Table A.6 Raw and Reduced Strain Data of *PS_P_G2.1*

Strain Time (sec)	Load Time (sec)	Load (kN)	Microstrains		
			L1	L2	L3
6	0	0.00	13	50	36
16	10	0.40	42	152	107
26	20	0.53	67	272	190
36	30	0.80	94	411	282
46	40	1.00	120	557	387
56	50	1.20	141	696	486
66	60	1.53	162	841	593
76	70	1.80	178	995	714
160	140	2.00	201	1334	988
170	150	2.33	226	1509	1134
180	160	2.60	249	1683	1279
190	170	2.86	265	1850	1416
200	175	3.53	283	2022	1556
260	245	3.66	266	2199	1693
270	255	4.00	292	2371	1839
280	265	4.33	315	2549	1986
290	275	4.60	335	2723	2132
300	285	4.93	350	2894	2271
310	295	5.20	366	3067	2409
320	305	5.40	377	3228	2538
396	375	5.47	333	3361	2620
406	385	5.80	361	3547	2774
416	395	6.07	384	3729	2916
426	405	6.33	406	3916	3054
436	415	6.60	422	4100	3191
446	425	6.73	438	4283	3317
456	435	7.13	450	4466	3441
571	515	7.33	484	5459	3947
581	525	7.67	506	5680	4041
591	535	7.94	520	5908	4148
601	545	8.07	528	6125	4245
611	555	8.20	538	6343	4345
621	565	8.47	544	6564	4441
631	575	8.54	552	6766	4535
641	585	8.67	561	6974	4631
651	595	8.74	590	7246	4706
661	605	8.94	583	7434	4762
671	615	9.00	577	7633	4850
681	625	9.07	568	7826	4954
691	635	9.20	562	8012	5040
701	645	9.34	545	8171	5126

Table A.7 Raw and Reduced Strain Data of *PS_P_G2.2*

Strain Time (sec)	Load Time (sec)	Load (kN)	Microstrains		
			L1	L2	L3
22	0	0.00	Sensor Failure	183	117
32	10	0.46		341	223
42	20	0.80		529	347
52	30	1.13		688	444
62	40	1.53		904	586
72	50	2.00		1135	739
82	60	2.46		1353	873
92	70	2.93		1607	1037
102	80	3.40		1839	1177
153	150	4.07		1934	1163
163	160	4.33		1923	1149
173	170	4.83		1939	1157
183	180	5.20		1988	1189
193	190	5.67		2199	1368
213	210	6.00		2723	1681
223	220	6.47		2985	1842
233	230	6.93		3239	1990
243	240	7.27		3504	2142
332	310	7.47		3815	2233
342	320	7.87		4075	2406
352	330	8.27		4341	2570
362	340	8.54		4601	2716
372	350	8.94		4839	2838
450	420	8.65		4940	2776
460	430	9.20		5186	2944
470	440	9.54		5461	3094
480	450	9.74		5735	3243
490	460	9.87		5983	3357
500	470	10.07		6254	3485
510	480	10.27		6521	3608

Table A.8 Raw and Reduced Strain Data of *PS_P_G2.3*

Strain Time (sec)	Load Time (sec)	Load (kN)	Microstrains		
			L1	L2	L3
15	0	0.00	162	246	155
25	10	0.80	256	434	269
35	20	1.26	319	614	372
45	30	1.66	388	827	494
146	100	1.93	401	1315	715
156	110	2.46	460	1556	847
166	120	2.86	509	1811	985
176	130	3.40	544	2081	1122
186	140	3.80	550	2348	1243
274	210	4.13	405	2703	1328
284	220	4.53	462	2957	1463
294	230	5.07	487	3225	1596
304	240	5.47	519	3523	1743
414	310	5.67	441	2079	2079
424	320	6.07	461	4762	2212
434	330	6.60	488	5072	2350
444	340	7.00	488	5368	2459
454	350	7.20	499	5680	2587
555	420	7.27	429	6441	2779
565	430	7.67	438	6732	2891
575	440	8.07	441	7030	2999
585	450	8.34	438	7330	3093
595	460	8.74	451	7674	3199
605	470	9.00	435	7999	3291
695	550	9.27	319	8408	3235
705	560	9.74	351	8724	3371
715	570	10.05	351	9033	3477
725	580	10.14	347	9364	3569
735	590	10.47	333	9519	3656
745	600	10.67	316	9834	3788
870	700	10.74	-167	1948	3359
880	710	10.74	-155	1984	3450
890	720	10.67	-168	1991	3492

Table A.9 Raw and Reduced Strain Data of *PS_P_G2.4*

Strain Time (sec)	Load Time (sec)	Load (kN)	Microstrains		
			L1	L2	L3
38	0	0.00	29	53	56
48	10	0.13	9	131	97
58	20	0.33	24	279	206
68	30	0.60	40	452	338
78	40	0.93	52	640	473
88	50	1.46	48	831	602
98	60	1.80	45	1027	730
196	130	2.33	67	1519	1037
206	140	2.80	80	1762	1204
216	150	3.20	94	2018	1376
226	160	3.66	65	2215	1478
320	230	3.87	138	2798	1849
330	240	4.27	129	3076	2025
340	270	4.87	147	3365	2217
350	260	5.40	147	3652	2390
459	340	6.00	168	4479	2833
469	350	6.27	169	4771	3011
479	360	6.67	185	5070	3189
489	370	7.00	192	5372	3356
499	380	7.40	198	5653	3506
604	470	7.67	202	6602	3930
614	480	8.20	208	6911	4087
624	490	8.34	186	7211	4222
634	500	8.67	238	7557	4385
737	560	9.00	221	8468	4692
747	570	9.34	225	8778	4843
757	580	9.67	212	9103	4985
767	590	10.07	214	9417	5117
777	600	10.40	212	9726	5237
787	610	10.54	224	10045	5368
797	620	10.80	243	10375	5497

Table A.10 Raw and Reduced Strain Data of *PS_P_G2.5*

Strain Time (sec)	Load Time (sec)	Load (kN)	Microstrains		
			L1	L2	L3
15	0	0.00	143	319	173
25	10	0.60	218	557	296
35	20	1.13	291	826	426
45	30	1.60	357	1113	561
55	40	2.20	369	1337	651
159	110	2.46	441	2250	1019
169	120	3.13	530	2623	1186
179	130	3.87	566	2986	1343
189	140	4.33	595	3370	1503
199	150	4.73	626	3750	1657
209	160	5.27	648	4131	1807
219	170	5.73	652	4489	1941
318	240	6.00	553	5307	2172
328	250	6.60	648	5296	2320
338	260	6.93	585	N/A	2444
438	330	7.13	545	N/A	2768
448	340	7.73	599	N/A	2917
458	350	8.14	620	N/A	2997
468	360	8.54	527	N/A	3108
478	370	8.80	498	N/A	3218
488	380	9.07	441	N/A	3284

Table A.11 Raw and Reduced Strain Data of *PS_P_G3.1*

Strain Time (sec)	Load Time (sec)	Load (kN)	Microstrains		
			L1	L2	L3
3	0	0.00	16	18	14
13	10	0.26	71	80	81
23	20	0.53	169	182	189
33	30	0.86	304	329	327
43	40	1.26	444	488	495
53	50	1.73	591	651	676
63	60	2.26	736	817	860
73	70	2.60	876	978	1046
147	140	3.00	984	1092	1215
157	150	3.53	1150	1286	1446
229	220	4.60	1460	1646	1876
239	230	5.27	1651	1887	2140
249	240	5.67	1842	2128	2402
326	310	6.20	2046	2347	2691
336	320	6.87	2235	2575	2977
346	330	7.53	2421	2799	3260
356	340	7.87	2596	3016	3545
366	350	8.47	2760	3219	3833
376	360	8.94	2920	3415	4114
450	430	9.34	3037	3506	4363
460	440	9.94	3210	3707	4654
470	450	10.40	3373	3902	4967
480	460	10.85	3523	4070	5262
490	470	11.20	3655	4220	5560
573	550	11.34	3794	4327	6037
583	560	11.81	3937	4488	6355
593	570	12.07	4049	4615	6704
603	580	11.81	4206	4756	6950

Table A.12 Raw and Reduced Strain Data of *PS_P_G3.2*

Strain Time (sec)	Load Time (sec)	Load (kN)	Microstrains		
			L1	L2	L3
10	0	0.00	166	148	126
20	10	0.60	355	318	288
30	20	1.00	508	456	403
40	30	1.53	690	621	567
50	40	2.00	862	779	738
153	110	2.40	1369	1237	1228
163	120	3.06	1561	1412	1402
173	130	4.00	1759	1593	1591
183	140	4.27	1953	1765	1766
193	150	4.80	2162	1957	1968
203	160	5.40	2363	2140	2162
291	230	6.00	2714	2439	2471
301	240	6.40	2912	2624	2659
311	250	7.13	3084	2782	2822
405	320	7.40	3440	3081	3128
415	330	8.00	3635	3261	3313
425	340	8.60	3831	3443	3506
435	350	8.94	3965	3564	3620
531	420	9.27	4359	3893	3971
541	430	9.60	4530	4055	4117
551	440	10.02	4698	4209	4280
571	460	10.67	5013	4501	4577
694	540	11.14	5659	5061	5161
704	550	11.47	5772	5166	5253
714	560	11.67	5867	5248	5328
724	570	11.81	5971	5365	5582
734	580	12.01	6088	5474	5703
744	590	12.14	6187	5565	5806
754	600	12.27	6271	5637	5889
764	610	12.41	6374	5722	5958

Table A.13 Raw and Reduced Strain Data of *PS_P_G3.3*

Strain Time (sec)	Load Time (sec)	Load (kN)	Microstrains		
			L1	L2	L3
23	0	0.00	30	47	12
33	10	0.33	120	139	71
43	20	0.73	260	266	158
53	30	1.33	400	389	231
63	40	1.86	562	341	359
148	100	1.80	711	656	459
158	110	2.46	880	812	586
168	120	3.26	1056	959	703
178	130	3.93	1220	1109	835
256	190	4.00	1305	1147	879
266	200	4.73	1505	1322	1028
276	210	5.53	1705	1503	1185
355	270	5.60	1803	1548	1251
365	280	6.67	1994	1713	1379
375	290	7.13	2219	1903	1554
385	300	7.73	2424	2075	1704
467	360	7.60	2547	2103	1765
477	370	8.47	2756	2282	1901
487	380	9.40	2970	2460	2076
570	440	9.20	3122	2500	2154
580	450	10.14	3352	2697	2344
600	470	11.60	3756	3018	2647
678	530	11.34	3857	2990	2681
688	540	12.47	4073	3172	2836
698	550	13.21	4266	3329	2983
781	610	12.74	4418	3347	3056
791	620	13.74	4629	3521	3211
801	630	14.34	4810	3647	3344
811	640	14.61	4978	3774	3462
893	700	14.30	5031	3697	3442
903	710	15.14	5237	3866	3593
913	720	15.61	5412	4007	3721
923	730	16.08	5564	4123	3837
947	790	15.81	5471	3989	3739
957	800	16.41	5439	3946	3706
967	810	16.81	5438	3930	3719
987	820	16.94	5417	3887	3687
997	830	17.08	5404	3869	3679
1007	840	17.28	5579	4015	3797
1017	850	17.34	5765	4169	3938
1027	860	17.48	5877	4256	4011

Table A.14 Raw and Reduced Strain Data of *PS_P_G3.4*

Strain Time (sec)	Load Time (sec)	Load (kN)	Microstrains		
			L1	L2	L3
5	0	0.00	90	87	56
15	10	0.66	242	228	153
25	20	1.06	404	368	265
35	30	1.53	548	497	375
45	40	1.93	669	604	476
126	100	2.00	753	655	534
136	110	2.53	931	816	672
146	120	3.13	1100	970	812
156	130	3.60	1281	1132	962
233	190	3.53	1364	1183	1015
243	200	4.27	1550	1349	1168
253	210	4.53	1738	1521	1329
263	220	5.33	1917	1675	1477
342	280	5.27	2040	1750	1566
352	290	5.93	2240	1927	1732
362	300	6.53	2432	2096	1894
372	310	7.13	2610	2247	2077
450	370	6.73	2708	2285	2134
460	380	7.53	2896	2446	2305
470	390	8.20	3099	2619	2474
480	400	8.74	3285	2791	2638
570	470	8.80	3589	2988	2862
580	480	9.40	3791	3162	3029
590	490	10.07	3955	3298	3162
600	500	10.47	4125	3448	3305
610	510	10.80	4288	3587	3441
699	570	10.34	4555	3738	3589
709	580	11.07	4715	3874	3710
719	590	11.40	4832	3954	3795
729	600	11.67	4954	4056	3889
739	610	11.87	5080	4108	3943
749	620	11.94	5192	4180	4002
759	630	12.01	5306	4261	4081
769	640	12.07	5388	4305	4137
779	650	12.01	5504	4399	4303

Table A.15 Raw and Reduced Strain Data of *PS_SG_G3.1*

Strian Time (sec)	Load Time (sec)	Load (kN)	Microstrains		
			L1	L2	L3
4	0	0.00	39	22	16
14	10	0.40	195	109	93
24	20	0.73	397	246	213
34	30	1.00	630	394	346
44	40	1.46	859	463	490
54	50	1.73	1045	591	600
128	120	2.20	1372	874	796
138	130	2.60	1630	1017	934
148	140	3.06	1914	1175	1086
158	150	3.53	2215	1337	1249
168	160	4.07	2509	1498	1409
243	230	4.53	2895	165	1628
253	240	5.00	3151	591	1764
325	310	5.60	3559	1575	1993
335	320	6.27	3891	1885	2167
419	390	6.67	4616	2572	2577
429	400	7.27	4963	2775	2768
439	410	8.34	5296	2917	2933
505	480	8.67	5806	3145	3199
515	490	9.27	6206	3331	3390
525	500	9.67	6605	3422	3564
535	510	10.00	6923	3561	3731
610	580	10.27	7460	3730	3952
620	590	10.80	7862	3898	4124
630	600	11.20	8262	4016	4270
640	610	11.54	8692	4133	4400
650	620	11.67	9074	4224	4493

Table A.16 Raw and Reduced Strain Data of *PS_SG_G3.2*

Strain Time (sec)	Load Time (sec)	Load (kN)	Microstrains		
			L1	L2	L3
12	0	0.00	Sensor Failure	86	61
22	10	0.53		177	136
32	20	0.86		349	247
42	30	1.26		460	342
52	40	1.66		618	458
62	50	2.00		774	567
155	120	2.40		1036	749
165	130	2.93		1211	877
175	140	3.46		1364	1003
185	150	3.93		1512	1128
280	220	4.27		1810	1357
290	230	4.87		1930	1486
300	240	5.40		2105	1622
393	310	5.87		2378	1864
403	320	6.40		2554	2019
413	330	7.09		2660	2142
423	340	7.33		2841	2297
519	410	7.73		3103	2541
529	420	8.27		3281	2702
539	430	8.80		3408	2840
549	440	9.27		3556	2979
650	510	9.40		3869	3297
660	520	10.00		4055	3452
670	530	10.47		4220	3595
680	540	10.87		4339	3715
690	550	11.20		4447	3824
700	560	11.54		4632	3982
710	570	11.81		4739	4073
720	580	12.14		4877	4189
730	590	12.81		5009	4308

Table A.17 Raw and Reduced Strain Data of *PS_SG_G3.3*

Strain Time (sec)	Load Time (sec)	Load (kN)	Microstrains		
			L1	L2	L3
9	0	0.00	117	116	Sensor Failure
19	10	0.80	248	243	
29	20	1.26	425	431	
39	30	1.66	589	608	
49	40	2.13	759	789	
133	110	2.60	915	966	
143	120	3.13	1061	1109	
153	130	3.60	1252	1330	
163	200	3.40	1423	1516	
268	220	4.60	1955	2107	
278	230	5.20	2136	2308	
288	240	5.60	2310	2499	
379	310	6.27	2624	2856	
389	320	6.80	2804	3047	
399	330	7.27	2961	3198	
493	400	7.80	3296	3577	
503	410	8.20	3470	3746	
513	420	8.80	3681	3991	
523	430	9.34	3834	4134	
637	500	10.20	4539	4880	
647	510	10.67	4743	5101	
657	520	11.14	4929	5298	
667	530	11.54	5118	5504	
677	540	12.01	5294	5680	
687	550	12.41	5454	5855	
797	570	12.85	6057	6486	
807	580	13.05	6223	6661	
817	590	13.34	6367	6803	
827	600	13.67	6512	6952	
837	610	13.94	6621	7063	
847	620	14.07	6757	7205	

Table A.18 Raw and Reduced Strain Data of *PS_SG_G3.4*

Strain Time (sec)	Load Time (sec)	Load (kN)	Microstrains		
			L1	L2	L3
13	0	0.00	152	139	96
23	10	0.66	270	251	172
33	20	1.20	432	397	276
43	30	1.60	550	514	361
53	40	2.13	730	666	469
140	140	3.33	842	751	525
150	150	4.07	997	894	637
160	160	4.73	1153	1029	747
170	170	5.33	1302	1163	858
180	180	5.93	1406	1260	938
292	250	6.33	1760	1533	1190
302	260	6.93	1908	1663	1312
312	270	7.53	2055	1791	1432
404	340	7.07	2285	1941	1607
414	350	7.94	2447	2076	1743
424	360	8.60	2610	2216	1881
505	430	8.54	517	297	241
515	440	9.40	647	425	332
525	450	10.07	789	548	428
605	520	10.87	864	618	467
615	530	10.20	1020	758	579
625	540	11.07	1200	918	710
635	550	11.60	1355	1059	830
729	620	12.54	1626	1299	1037
739	630	11.47	1797	1450	1173
749	640	12.41	1952	1593	1304
759	650	12.94	2093	1723	1426
781	720	13.74	2124	1727	1438
791	730	13.87	2093	1701	1416
801	740	13.87	2100	1701	1416
811	750	14.01	2070	1675	1398
821	760	14.14	2093	1683	1403
831	770	14.27	2064	1660	1388
841	780	14.34	2168	1745	1469
851	790	13.61	2365	1911	1626
861	800	13.41	2519	2050	1766
871	810	13.94	2704	2207	1920
935	880	14.41	2614	2094	1845
945	890	14.61	2649	2104	1860
955	900	14.47	2753	2208	1964
965	910	14.54	2966	2385	2135
975	920	14.54	3158	2541	2295
985	930	14.54	3299	2665	2422

Table A.19 Raw and Reduced Strain Data of *PS_P_G4.1*

Strain Time (sec)	Load Time (sec)	Load (kN)	Microstrains
			L1
5	0	0.00	20
15	10	0.40	76
25	20	0.73	154
35	30	1.13	312
45	40	1.66	502
55	50	2.26	692
129	120	2.93	926
139	130	3.60	1136
213	200	4.40	1394
223	210	5.27	1629
233	220	5.93	1831
308	290	6.80	2111
318	300	7.33	2316
379	360	7.40	2286
389	370	8.40	2553
399	380	9.34	2786
473	450	10.00	3017
483	460	10.94	3235
557	530	11.47	3477
567	540	12.27	3754
577	550	13.01	3992
649	620	13.74	4233
659	630	14.34	4512
714	700	14.87	4465
724	710	15.79	4522
734	720	16.34	4818
744	730	16.94	5120
754	740	17.48	5419
764	750	17.94	5699
774	760	18.21	5942

Table A.20 Raw and Reduced Strain Data of *PS_P_G4.2*

Strain Time (sec)	Load Time (sec)	Load (kN)	Microstrains
			L1
9	0	0.00	129
19	10	0.60	348
29	20	0.93	586
39	30	1.40	823
49	40	1.86	1038
143	60	2.33	1495
153	70	2.80	1756
163	80	3.26	2002
173	140	3.80	2234
268	210	4.27	2735
278	220	4.87	3003
288	230	5.40	3265
298	240	5.80	3529
392	310	6.33	4034
402	320	6.80	4321
412	330	7.33	4590
422	340	7.73	4903
516	360	8.20	5430
526	370	8.67	5716
536	380	9.20	5995
546	440	9.60	6316
645	460	9.60	7015
655	470	10.20	7303
665	480	10.60	7591
675	490	10.87	7905
685	550	11.20	8199
784	570	11.27	8929
794	580	11.74	9252
804	590	12.01	9539
814	600	12.41	9840
824	610	12.61	10133
834	670	12.94	10393

Table A.21 Raw and Reduced Strain Data of *PS_P_G4.3*

Strain Time (sec)	Load Time (sec)	Load (kN)	Microstrains
			L1
10	0	0.00	60
20	10	0.53	202
30	20	1.00	353
40	30	1.53	484
138	100	2.00	815
148	110	2.66	968
158	120	3.26	1166
168	130	3.87	1334
264	200	4.67	1677
274	210	5.33	1875
284	220	6.13	2098
382	320	8.00	2253
392	330	9.14	2478
402	340	10.00	2674
412	350	10.74	2899
506	420	11.34	3261
516	430	12.07	3498
526	440	12.94	3709
622	510	13.27	4146
632	520	14.01	4396
642	530	14.61	4598
726	600	14.87	4800
736	610	15.54	5012
746	620	16.08	5271
756	630	16.28	5484
862	710	16.88	6197
872	720	16.94	6425
882	730	17.28	6732

Table A.22 Raw and Reduced Strain Data of *PS_P_G4.4*

Strain Time (sec)	Load Time (sec)	Load (kN)	Microstrains
			L1
11	0	0.00	138
21	10	0.60	342
31	20	1.13	623
41	30	1.73	1040
51	40	2.46	1642
129	190	4.40	1812
139	200	5.47	3900
149	210	6.33	6353
159	220	7.20	10091

Table A.23 Raw and Reduced Strain Data of *PS_SG_G4.1*

Strain Time (sec)	Load Time (sec)	Load (kN)	Microstrains
			L1
3	0	0.00	57
13	10	0.86	229
23	20	1.60	458
33	30	2.26	714
107	100	3.13	1015
117	110	3.93	1310
191	180	4.87	1602
201	190	5.67	1918
275	260	6.47	2222
285	270	7.40	2547
359	340	8.20	2872
369	350	9.14	3185
444	420	9.80	3526
454	430	10.67	3869
525	500	11.40	4078
535	510	12.21	4425
545	520	13.14	4777
555	530	13.34	5129
565	540	14.25	5589
642	610	14.74	5939
652	620	15.54	6304
662	630	16.08	6662
736	700	16.34	7025
746	710	17.08	7397
821	780	17.48	7571
831	790	18.14	7945
841	800	18.61	8312
851	810	18.88	8679
871	830	19.14	9395
966	920	19.57	10510
1049	1000	19.61	11538
1059	1010	19.95	11936
1069	1020	20.15	11544

Table A.24 Raw and Reduced Strain Data of *PS_SG_G4.2*

Strain Time (sec)	Load Time (sec)	Load (kN)	Microstrains
			L1
7	0	0.00	148
17	10	0.93	376
27	20	1.53	608
37	30	2.33	846
129	100	3.06	1230
139	110	3.87	1482
149	120	4.87	1736
243	190	5.60	2226
253	200	6.67	2501
263	210	7.67	2781
353	280	8.40	3192
363	290	9.40	3466
455	360	10.20	3952
465	370	11.27	4259
475	380	12.34	4544
568	450	13.07	5052
578	460	14.01	5357
588	470	14.81	5641
680	540	15.47	6195
690	550	16.48	6503
700	560	17.14	6812
792	630	17.41	7370
802	640	18.21	7680
812	650	18.81	8096
915	720	18.61	8955
925	730	19.48	9264
935	740	20.28	9671
945	750	20.55	10028
955	760	20.88	10245

Table A.25 Raw and Reduced Strain Data of *PS_SG_G4.3*

Strain Time (sec)	Load Time (sec)	Load (kN)	Microstrains
			L1
10	0	0.00	46
20	10	0.46	213
30	20	1.06	399
40	30	1.80	582
136	100	2.46	917
146	110	3.20	1125
156	120	4.07	1333
252	190	4.80	1750
262	200	5.67	2003
272	210	6.67	2242
369	280	7.47	2737
379	290	8.40	3017
389	300	9.34	3230
484	370	10.14	3766
494	380	10.94	4043
504	390	11.87	4237
597	460	12.81	4761
607	470	13.67	5026
617	480	14.54	5299
712	550	15.07	5821
722	560	15.94	6131
732	570	16.68	6409
830	640	16.94	7020
840	650	17.88	7304
850	660	18.54	7592
860	670	19.01	7840
960	740	19.01	8519
970	750	19.75	8914
980	760	20.08	9208
990	770	20.55	9505
1000	780	20.95	9780

Table A.26 Raw and Reduced Strain Data of *PS_SG_G4.4*

Strain Time (sec)	Load Time (sec)	Load (kN)	Microstrains
			L1
7	40	1.66	110
17	50	2.60	284
27	60	3.26	463
37	70	4.20	660
133	130	5.00	1067
153	150	5.73	1524
163	160	6.60	1761
255	220	7.53	2178
275	240	8.34	2687
355	310	8.74	2796
365	320	10.00	3067
375	330	10.87	3327
457	390	11.81	3529
477	410	12.47	4078
487	420	13.41	4355
568	480	14.21	4515
588	500	14.61	5078
598	510	15.54	5368
681	570	16.28	5587
701	590	16.54	6164
711	600	17.34	6451
783	660	18.01	6462
803	680	18.08	6951
813	690	18.81	7258
823	700	19.41	7541
898	790	20.35	7579
908	800	20.68	7836
918	810	20.88	8147
928	820	21.15	8438
938	830	21.35	8735
948	840	21.41	9027

Table A.27 Raw and Reduced Strain Data of *PS_P_G5.1*

Strain Time (sec)	Load Time (sec)	Load (kN)	Microstrains
			L1
8	0	0.00	97
18	10	0.73	268
28	20	1.33	483
38	30	2.00	686
131	100	2.66	1086
141	110	3.33	1360
151	120	3.93	1587
243	190	4.73	2008
253	200	5.40	2267
263	210	6.07	2513
356	280	6.67	2946
366	290	7.33	3186
376	300	8.00	3409
469	370	8.60	3851
479	380	9.27	4107
489	390	9.94	4353
593	460	10.87	5068
603	470	11.40	5335
613	480	11.94	5566
684	550	12.07	5477
694	560	12.74	5629
704	570	13.14	5892
714	580	13.54	6175
724	590	13.81	6427
734	650	12.87	6664

Table A.28   Raw and Reduced Strain Data of *PS_P_G5.2*

Strain Time (sec)	Load Time (sec)	Load (kN)	Microstrains
			L1
8	0	0.00	186
18	10	0.86	412
28	20	1.46	723
38	30	2.13	994
140	100	3.33	1711
150	110	4.07	2036
242	170	4.67	2490
252	180	5.40	2818
262	190	5.93	3086
357	260	6.47	3657
367	270	7.13	4021
377	280	7.80	4310
387	290	8.34	4569
484	360	8.80	5239
494	370	9.34	5555
504	380	9.87	5884
514	390	10.34	6176
524	400	10.74	6497
622	470	10.94	7174
632	480	11.54	7506
642	490	12.01	7778
652	500	12.41	8113
662	510	12.54	8440

Table A.29 Raw and Reduced Strain Data of *PS_P_G5.3*

Strain Time (sec)	Load Time (sec)	Load (kN)	Microstrains
			L1
10	0	0.00	120
20	10	0.80	316
30	20	1.33	487
40	30	1.93	692
137	100	2.53	1033
147	110	3.13	1278
157	120	3.73	1461
253	190	4.33	1870
263	200	4.93	2096
273	210	5.60	2292
364	280	6.04	2641
374	290	6.73	2865
384	300	7.33	3062
479	370	7.80	3507
489	380	8.40	3717
499	390	8.94	3953
593	460	9.27	4377
603	470	9.94	4600
613	480	10.40	4829
623	490	10.80	5067
720	560	11.07	5552
730	570	11.54	5809
740	580	12.07	6016
750	590	12.47	6252
760	600	12.81	6487
854	670	12.81	6839
864	680	13.34	7106
874	690	13.74	7332

Table A.30 Raw and Reduced Strain Data of *PS_P_G5.4*

Strain Time (sec)	Load Time (sec)	Load (kN)	Microstrains
			L1
6	0	0.00	83
16	10	0.86	233
26	20	1.46	396
36	30	2.33	578
126	100	3.40	993
136	110	4.47	1267
146	120	5.53	1535
234	190	6.60	1909
244	200	7.60	2175
332	270	8.67	2622
342	280	9.74	2919
352	290	10.87	3160
439	360	11.74	3630
449	370	13.01	3918
459	380	14.01	4170
545	450	14.87	4616
555	460	15.88	4909
565	470	16.68	5196
653	540	17.41	5686
663	550	18.28	6263
673	560	18.94	6610
765	630	19.34	7390
775	640	20.35	7730
785	650	21.01	8065

Table A.31 Raw and Reduced Strain Data of *PS_SG_G5.1*

Strain Time (sec)	Load Time (sec)	Load (kN)	Microstrains
			L1
13	0	0.00	94
23	10	0.46	137
33	20	0.80	209
43	30	1.20	321
53	40	1.86	539
63	50	2.60	799
154	120	3.60	1311
164	130	4.67	1608
174	140	5.60	1907
184	150	6.40	2211
276	220	7.20	2726
286	230	8.54	3028
296	240	9.07	3319
306	250	9.87	3620
407	320	10.54	4142
417	330	11.40	4460
427	340	12.85	4774
437	350	13.21	5071
521	420	13.81	5442
531	430	14.67	5762
623	500	15.47	6476
633	510	15.94	6813
643	520	16.74	7123
663	540	17.34	7798
764	610	17.88	8829
774	620	19.08	9183
784	630	19.41	9537
794	640	19.75	9892
886	710	19.68	10767
896	720	20.12	11159
906	730	20.55	11566
926	750	20.68	12399
936	760	20.88	12773
946	770	20.95	13174

Table A.32 Raw and Reduced Strain Data of *PS_SG_G5.2*

Strain Time (sec)	Load Time (sec)	Load (kN)	Microstrains
			L1
9	0	0.00	8
19	10	0.46	117
29	20	1.06	276
39	30	1.86	451
49	40	2.66	700
144	110	3.66	1281
154	120	4.53	1552
164	130	5.67	1833
174	140	6.48	2119
184	150	7.47	2409
272	220	8.58	2816
282	230	9.34	3090
360	290	9.07	3339
370	300	10.14	3642
380	310	11.07	3952
390	320	12.41	4529
400	330	12.94	4579
487	400	13.87	5075
497	410	14.74	5364
571	470	14.47	5543
581	480	15.88	5859
591	490	16.41	6192
601	500	17.01	6494
699	580	18.01	7306
709	590	18.68	7616
719	600	19.21	7940
825	670	19.28	9104
835	680	19.95	9434
845	690	20.48	9772
855	700	20.95	10087
865	710	21.28	10438
875	720	21.68	10761
885	730	21.95	11210

Table A.33 Raw and Reduced Strain Data of *PS_SG_G5.3*

Strain Time (sec)	Load Time (sec)	Load (kN)	Microstrains
			L1
0	0	0.00	0
7	10	0.46	32
17	20	1.06	152
27	30	1.86	323
37	40	2.66	516
100	100	2.66	518
110	110	3.66	525
120	120	4.53	676
130	130	5.67	942
140	140	6.48	1216
150	150	7.47	1453
242	210	7.47	1908
252	220	8.58	2196
262	230	9.34	2470
331	300	10.14	2487
341	310	11.07	2587
351	320	12.41	2869
361	330	12.94	3143
463	400	13.87	3541
473	410	14.74	3833
554	480	15.88	3975
564	490	16.41	4259
644	570	17.14	4573
654	580	18.01	4686
664	590	18.68	5009
674	600	19.21	5272
739	670	19.28	5256
749	680	19.95	5282
759	690	20.48	5278
769	700	20.95	5505
779	710	21.28	5793
789	720	21.68	6114
799	730	21.95	6378

Table A.34 Raw and Reduced Strain Data of *PS_SG_G5.4*

Strain Time (sec)	Load Time (sec)	Load (kN)	Microstrains
			L1
6	0	0.00	99
16	10	0.93	261
26	20	1.80	484
117	90	2.66	835
127	100	3.60	1087
137	110	4.53	1347
232	180	5.47	1823
242	190	6.47	2090
252	200	7.40	2346
343	270	8.14	2728
353	280	9.14	2980
363	290	10.00	3260
458	360	10.87	3773
468	370	11.81	4043
478	380	12.74	4318
488	390	13.54	4576
580	460	14.14	5013
590	470	15.01	5290
600	480	15.81	5556
691	550	16.21	5966
701	560	17.01	6239
711	570	17.68	6520
822	650	18.54	7504
832	660	19.01	7781
842	670	19.41	8065
852	680	19.95	8351
862	690	20.21	8634
977	770	20.61	9706
987	780	21.08	9968
997	790	21.35	10235
1007	800	21.35	10576
1017	810	20.88	10852

Table A.35 Raw and Reduced Strain Data of *PS_A_G5.1*

Strain Time (sec)	Load Time (sec)	Load (kN)	Microstrains
			L1
13	0	0.00	0
23	10	0.53	410
33	20	0.93	685
43	30	1.26	978
53	40	1.73	1287
63	50	2.13	1590
148	120	2.60	2285
158	130	2.86	2582
168	140	3.40	2940
178	150	3.80	3271
188	160	4.20	3586
287	230	4.67	4346
297	240	5.07	4693
307	250	5.53	5018
317	260	5.93	5367
327	270	6.33	5735
337	280	6.73	6087
436	350	7.07	6914
446	360	7.47	7267
456	370	7.87	7604
466	380	8.20	7993
476	390	8.60	8338
486	400	8.87	8749
585	470	9.07	9615
595	480	9.47	9986
605	490	9.80	10344

Table A.36 Raw and Reduced Strain Data of *PS_A_G5.2*

Strain Time (sec)	Load Time (sec)	Load (kN)	Microstrains
			L1
8	0	0.00	126
18	10	0.86	355
28	20	1.66	507
38	30	2.46	787
130	100	3.20	1167
140	110	4.00	1389
150	120	4.80	1648
241	190	5.53	2009
251	200	6.33	2240
261	210	7.13	2481
355	280	7.87	2909
365	290	8.67	3148
375	300	9.40	3413
480	370	10.94	4147
490	380	11.47	4391
500	390	12.27	4626
595	460	12.67	5126
605	470	13.41	5386
615	480	13.94	5640
625	490	14.41	5924
721	560	14.54	6443
731	570	15.27	6675
741	580	15.81	6956
751	590	16.14	7176
761	600	16.48	7407
867	680	16.68	7799
877	690	17.34	8024
887	700	17.61	8204

Table A.37 Raw and Reduced Strain Data of *PS_A_G5.3*

Strain Time (sec)	Load Time (sec)	Load (kN)	Microstrains
			L1
12	0	0.00	0
22	10	1.00	203
32	20	1.66	415
42	30	2.40	706
124	90	2.26	880
134	100	3.20	1213
144	110	4.00	1528
154	120	4.82	1874
237	180	4.60	2115
247	190	5.53	2459
257	200	6.33	2779
267	210	7.20	3086
351	270	6.87	3369
361	280	7.94	3728
371	290	8.80	4138
381	300	9.60	4555
391	310	10.34	5021
474	370	9.87	5416
484	380	10.94	6228
494	390	11.67	8928
504	400	12.47	14795
565	460	11.74	15208
575	470	12.94	15269
585	480	13.67	16897
595	490	14.21	18193
605	500	14.81	21631

Table A.38 Raw and Reduced Strain Data of *PS_A_G5.4*

Strain Time (sec)	Load Time (sec)	Load (kN)	Microstrains
			L1
6	0	0.00	75
16	10	0.73	290
26	20	1.46	523
36	30	2.20	754
131	100	2.93	1256
141	110	3.66	1527
151	120	4.40	1778
161	130	5.31	2067
252	200	5.87	2488
262	210	6.60	2752
272	220	7.33	3047
355	280	7.07	3242
365	290	8.07	3521
375	300	8.87	3799
385	310	9.54	4095
490	380	10.80	4903
500	390	11.47	5199
510	400	12.07	5485
605	470	12.54	6034
615	480	13.07	6332
625	490	13.74	6622
635	500	14.14	6924
732	570	14.27	7509
742	580	14.87	7808
752	590	15.47	8093
762	600	15.81	8386
772	610	16.14	8666
894	680	16.48	9939
904	690	16.88	10229
914	700	17.21	10503
924	710	17.48	10778
934	720	17.68	11197
944	730	17.74	11500

Table A.39 Raw and Reduced Strain Data of *PS_H_G5.1*

Strain Time (sec)	Load Time (sec)	Load (kN)	Microstrains L1
---	0	0.00	Sensor Failure
---	10	0.73	
---	20	1.53	
---	30	2.34	
---	100	3.27	
---	110	4.27	
---	120	5.20	
---	190	6.21	
---	200	7.21	
---	210	8.27	
---	280	9.34	
---	290	10.21	
---	300	11.08	
---	370	12.01	
---	380	13.14	
---	390	14.01	
---	460	14.68	
---	470	15.68	
---	540	16.21	
---	550	17.08	
---	620	17.75	
---	630	18.68	
---	640	19.28	
---	710	19.48	
---	720	20.35	
---	730	21.02	
---	800	21.08	
---	810	21.82	
---	820	22.42	
---	880	22.89	
---	910	23.42	
---	920	23.89	
---	930	24.29	
---	940	24.42	
---	1020	24.69	
---	1030	25.22	
---	1040	25.49	
---	1060	25.69	
---	1070	25.76	
---	1080	25.89	
---	1090	25.96	
---	1100	26.16	

Table A.40 Raw and Reduced Strain Data of *PS_H_G5.2*

Strain Time (sec)	Load Time (sec)	Load (kN)	Microstrains
			L1
8	0	0.00	154
18	10	0.80	346
28	20	1.73	560
38	30	2.66	817
128	100	3.66	1236
138	110	4.80	1534
227	180	5.80	1957
237	190	6.87	2264
327	260	7.87	2702
337	270	9.07	3050
429	340	10.07	3568
439	350	11.07	3913
449	360	12.27	4252
540	430	13.07	4774
550	440	14.14	5070
639	510	15.01	5587
649	520	16.08	5941
738	590	16.81	6451
748	600	17.74	6792
840	690	18.08	7421
850	700	19.21	7761
860	710	19.95	8124
955	780	20.15	8872
965	790	21.28	9210
975	800	21.88	9570
985	810	22.48	9926
1090	890	23.28	10982
1100	900	23.88	11323
1110	910	24.35	11662
1120	920	24.75	12035
1248	1010	25.15	14108
1258	1020	25.55	14610
1268	1030	25.82	14965
1278	1040	26.02	15885

Table A.41 Raw and Reduced Strain Data of *PS_H_G5.3*

Strain Time (sec)	Load Time (sec)	Load (kN)	Microstrains
			L1
12	0	0.00	93
22	10	0.46	249
32	20	1.13	450
42	30	1.93	662
52	40	2.86	920
159	110	5.00	1726
169	120	6.07	2016
263	190	7.07	2487
273	200	8.20	2785
283	210	9.34	3097
376	280	10.27	3609
386	290	11.40	3925
478	360	12.34	4410
488	370	13.47	4726
541	440	14.41	4787
551	450	15.34	4789
571	470	16.19	4949
581	480	17.21	5275
591	490	18.14	5594
675	560	18.54	5867
685	570	19.68	6192
695	580	20.28	6507
791	650	20.55	7202
801	660	21.48	7533
811	670	22.21	7870
821	680	22.68	8203
899	750	23.55	8283
909	760	24.02	8602
919	770	24.55	8947
949	800	24.62	9906
996	860	25.28	9948
1006	870	25.62	9953
1016	880	25.95	9954
1026	890	26.22	9982
1066	930	26.48	11256
1076	940	26.95	11572

Table A.42 Raw and Reduced Strain Data of *PS_H_G5.4*

Strain Time (sec)	Load Time (sec)	Load (kN)	Microstrains
			L1
7	0	0.00	55
17	10	0.80	184
27	20	1.53	357
37	30	2.46	580
130	100	3.26	974
140	110	4.40	1226
150	120	5.40	1479
241	190	6.40	1865
251	200	7.40	2124
261	210	8.54	2376
357	280	9.34	2897
367	290	10.47	3149
377	300	11.47	3416
387	310	12.47	3653
480	380	13.34	4113
490	390	14.21	4381
500	400	15.14	4647
510	410	16.01	4920
606	480	16.54	5438
616	490	17.54	5721
626	500	18.21	5990
636	510	18.88	6260
728	580	19.21	6661
738	590	20.08	6932
748	600	20.75	7221
843	670	20.95	7731
853	680	21.68	7995
863	690	22.28	8267
873	700	22.68	8533
979	780	23.15	9323
989	790	23.75	9586
999	800	24.15	9841
1009	810	24.42	10104
1055	890	24.62	10075
1065	900	25.02	10067
1075	910	25.35	10043
1085	920	25.48	10038
1095	930	25.75	10298
1105	940	25.82	10562
1115	950	26.02	10822
1135	970	26.08	11386
1145	980	26.22	11648
1155	990	26.42	11873

Table A.43 Raw and Reduced Strain Data of *FS_SG_G7.1*

Time (sec)	Load (kN)	Microstrains		
		L1	L3	L7
0	0.00	0	0	0
20	6.36	239	195	138
75	14.15	522	500	246
133	21.15	840	783	360
190	34.11	1426	1398	478
244	45.55	1928	1891	523
277	59.36	2407	2401	704
340	72.34	2788	2822	917
384	85.47	3181	3235	1148
440	99.73	3573	3674	1389
480	112.23	3955	4094	1624
505	125.62	4360	4516	1861
545	137.48	4691	4876	2061
588	150.21	4897	4439	2259
647	158.89	N/A	4841	2405

Table A.44 Raw and Reduced Strain Data of *FS_SG_G7.2*

Time (sec)	Load (kN)	Microstrains					
		L1	L2	L4	L6	L10	L12
0	0.00	0	0	0	0	0	0
16	7.05	134	195	92	238	275	245
88	14.55	357	278	175	430	472	380
97	21.30	577	462	293	581	613	467
160	32.16	1120	839	495	701	771	557
226	44.09	1879	1404	733	817	908	634
283	59.52	2687	2007	1006	1160	1350	920
353	73.52	3321	2483	1169	1457	1743	1167
411	85.57	3855	2880	1236	1694	2066	1363
507	99.41	367	3351	1201	1961	2422	1627
543	113.43	131	3919	954	2265	2852	1908
591	126.58	N/A	4243	510	2504	3221	2205
657	137.39	N/A	N/A	168	2760	3622	2445
690	139.34	N/A	N/A	-223	2693	4711	2140

Table A.45 Raw and Reduced Strain Data of *FS_SG_G7.3*

Time (sec)	Load (kN)	Microstrains					
		L1	L2	L4	L6	L10	L12
0	0.00	0	0	0	0	0	0
104	7.43	147	184	269	160	187	145
119	14.30	322	365	524	297	343	265
161	21.63	557	622	819	394	467	371
213	32.52	972	1049	1299	479	571	444
260	45.05	1590	1583	1963	534	639	468
307	59.05	2171	2169	2735	754	864	632
397	73.02	2609	2638	3335	934	1113	793
450	86.11	2960	3185	3933	1142	1359	974
458	99.40	3360	3789	4477	1335	1578	1154
520	112.53	3786	4405	5013	1497	1794	1327
572	127.52	4243	5119	5569	1716	2046	1523
618	141.46	4698	5880	3644	1905	2262	1712
-35	173.48	2482	N/A	N/A	N/A	N/A	443

Table A.46 Raw and Reduced Strain Data of *FS_SG_G7.4*

Time (sec)	Load (kN)	Microstrains		
		L1	L3	L7
0	0.00	0	0	0
13	7.03	172	197	97
55	14.39	391	446	200
110	21.90	634	721	304
155	32.35	989	1116	439
199	45.99	1493	1677	589
254	59.21	1987	2217	747
306	72.94	2405	2722	958
349	86.30	2726	3180	1151
397	99.30	3047	3664	1334
466	113.08	3164	4318	1548
491	126.43	3665	5042	1781
540	138.35	4542	6380	2066
617	150.53	-156	-50	3291

Table A.47 Raw and Reduced Strain Data of *FS_SG_G7.5*

Time (sec)	Load (kN)	Microstrains						
		L1	L2	L5	L6	L8	L9	L10
0	0.00	0	0	0	0	0	0	0
8	7.09	278	330	-34	151	-17	-124	193
102	9.94	555	665	-86	307	-57	-276	413
121	21.76	808	963	-107	441	-102	-425	589
207	32.97	1054	1475	-129	643	-169	-673	856
222	45.41	1794	2080	-157	868	-209	-989	1151
273	58.81	2366	2727	46	1168	30	-1411	1548
328	72.44	2927	3425	-203	1499	999	-1833	2013
383	85.97	3415	4209	-203	1817	3586	-2194	2468
451	99.84	4066	4875	-188	2128	2805	-2512	2944
507	113.25	4814	5589	-173	2433	1316	-2786	3446
553	126.51	6036	18619	-143	2775	1281	-572	1105
652	135.19	1131	694	1112	892	1246	-2248	1488

Table A.48 Raw and Reduced Strain Data of *FS_SG_G7.6*

Time (sec)	Load (kN)	Microstrains						
		L1	L2	L5	L6	L8	L9	L10
0	0.00	0	0	0	0	0	0	0
54	14.00	611	676	-821	265	-200	-3980	209
108	26.16	1302	1398	-940	512	204	-4068	392
166	40.51	2084	2239	-1044	869	-2166	-4236	697
212	54.71	2708	3030	-1187	1196	-2166	-4408	995
258	68.86	3246	3834	-1290	1364	-2166	-4554	1262
304	82.63	3900	4960	-1103	1416	-2166	-4695	1503
349	93.88	4302	6954	-1148	1655	-2166	-4800	1744

Table A.49 Raw and Reduced Strain Data of *FS_SG_G7.7*

Time (sec)	Load (kN)	Microstrains						
		L1	L2	L5	L6	L8	L9	L10
0	0.00	0	Sensor Failure	0	0	0	0	0
51	15.54	371		-92	144	-108	86	189
133	27.84	665		-166	254	-199	156	338
138	40.78	975		-244	387	-326	254	531
187	54.25	1229		-342	550	-489	374	773
265	70.37	1500		-454	743	-678	509	1029
307	85.81	1747		-598	957	-857	654	1304
361	98.52	5897		-723	1111	-992	760	1511
407	113.07	2033		-883	1523	-1134	913	1774
455	126.48	-614		-1048	1486	347	1234	2246
545	132.40	350		-143	538	473	-4621	100

Table A.50 Raw and Reduced Strain Data of *FS_SG_G7.8*

Time (sec)	Load (kN)	Microstrains						
		L1	L2	L4	L5	L6	L11	L12
0	0	0	0	0	0	0	0	0
45	12.53	453	580	446	-65	88	-89	62
88	23.34	882	1117	866	-119	162	-193	146
130	37.26	1507	1878	1470	-162	214	-287	228
174	54.79	2204	2869	2251	-307	410	-557	450
216	71.36	2712	3602	2902	-488	600	-833	633
254	85.08	3107	4068	3465	-674	762	-1004	784
294	99.65	3499	4516	4095	-880	931	-1321	939
341	113.46	4004	5236	4859	-1112	1105	-1587	1092
384	126.16	4311	2531	5560	-1266	1303	-1967	1284
473	136.45	-276	1395	-236	-1479	1694	-1635	2247

Table A.51 Raw and Reduced Strain Data of *FS_SG_G7.9*

Time (sec)	Load (KN)	Microstrains			
		L1	L4	L11	L12
0	0.00	0	0	0	0
27	14.78	8	8	-1	2
71	28.27	448	504	-134	159
107	41.96	957	1064	-275	324
179	57.09	1498	1675	-413	498
222	82.61	2062	2332	-549	686
254	94.27	2823	3350	-807	1059
292	116.25	3188	3826	-926	1233
328	132.33	3845	4679	-1134	1548
362	145.48	4101	5298	-1320	1822
399	163.68	4485	5904	-1468	2073
454	176.59	6081	6846	-1658	2424

Table A.52 Raw and Reduced Strain Data of *FS_SG_G7.10*

Time (sec)	Load (KN)	Microstrains			
		L1	L4	L11	L12
0	0.00	0	0	0	0
31	14.30	342	485	-138	217
72	28.13	713	992	-233	391
118	41.67	1114	1521	-325	544
154	55.88	1552	2102	-405	711
191	68.55	1871	2597	-477	901
231	81.74	2143	3071	-535	1098
267	99.05	2563	3740	-676	1339
307	117.45	2966	4508	-755	1582
344	130.79	3270	5167	-806	1761
395	147.11	3617	6060	-833	2024
441	163.93	4210	7142	-809	2213

Table A.53 Raw and Reduced Deflection Data of *PS_P_G1*

Platform 1		Platform 2		Platform 3		Platform 4		Platform 5	
Load (kN)	Defl. (mm)	Load (kN)	Defl. (mm)	Load (kN)	Defl. (mm)	Load (kN)	Defl. (mm)	Load (kN)	Defl. (mm)
0.00	0.00	0.00	0.00	0.00	0.00	0.00	0.00	0.00	0.00
0.27	0.08	0.33	0.36	0.33	0.38	0.40	0.25	0.73	0.46
0.53	0.48	0.47	0.97	0.67	0.84	0.60	0.51	1.13	0.79
0.60	0.89	0.93	1.35	1.13	1.27	1.00	0.86	1.73	1.24
0.80	1.30	1.47	1.83	1.60	1.68	1.33	1.24	2.27	1.68
1.20	1.68	1.87	2.21	2.20	2.18	2.07	1.70	2.07	1.68
1.60	2.08	1.73	2.21	2.00	2.18	2.47	2.06	2.67	2.06
1.87	2.51	2.40	2.64	2.74	2.62	2.20	2.06	3.34	2.44
1.53	2.51	3.00	3.00	3.40	3.05	2.94	2.44	4.05	2.87
2.27	2.87	3.60	3.43	4.07	3.51	3.60	2.92	4.80	3.23
2.60	3.28	4.07	3.84	3.67	3.51	3.40	2.92	5.34	3.73
3.00	3.68	3.74	3.84	4.54	3.91	4.07	3.28	4.80	3.73
3.47	4.11	4.60	4.22	5.27	4.29	4.80	3.71	5.87	4.09
3.80	4.50	5.07	4.50	5.94	4.75	5.54	4.14	6.54	4.52
3.40	4.50	4.87	4.50	6.47	5.13	5.20	4.14	7.14	5.38
4.00	4.88	5.54	5.00	7.14	5.56	6.07	4.55	7.81	5.38
4.47	5.31	6.27	5.41	7.74	6.02	6.74	5.00	7.21	5.77
4.80	5.69	6.87	5.79	8.34	6.43	7.34	5.41	8.07	6.17
5.20	6.10	7.34	6.22	8.87	6.83	6.87	5.41	8.52	6.58
5.54	6.48	7.07	6.22	8.01	6.83	7.74	5.79	9.34	6.99
5.00	6.48	7.94	6.76	9.07	7.19	8.41	6.22	10.01	6.99
5.80	6.93	8.43	7.04	9.61	7.59	8.94	6.63	9.41	7.39
6.07	7.37	8.87	7.39	10.28	8.00	8.47	6.63	10.14	7.57
6.47	7.77	9.27	7.77	10.68	8.43	9.41	7.01	10.81	8.28
6.74	8.15	8.61	7.77	9.94	8.43	10.08	7.39	11.41	8.71
7.07	8.59	9.47	8.15	10.74	8.81	10.56	7.75	11.88	9.07
7.34	9.12	9.94	8.53	11.34	9.17	11.08	8.20	12.19	9.45
7.01	9.12	10.54	8.92	11.88	9.63	10.88	8.20	12.54	9.45
7.54	9.50	10.88	9.35	12.32	10.03	11.48	8.61	11.25	9.78
8.21	9.86	10.01	9.12	12.88	10.41	11.88	8.92	12.34	10.24
8.34	10.31	10.88	9.73	11.94	10.41	12.41	9.32	13.08	10.64
8.54	10.87	11.34	10.16	12.88	10.80	12.88	9.70	13.41	11.00
8.74	11.18	11.94	10.64	13.41	11.28	12.01	9.70	13.81	11.51
9.01	11.56	12.21	10.92	13.88	11.63	12.74	10.03	14.15	11.51
8.47	12.14	11.01	11.28	14.21	12.17	13.41	10.49	13.08	11.96
8.94	12.14	---	---	14.41	12.55	13.81	12.27	13.88	12.24
9.34	12.55	---	---	13.34	12.55	13.21	14.55	14.35	12.70
9.54	12.98	---	---	14.08	12.93	13.28	19.38	14.81	13.08
8.67	13.39	---	---	14.68	13.36	13.41	23.44	15.01	13.13
---	---	---	---	14.95	13.74	13.68	12.47	---	---
---	---	---	---	---	---	13.34	12.83	---	---
---	---	---	---	---	---	13.41	13.54	---	---
---	---	---	---	---	---	13.41	10.74	---	---

Table A.54 Raw and Reduced Deflection Data of *PS_P_G2*

Platform 1		Platform 2		Platform 3		Platform 4		Platform 5	
Load (kN)	Defl. (mm)	Load (kN)	Defl. (mm)	Load (kN)	Defl. (mm)	Load (kN)	Defl. (mm)	Load (kN)	Defl. (mm)
0.00	0.00	0.00	0.00	0.00	0.00	0.00	0.00	0.00	0.00
0.40	0.13	0.47	0.20	0.80	0.64	0.13	0.41	0.60	0.43
0.53	0.48	0.80	0.58	1.27	1.12	0.33	0.76	1.13	0.79
0.80	0.81	1.13	0.99	1.67	1.60	0.60	1.07	1.60	1.22
1.00	1.14	1.53	1.40	1.60	1.60	0.93	1.45	2.20	1.65
1.20	1.45	2.00	1.88	1.93	1.93	1.47	1.91	2.07	1.65
1.53	1.78	2.47	2.31	2.47	2.39	1.80	2.29	2.47	2.01
1.80	2.06	2.94	2.72	2.87	2.82	1.87	2.29	3.14	2.44
1.47	2.11	3.40	3.15	3.40	3.28	2.34	2.69	3.87	3.00
2.00	2.39	3.20	3.15	3.80	3.71	2.80	3.15	4.34	3.30
2.34	2.72	4.07	3.56	3.47	3.71	3.20	3.51	4.74	3.66
2.60	3.00	4.34	3.94	4.14	4.09	3.67	3.89	5.27	4.06
2.87	3.33	4.84	4.55	4.54	4.50	3.40	3.89	5.74	4.50
3.54	3.99	5.20	4.93	5.07	4.95	3.87	4.19	5.27	4.50
3.14	4.01	5.67	5.28	5.47	5.38	4.27	4.55	6.01	4.83
3.67	4.37	5.34	5.28	4.94	5.38	4.87	4.95	6.61	5.36
4.00	4.62	6.01	5.64	5.67	5.77	5.40	5.44	6.94	5.72
4.34	4.93	6.47	6.10	6.07	6.17	5.27	5.44	6.61	5.72
4.60	5.26	6.94	6.48	6.61	6.60	5.40	5.77	7.14	6.10
4.94	5.59	7.27	6.93	7.01	7.16	6.01	6.12	7.74	6.50
5.20	5.89	6.81	6.93	7.21	7.57	6.27	6.40	8.14	6.93
5.40	6.22	7.47	7.32	6.67	7.57	6.67	7.19	8.54	7.37
4.94	6.22	7.87	7.72	7.27	8.00	7.01	7.14	8.81	7.87
5.47	6.50	8.27	8.13	7.67	8.41	7.41	7.54	9.07	8.38
5.80	6.83	8.54	8.53	8.07	8.86	7.01	7.54	8.34	8.38
6.07	7.14	8.94	8.99	8.34	9.27	7.67	7.95	8.87	8.86
6.34	7.47	8.21	8.99	8.74	9.73	8.21	8.36	9.21	9.42
6.61	7.80	8.65	9.35	9.01	10.19	8.34	8.71	9.54	9.86
6.74	8.08	9.21	9.75	7.87	10.19	8.67	9.09	9.74	10.34
7.14	8.41	9.54	10.19	8.87	10.59	9.07	9.55	9.94	10.72
6.47	8.43	9.74	10.59	9.27	11.10	8.41	9.55	10.08	11.13
7.01	8.71	9.88	10.97	9.74	11.40	9.01	9.98	---	---
7.34	9.04	10.08	11.40	10.01	11.76	9.34	10.36	---	---
7.67	9.35	10.28	11.76	10.14	12.19	9.67	10.72	---	---
7.94	9.70	---	---	10.48	11.40	10.08	11.10	---	---
8.07	10.03	---	---	10.68	13.11	10.41	11.58	---	---
8.21	10.29	---	---	9.47	10.82	10.54	11.99	---	---
8.47	10.57	---	---	9.94	13.49	10.81	12.40	---	---
8.54	10.92	---	---	10.32	14.00	7.27	12.40	---	---
8.67	11.23	---	---	10.61	14.33	7.61	12.75	---	---
8.74	11.56	---	---	10.74	14.78	7.67	13.06	---	---
8.94	11.89	---	---	10.74	15.29	7.61	13.46	---	---
9.01	12.17	---	---	10.68	15.67	---	---	---	---
9.07	12.47	---	---	---	---	---	---	---	---
9.21	12.78	---	---	---	---	---	---	---	---
9.34	13.11	---	---	---	---	---	---	---	---
9.01	13.41	---	---	---	---	---	---	---	---
8.56	13.74	---	---	---	---	---	---	---	---
8.47	14.02	---	---	---	---	---	---	---	---
7.74	14.35	---	---	---	---	---	---	---	---

Table A.54 (continued)

Platform 1		Platform 2		Platform 3		Platform 4		Platform 5	
Load (kN)	Defl. (mm)	Load (kN)	Defl. (mm)	Load (kN)	Defl. (mm)	Load (kN)	Defl. (mm)	Load (kN)	Defl. (mm)
7.07	14.68	---	---	---	---	---	---	---	---
7.07	15.01	---	---	---	---	---	---	---	---
7.14	15.32	---	---	---	---	---	---	---	---
7.21	15.65	---	---	---	---	---	---	---	---
7.14	15.95	---	---	---	---	---	---	---	---
7.14	16.26	---	---	---	---	---	---	---	---
7.07	16.59	---	---	---	---	---	---	---	---
7.07	16.92	---	---	---	---	---	---	---	---
7.01	17.22	---	---	---	---	---	---	---	---
6.94	17.53	---	---	---	---	---	---	---	---
7.01	17.83	---	---	---	---	---	---	---	---
6.67	18.14	---	---	---	---	---	---	---	---
6.54	18.42	---	---	---	---	---	---	---	---

Table A.55 Raw and Reduced Deflection Data of *PS_P_G3*

Platform 1		Platform 2		Platform 3		Platform 4	
Load (kN)	Defl. (mm)	Load (kN)	Defl. (mm)	Load (kN)	Defl. (mm)	Load (kN)	Defl. (mm)
0.00	0.00	0.00	0.00	0.00	0.00	0.00	0.00
0.27	0.33	0.60	0.43	0.33	0.53	0.67	0.41
0.53	0.79	1.00	0.84	0.73	1.04	1.07	0.81
0.87	1.17	1.53	1.30	1.33	1.45	1.53	1.22
1.27	1.60	2.00	1.73	1.87	1.96	1.93	1.68
1.73	2.03	1.87	1.73	1.80	1.96	2.00	1.68
2.27	2.49	2.40	2.06	2.47	2.44	2.54	2.01
2.60	2.95	3.07	2.59	3.27	2.87	3.14	2.49
2.40	2.95	4.00	3.05	3.94	3.30	3.60	2.90
3.00	3.28	4.27	3.53	4.00	3.30	3.54	2.90
3.54	3.76	4.80	3.91	4.74	3.73	4.27	3.33
3.40	3.76	5.40	4.45	5.54	4.19	4.54	3.71
4.60	4.50	5.40	4.45	5.60	4.19	5.34	4.14
5.27	4.95	6.01	4.85	6.67	4.80	5.27	4.14
5.67	5.41	6.41	5.18	7.14	5.05	5.94	4.55
5.47	5.41	7.14	5.69	7.74	5.41	6.54	4.95
6.21	5.79	6.87	5.69	7.61	5.41	7.14	5.41
6.87	6.25	7.41	6.05	8.47	5.82	6.74	5.41
7.54	6.65	8.01	6.45	9.41	6.25	7.54	5.79
7.87	7.06	8.61	6.93	9.21	6.25	8.21	6.22
8.47	7.47	8.94	7.34	10.14	6.65	8.74	6.63
8.94	7.95	8.61	7.34	10.81	7.06	9.14	7.01
8.61	7.95	9.27	7.70	11.61	7.57	8.81	7.01
9.34	8.36	9.61	8.15	11.34	7.57	9.41	7.34
9.94	8.76	10.08	8.56	12.48	8.00	10.08	7.80
10.41	9.17	10.48	8.94	13.21	8.43	10.48	8.23
10.85	9.58	10.68	9.40	12.74	8.43	10.81	8.64
11.21	10.01	10.21	9.40	13.75	8.92	10.34	8.64
10.48	10.01	10.68	9.78	14.35	9.30	11.08	9.07
11.14	10.49	11.14	10.16	14.61	9.70	11.41	9.47
11.34	10.77	11.48	10.57	14.30	9.70	11.68	9.88
11.81	11.13	11.68	11.07	15.15	10.08	11.88	10.26
12.08	11.53	11.81	11.43	15.61	10.44	11.94	10.64
11.81	12.37	12.01	11.86	16.08	10.92	12.01	11.07
11.94	12.80	12.14	12.24	15.81	10.92	12.08	11.53
11.81	13.23	12.28	12.67	16.41	11.28	12.01	11.86
11.88	13.64	12.41	13.03	16.81	11.76	---	---
11.52	14.07	---	---	16.95	12.12	---	---
11.34	14.58	---	---	17.08	12.52	---	---
10.45	15.34	---	---	17.28	12.85	---	---
10.68	15.85	---	---	17.35	13.26	---	---
10.54	16.38	---	---	17.48	13.74	---	---

Table A.56 Raw and Reduced Deflection Data of *PS_SG_G3*

Platform 1		Platform 2		Platform 3		Platform 4	
Load (kN)	Defl. (mm)	Load (kN)	Defl. (mm)	Load (kN)	Defl. (mm)	Load (kN)	Defl. (mm)
0.00	0.00	0.00	0.00	0.00	0.00	0.00	0.00
0.40	0.43	0.53	0.36	0.80	0.36	0.67	0.48
0.73	0.99	0.87	0.74	1.27	0.76	1.20	0.89
1.00	1.57	1.27	1.14	1.67	1.09	1.60	1.27
1.47	1.96	1.67	3.84	2.14	1.52	2.14	1.70
1.73	2.46	2.00	1.98	1.93	1.52	1.93	1.70
1.67	2.46	1.93	1.98	2.60	1.85	2.54	2.01
2.20	2.84	2.40	2.31	3.14	2.29	3.07	2.39
2.60	3.33	2.94	2.77	3.60	2.74	3.54	2.84
3.07	3.73	3.47	3.20	3.40	2.74	3.34	2.84
3.54	4.17	3.94	3.58	4.07	3.12	4.07	3.20
4.07	4.65	3.74	3.58	4.60	3.51	4.74	3.61
3.94	4.65	4.27	3.96	5.20	3.91	5.34	4.01
4.54	5.00	4.87	4.39	5.60	4.34	5.94	4.42
5.00	5.44	5.40	4.83	5.54	4.34	5.60	4.19
5.07	5.44	5.27	4.83	6.27	4.72	6.34	4.72
5.60	5.79	5.87	5.23	6.81	5.11	6.94	5.13
6.27	6.30	6.41	5.69	7.27	5.54	7.54	5.56
6.07	6.30	7.09	6.07	7.07	5.54	7.54	5.56
6.67	6.65	7.34	6.73	7.81	5.94	7.07	5.89
7.27	7.11	7.01	6.73	8.21	6.30	7.94	6.35
8.34	7.92	7.74	6.91	8.81	6.65	8.61	5.56
8.01	7.92	8.27	7.29	9.34	7.04	9.07	5.56
8.67	8.36	8.81	7.70	8.81	7.04	8.54	5.89
9.27	8.79	9.27	8.13	10.21	7.77	9.41	6.35
9.67	9.17	8.81	8.13	10.68	8.10	10.08	6.73
10.01	9.60	9.41	8.46	11.14	8.56	10.54	6.73
9.61	9.60	10.01	8.92	11.54	8.94	10.88	7.09
10.28	9.96	10.48	9.32	12.01	9.35	10.21	7.49
10.81	10.41	10.88	9.73	12.41	9.73	11.08	7.90
11.21	10.85	11.21	10.16	11.52	10.13	11.61	8.31
11.54	11.18	11.54	10.54	12.86	10.52	12.08	8.31
11.68	11.63	11.81	10.97	13.06	10.87	12.54	8.69
10.68	11.63	12.14	11.33	13.34	11.28	11.48	9.09
11.34	11.96	12.81	11.79	13.68	11.68	12.41	9.47
11.88	12.42	11.48	11.79	13.95	12.07	12.94	9.88
12.28	12.83	12.14	12.19	14.08	12.42	13.41	9.88
12.14	13.26	12.81	12.57	14.21	12.42	13.75	10.26
12.34	13.64	13.14	13.00	13.14	12.85	13.88	10.59
12.54	14.12	13.34	13.39	14.21	13.23	13.88	11.05
12.61	14.58	13.54	13.79	14.41	13.61	14.01	11.43
12.41	15.04	13.68	14.27	14.59	13.97	14.15	11.81
12.48	15.34	13.75	14.63	---	---	14.28	12.27
12.08	15.80	13.88	15.04	---	---	14.35	12.67
---	---	14.01	15.47	---	---	13.61	13.08
---	---	14.15	15.90	---	---	13.41	13.56
---	---	14.08	16.28	---	---	13.95	13.92
---	---	13.81	16.69	---	---	14.21	13.92
---	---	13.88	17.07	---	---	14.41	14.20
---	---	13.81	17.48	---	---	14.61	14.55

Table A.56 (continued)

Platform 1		Platform 2		Platform 3		Platform 4	
Load (kN)	Defl. (mm)	Load (kN)	Defl. (mm)	Load (kN)	Defl. (mm)	Load (kN)	Defl. (mm)
---	---	---	---	---	---	14.48	14.96
---	---	---	---	---	---	14.55	15.34
---	---	---	---	---	---	14.55	15.75
---	---	---	---	---	---	14.55	16.18

Table A.57 Raw and Reduced Deflection Data of *PS_P_G4*

Platform 1		Platform 2		Platform 3		Platform 4	
Load (kN)	Defl. (mm)	Load (kN)	Defl. (mm)	Load (kN)	Defl. (mm)	Load (kN)	Defl. (mm)
0.00	0.00	0.00	0.00	0.00	0.00	0.00	0.00
0.40	0.58	0.60	0.46	0.53	0.38	0.60	0.56
0.73	1.02	0.93	0.84	1.00	0.81	1.13	0.99
1.13	1.60	1.40	1.27	1.53	1.24	1.73	1.45
1.67	1.98	1.87	1.68	1.27	1.24	2.47	1.85
2.27	2.46	1.60	1.68	2.00	1.68	2.14	1.85
2.27	2.46	2.34	2.06	2.67	2.11	3.14	2.24
2.94	2.84	2.80	2.49	3.27	2.54	4.07	2.67
3.60	3.30	3.27	2.90	3.87	2.95	4.80	3.10
3.47	3.30	3.80	3.30	3.60	2.95	4.40	3.10
4.40	3.68	3.60	3.30	4.67	3.35	5.47	3.53
5.27	4.09	4.27	3.71	5.34	3.78	6.34	3.94
5.94	4.52	4.87	4.11	6.14	4.19	7.21	4.34
5.74	4.52	5.40	4.52	5.87	4.19	6.94	4.34
6.81	4.93	5.80	4.93	6.81	4.57	8.01	4.75
7.34	5.36	5.60	4.93	7.67	4.98	9.01	5.18
7.41	5.36	6.34	5.31	8.54	5.38	9.88	5.56
8.41	5.79	6.81	5.74	8.01	5.38	9.27	5.56
9.34	6.25	7.34	6.15	9.14	5.82	10.41	5.97
9.01	6.25	7.74	6.55	10.01	6.20	11.41	6.38
10.01	6.60	7.41	6.55	10.74	6.60	12.28	6.78
10.94	7.01	8.21	6.96	10.34	6.60	11.34	6.78
10.61	7.01	8.67	7.34	11.34	6.99	12.81	7.16
11.48	7.39	9.21	7.77	12.08	7.37	13.75	7.59
12.28	7.75	9.61	8.18	12.94	7.80	14.41	8.00
13.01	8.18	8.87	8.18	12.08	7.80	13.48	8.00
12.54	8.18	9.61	8.56	13.28	8.23	14.75	8.41
13.75	8.59	10.21	8.97	14.01	8.66	15.55	8.84
14.35	8.84	10.61	9.37	14.61	9.02	16.15	9.25
13.81	8.84	10.88	9.78	13.75	9.02	12.21	9.25
14.88	9.40	11.21	10.21	14.88	9.42	15.21	9.88
15.79	9.78	10.54	10.21	15.55	9.83	15.95	10.29
16.35	10.19	11.28	10.62	16.08	10.19	16.55	10.74
16.95	10.62	11.74	11.02	16.28	10.64	17.15	11.15
17.48	11.02	12.01	11.43	15.08	10.64	17.61	11.58
17.95	11.53	12.41	11.84	16.21	11.02	18.02	11.99
18.22	11.86	12.61	12.24	16.88	11.43	15.46	11.99
17.10	11.86	12.94	12.65	16.95	11.86	17.61	12.37
18.02	12.22	11.88	12.65	17.28	12.22	17.46	12.83
18.82	12.65	12.74	13.03	---	---	---	---
19.22	13.13	13.14	13.46	---	---	---	---
19.42	13.54	13.54	13.87	---	---	---	---
17.21	13.54	13.81	14.27	---	---	---	---
18.62	13.97	14.01	14.66	---	---	---	---
19.02	14.35	---	---	---	---	---	---
19.42	14.78	---	---	---	---	---	---
19.68	15.21	---	---	---	---	---	---
18.48	15.65	---	---	---	---	---	---

Table A.58 Raw and Reduced Deflection Data of *PS_SG_G4*

Platform 1		Platform 2		Platform 3		Platform 4	
Load (kN)	Defl. (mm)	Load (kN)	Defl. (mm)	Load (kN)	Defl. (mm)	Load (kN)	Defl. (mm)
0.00	0.00	0.00	0.00	0.00	0.00	0.00	0.00
0.87	0.43	0.93	0.41	0.47	0.43	0.73	1.04
1.60	0.89	1.53	0.84	1.07	0.89	1.33	1.50
2.27	1.32	2.34	1.27	1.80	1.30	1.93	1.96
2.14	1.32	2.07	1.27	1.67	1.30	1.67	1.96
3.14	1.75	3.07	1.57	2.47	1.60	2.60	2.41
3.94	2.18	3.87	2.03	3.20	2.08	3.27	2.84
3.80	2.18	4.87	2.64	4.07	2.49	4.20	3.28
4.87	2.57	4.54	2.64	3.74	2.49	5.00	3.73
5.67	3.02	5.60	3.05	4.80	2.84	4.67	3.73
5.40	3.02	6.67	3.51	5.67	3.28	5.74	4.17
6.47	3.40	7.67	3.91	6.67	3.66	6.61	4.57
7.41	3.86	7.21	3.91	6.34	3.66	7.54	5.00
7.07	3.86	8.41	4.32	7.47	4.01	7.14	5.00
8.21	4.24	9.41	4.78	8.41	4.42	8.34	5.41
9.14	4.67	9.34	4.78	9.34	4.83	9.34	5.82
8.81	4.67	10.21	5.18	8.87	4.83	8.74	5.82
9.81	5.00	11.28	5.59	10.14	5.21	10.01	6.22
10.68	5.49	12.34	6.02	10.94	5.61	10.88	6.71
10.48	5.49	11.68	6.02	11.88	5.99	11.81	7.09
11.41	5.84	13.08	6.43	11.41	5.99	11.34	7.09
12.21	6.27	14.01	6.86	12.81	6.40	12.48	7.47
13.14	6.65	14.81	7.26	13.68	6.78	13.41	7.85
13.34	7.09	14.21	7.26	14.55	7.19	14.21	8.26
14.26	7.49	15.48	7.67	13.88	7.19	13.41	8.26
13.95	7.49	16.48	8.08	15.08	7.57	14.61	8.69
14.75	7.85	17.15	8.51	15.95	8.00	15.55	9.09
15.55	8.26	16.15	8.51	16.68	8.41	16.28	9.50
16.08	8.69	17.41	8.94	15.88	8.41	15.28	9.50
15.28	8.69	18.22	9.32	16.95	8.74	16.55	9.88
16.35	9.17	18.82	9.73	17.88	9.17	17.35	10.29
17.08	9.50	18.55	9.73	18.55	9.58	18.02	10.72
15.95	9.50	18.62	10.03	19.02	9.98	16.88	10.72
17.48	10.01	19.48	10.49	17.82	9.98	18.08	11.13
18.15	10.49	20.28	10.92	19.02	10.34	18.82	11.53
18.62	10.85	20.55	11.35	19.75	10.72	19.42	11.94
18.88	11.20	20.88	11.76	20.08	11.18	19.88	12.34
19.15	11.71	19.11	11.76	20.55	11.56	18.35	12.34
17.95	11.71	20.28	12.14	20.95	11.96	19.55	12.78
18.68	12.07	21.15	12.60	19.48	11.96	20.35	13.16
19.13	12.47	---	---	20.55	12.37	20.68	13.59
19.57	12.93	---	---	21.35	12.73	20.88	13.97
18.42	12.93	---	---	21.82	13.13	21.15	14.35
19.02	13.34	---	---	21.75	13.64	21.35	14.81
19.62	13.69	---	---	21.35	13.84	21.42	15.16
19.95	14.15	---	---	21.55	14.20	---	---
20.15	14.58	---	---	---	---	---	---
19.68	14.99	---	---	---	---	---	---
19.28	15.44	---	---	---	---	---	---
18.88	15.72	---	---	---	---	---	---

Table A.58 (continued)

Platform 1		Platform 2		Platform 3		Platform 4	
Load (kN)	Defl. (mm)	Load (kN)	Defl. (mm)	Load (kN)	Defl. (mm)	Load (kN)	Defl. (mm)
18.62	16.15	---	---	---	---	---	---
17.55	16.66	---	---	---	---	---	---
17.21	16.99	---	---	---	---	---	---
17.21	17.50	---	---	---	---	---	---
16.88	17.91	---	---	---	---	---	---

Table A.59 Raw and Reduced Deflection Data of *PS_P_G5*

Platform 1		Platform 2		Platform 3		Platform 4	
Load (kN)	Defl. (mm)	Load (kN)	Defl. (mm)	Load (kN)	Defl. (mm)	Load (kN)	Defl. (mm)
0.00	0.00	0.00	0.00	0.00	0.00	0.00	0.00
0.73	0.38	0.87	0.41	0.80	0.43	0.87	0.48
1.33	0.81	1.47	0.84	1.33	0.84	1.47	0.89
2.00	1.24	2.14	1.27	1.93	1.22	2.34	1.32
1.80	1.24	1.93	1.27	1.87	1.22	2.14	1.32
2.67	1.63	3.34	1.80	2.54	1.57	3.40	1.73
3.34	2.03	4.07	2.46	3.14	1.96	4.47	2.18
3.94	2.46	3.80	2.46	3.74	2.34	5.54	2.54
3.87	2.46	4.67	2.84	3.54	2.34	5.14	2.54
4.74	2.87	5.40	3.28	4.34	2.69	6.61	2.92
5.40	3.28	5.94	3.68	4.94	3.10	7.61	3.33
6.07	3.71	5.60	3.68	5.60	3.48	7.27	3.33
5.87	3.71	6.47	4.06	5.34	3.48	8.67	3.71
6.67	4.09	7.14	4.50	6.05	3.84	9.74	4.09
7.34	4.50	7.81	4.93	6.74	4.19	10.88	4.50
8.01	4.93	8.34	5.31	7.34	4.57	10.41	4.50
7.67	4.93	7.87	5.31	7.01	4.57	11.74	4.90
8.61	5.33	8.81	5.72	7.81	4.93	13.01	5.28
9.27	5.72	9.34	6.12	8.41	5.31	14.01	5.69
9.94	6.17	9.88	6.53	8.94	5.74	13.41	5.69
9.47	6.17	10.34	6.96	8.47	5.74	14.88	6.07
10.88	6.93	10.74	7.34	9.27	6.10	15.88	6.50
11.41	7.34	10.14	7.34	9.94	6.50	16.68	6.91
11.94	7.75	10.94	7.75	10.41	6.83	15.95	6.91
11.14	7.75	11.54	8.15	10.81	7.26	17.41	7.29
12.08	8.13	12.01	8.56	10.21	7.26	18.28	7.70
12.74	8.56	12.41	9.04	11.08	7.65	18.95	8.08
13.14	8.97	12.54	9.37	11.54	8.03	18.02	8.08
13.54	9.37	11.61	9.37	12.08	8.41	19.35	8.51
13.81	9.78	12.41	9.75	12.48	8.81	20.35	8.89
12.88	9.78	13.01	10.19	12.81	9.17	21.02	9.30
13.75	10.16	13.34	10.59	11.88	9.17	19.75	9.30
14.28	10.54	13.54	11.00	12.81	9.55	21.08	9.68
14.48	10.92	13.81	11.43	13.34	9.93	21.95	10.06
14.68	11.33	13.88	11.81	13.75	10.31	22.55	10.46
14.95	11.76	---	---	12.81	10.31	22.95	10.85
15.15	12.17	---	---	13.54	10.69	23.42	11.25
15.28	12.55	---	---	14.01	11.07	21.69	11.25
15.48	13.00	---	---	14.35	11.46	22.95	11.63
15.68	13.39	---	---	14.48	11.84	23.89	11.99
---	---	---	---	14.68	12.22	24.35	12.40
---	---	---	---	---	---	24.75	12.78
---	---	---	---	---	---	25.09	13.16
---	---	---	---	---	---	23.02	13.16
---	---	---	---	---	---	24.22	13.54
---	---	---	---	---	---	24.29	14.05
---	---	---	---	---	---	24.82	14.48
---	---	---	---	---	---	25.22	14.91
---	---	---	---	---	---	25.42	15.27

Table A.60 Raw and Reduced Deflection Data of *PS_SG_P5*

Platform 1		Platform 2		Platform 3		Platform 4	
Load (kN)	Defl. (mm)	Load (kN)	Defl. (mm)	Load (kN)	Defl. (mm)	Load (kN)	Defl. (mm)
0.00	0.00	0.00	0.00	0.00	0.00	0.00	0.00
0.47	0.41	0.47	0.23	0.47	0.41	0.93	0.46
0.80	0.81	1.07	0.64	1.07	0.79	1.80	0.89
1.20	1.22	1.87	1.07	1.67	1.22	1.60	0.89
1.87	1.63	2.67	1.52	1.60	1.22	2.67	1.27
2.60	2.03	2.67	1.52	2.67	1.60	3.60	1.68
2.54	2.03	3.67	1.93	3.47	1.98	4.54	2.08
3.60	2.51	4.54	2.34	4.40	2.39	4.40	2.08
4.67	2.92	5.67	2.79	4.20	2.39	5.47	2.44
5.60	3.33	6.49	3.20	5.47	2.82	6.47	2.84
6.41	3.76	7.47	3.61	6.34	3.20	7.41	3.28
6.54	3.76	7.47	3.61	7.27	3.63	7.07	3.28
7.21	4.09	8.59	3.99	6.94	3.63	8.14	3.66
8.54	4.70	9.34	4.39	8.14	4.01	9.14	4.04
9.07	5.00	9.07	4.39	9.21	4.42	10.01	4.45
9.88	5.31	10.14	4.75	8.87	4.42	9.74	4.45
9.47	5.31	11.08	5.11	10.01	4.75	10.88	4.83
10.54	5.64	12.41	5.66	10.94	5.16	11.81	5.21
11.41	6.07	12.94	6.05	10.54	5.16	12.74	5.64
12.86	6.48	12.88	6.05	11.81	5.64	13.54	6.05
13.21	6.91	13.88	6.43	12.81	6.05	13.12	6.05
12.74	6.91	14.75	6.86	12.34	6.05	14.15	6.40
13.81	7.29	14.48	6.86	13.48	6.45	15.01	6.81
14.68	7.70	15.88	7.42	14.41	6.81	15.81	7.19
14.48	7.70	16.41	7.70	13.88	6.81	14.95	7.19
15.48	8.23	17.01	8.08	15.21	7.19	16.21	7.59
15.95	8.51	16.55	8.08	15.95	7.57	17.01	7.95
16.75	8.94	17.15	8.41	16.75	7.95	17.68	8.36
17.21	9.19	18.02	8.81	16.01	7.95	16.61	8.36
17.35	9.75	18.68	9.19	17.15	8.31	17.75	8.69
17.01	9.75	19.22	9.63	17.88	8.66	18.55	9.09
17.88	10.57	18.42	9.63	18.68	9.07	19.02	9.50
19.08	10.97	19.28	10.03	17.68	9.07	19.42	9.91
19.42	11.30	19.95	10.41	18.82	9.47	19.95	10.39
19.75	11.81	20.48	10.77	19.75	9.83	20.22	10.67
18.68	11.81	20.95	11.23	20.28	10.24	18.82	10.67
19.68	12.29	21.28	11.61	20.75	10.62	19.95	11.05
20.13	12.65	21.69	12.04	19.42	10.62	20.62	11.43
20.55	13.06	21.95	12.47	20.68	10.97	21.08	11.86
20.42	13.49	---	---	21.42	11.35	21.35	12.24
20.68	13.94	---	---	21.82	11.76	21.35	12.65
20.88	14.33	---	---	22.15	12.12	20.88	13.03
20.95	14.73	---	---	20.62	12.12	---	---
19.93	13.94	---	---	20.68	12.45	---	---
---	---	---	---	21.42	12.83	---	---
---	---	---	---	21.82	13.21	---	---
---	---	---	---	22.15	13.59	---	---
---	---	---	---	20.62	13.94	---	---
---	---	---	---	21.69	14.38	---	---

Table A.61 Raw and Reduced Deflection Data of *PS_A_G5*

Platform 1		Platform 2		Platform 3		Platform 4	
Load (kN)	Defl. (mm)	Load (kN)	Defl. (mm)	Load (kN)	Defl. (mm)	Load (kN)	Defl. (mm)
0.00	0.00	0.00	0.00	0.00	0.00	0.00	0.00
0.53	0.38	0.87	0.46	1.00	0.46	0.73	0.38
0.93	0.79	1.67	0.94	1.67	0.91	1.47	0.79
1.27	1.19	2.47	1.37	2.40	1.35	2.20	1.22
1.73	1.57	2.20	1.37	2.27	1.35	2.00	1.22
2.14	1.98	3.20	1.78	3.20	1.78	2.94	1.63
1.93	1.98	4.00	2.21	4.00	2.16	3.67	2.03
2.60	2.36	4.80	2.64	4.83	2.57	4.40	2.44
2.87	2.74	4.54	2.64	4.60	2.57	5.32	2.87
3.40	3.18	5.54	3.02	5.54	2.97	5.00	2.87
3.80	3.58	6.34	3.43	6.34	3.38	5.87	3.25
4.20	3.99	7.14	3.84	7.21	3.81	6.61	3.66
4.00	3.99	6.81	3.84	6.87	3.81	7.34	4.09
4.67	4.39	7.87	4.22	7.94	4.19	7.07	4.09
5.07	4.78	8.67	4.62	8.81	4.62	8.07	4.47
5.54	5.16	9.41	5.05	9.61	5.00	8.87	4.88
5.94	5.59	9.07	5.05	10.34	5.38	9.54	5.28
6.34	11.10	10.94	5.82	9.88	5.38	9.21	5.28
6.74	6.40	11.48	6.20	10.94	5.82	10.81	6.07
6.41	6.40	12.28	6.63	11.68	6.20	11.48	6.53
7.07	6.76	11.54	6.63	12.48	6.60	12.08	6.88
7.47	7.16	12.68	7.01	11.74	6.60	11.48	6.88
7.87	7.57	13.41	7.42	12.94	6.96	12.54	7.21
8.21	7.98	13.95	7.82	13.68	7.39	13.08	7.67
8.61	8.38	14.41	8.26	14.21	7.77	13.75	8.08
8.87	8.79	13.54	8.26	14.81	8.18	14.15	8.48
8.41	8.79	14.55	8.64	13.95	8.18	13.41	8.48
9.07	9.19	15.28	9.04	14.95	8.59	14.28	8.86
9.47	9.58	15.81	9.45	15.68	8.94	14.88	9.30
9.81	9.96	16.15	9.88	16.21	9.40	15.48	9.68
---	---	16.48	10.26	16.68	9.78	15.81	10.08
---	---	15.28	10.26	15.55	9.78	16.15	10.49
---	---	16.35	10.64	16.55	10.16	15.08	10.49
---	---	16.68	11.05	17.21	10.57	16.48	11.28
---	---	17.35	11.46	17.68	11.00	16.88	11.63
---	---	17.61	11.84	17.95	11.35	17.21	12.07
---	---	15.61	11.76	18.15	11.81	17.48	12.47
---	---	16.61	12.12	18.28	12.19	17.68	12.88
---	---	17.08	12.52	18.42	12.65	17.75	13.28
---	---	---	---	18.35	13.00	---	---

Table A.62 Raw and Reduced Deflection Data of *PS_H_G5*

Platform 1		Platform 2		Platform 3		Platform 4	
Load (kN)	Defl. (mm)	Load (kN)	Defl. (mm)	Load (kN)	Defl. (mm)	Load (kN)	Defl. (mm)
0.00	0.00	0.00	0.00	0.00	0.00	0.00	0.00
0.73	0.48	0.80	0.43	0.47	0.41	0.80	0.38
1.53	0.89	1.73	0.94	1.13	0.84	1.53	0.76
2.34	1.35	2.67	1.37	1.93	1.24	2.47	1.22
2.14	1.35	2.34	1.37	2.87	1.70	2.27	1.22
3.27	1.70	3.67	1.80	2.67	1.70	3.27	1.60
4.27	2.16	4.80	2.26	5.00	2.49	4.40	2.06
5.20	2.57	4.60	2.26	6.07	2.92	5.40	2.49
5.00	2.57	5.80	2.69	5.80	2.92	5.20	2.49
6.21	2.97	6.87	3.10	7.07	3.30	6.41	2.90
7.21	3.38	6.52	3.10	8.21	3.73	7.41	3.33
8.27	3.81	7.87	3.51	9.34	4.17	8.54	3.73
7.94	3.81	9.07	3.94	8.94	4.17	8.14	3.73
9.34	4.29	8.67	3.94	10.28	4.57	9.34	4.14
10.21	4.65	10.08	4.34	11.41	4.98	10.48	4.57
11.08	5.03	11.08	4.75	10.94	4.98	11.48	4.98
10.74	5.03	12.28	5.16	12.34	5.36	12.48	5.38
12.01	5.41	11.68	5.16	13.48	5.79	12.01	5.38
13.14	5.84	13.08	5.59	13.08	5.79	13.34	5.79
14.01	6.25	14.15	5.99	14.41	6.17	14.21	6.22
13.41	6.25	13.68	5.99	15.35	6.58	15.15	6.60
14.68	6.63	15.01	6.35	14.88	6.58	16.01	7.01
15.68	7.04	16.08	6.78	16.19	8.20	15.35	7.01
14.95	7.04	15.35	6.78	17.21	8.69	16.55	7.39
16.21	7.44	16.81	7.19	18.15	9.04	17.55	7.87
17.08	7.82	17.75	7.62	17.21	9.04	18.22	8.31
16.35	7.82	17.01	7.62	18.55	9.42	18.88	8.64
17.75	8.31	18.08	7.98	19.68	9.83	17.95	8.64
18.68	8.74	19.22	8.41	20.28	10.26	19.22	9.02
19.28	9.14	19.95	8.84	19.22	10.64	20.08	9.42
18.28	9.14	19.02	8.84	20.55	10.64	20.75	9.83
19.48	9.50	20.15	9.22	21.48	11.43	19.55	9.83
20.35	9.91	21.28	9.63	22.22	11.79	20.95	10.24
21.02	10.31	21.89	10.06	22.69	12.22	21.69	10.64
19.75	10.31	22.49	10.44	21.42	12.22	22.29	11.07
21.08	10.69	21.22	10.44	23.55	12.60	22.69	11.48
21.82	11.10	22.35	10.85	24.02	12.98	21.35	11.48
22.42	11.51	23.29	11.25	24.55	13.39	22.42	11.94
22.89	11.91	23.89	11.63	22.82	13.79	23.15	12.24
21.62	11.91	24.35	12.01	23.89	14.17	23.75	12.65
22.75	12.29	24.75	12.37	24.62	14.58	24.15	13.06
23.42	12.65	22.62	12.37	25.29	14.58	24.42	12.19
23.89	13.06	23.75	12.78	25.62	14.96	22.82	12.19
24.29	13.46	24.62	13.13	25.96	15.37	23.82	13.89
24.42	13.84	25.15	13.54	26.22	15.77	24.62	14.22
22.89	13.84	25.56	13.94	24.22	16.10	25.02	14.66
23.95	14.20	25.82	19.41	25.00	16.51	25.35	15.01
24.69	14.61	26.02	14.73	26.02	16.97	25.49	15.39
25.22	14.96	25.42	15.16	26.49	17.37	25.76	15.80
25.49	15.37	---	---	26.96	16.71	25.82	16.26

Table A.62 (continued)

Platform 1		Platform 2		Platform 3		Platform 4	
Load (kN)	Defl. (mm)	Load (kN)	Defl. (mm)	Load (kN)	Defl. (mm)	Load (kN)	Defl. (mm)
23.53	15.75	---	---	---	---	26.02	16.64
25.69	16.13	---	---	---	---	25.96	16.99
25.76	16.54	---	---	---	---	26.09	17.40
25.89	16.79	---	---	---	---	26.22	17.81
25.96	17.30	---	---	---	---	26.42	18.21
26.16	17.68	---	---	---	---	26.36	18.57
---	---	---	---	---	---	24.02	18.57
---	---	---	---	---	---	25.02	18.95
---	---	---	---	---	---	25.62	19.33

Table A.63 Raw and Reduced Deflection Data of *FS_SG_G7*

Platform 1		Platform 2		Platform 3		Platform 4		Platform 5	
Load (kN)	Defl. (mm)	Load (kN)	Defl. (mm)	Load (kN)	Defl. (mm)	Load (kN)	Defl. (mm)	Load (kN)	Defl. (mm)
0.00	0.00	0.00	0.00	0.00	0.00	0.00	0.00	0.00	0.00
7.79	2.95	7.33	3.89	6.88	2.84	7.49	2.74	7.74	3.00
14.79	5.99	14.08	7.21	14.20	5.82	15.00	5.51	14.67	5.54
27.75	12.04	24.94	12.09	25.09	10.19	25.45	9.42	25.88	9.83
39.19	17.50	36.87	18.21	37.71	15.93	39.09	14.83	38.32	14.96
52.99	23.27	52.30	25.30	51.62	22.00	52.31	20.37	51.72	20.62
65.97	28.09	66.29	30.96	65.59	27.48	66.04	25.65	65.35	26.42
79.10	32.99	78.35	35.92	78.68	32.69	79.40	30.94	78.88	31.67
---	---	---	---	91.96	38.20	92.40	36.63	92.75	36.98
Platform 6		**Platform 7**		**Platform 8**		**Platform 9**		**Platform 10**	
Load (kN)	**Defl. (mm)**	**Load (kN)**	**Defl. (mm)**	**Load (kN)**	**Defl. (mm)**	**Load (kN)**	**Defl. (mm)**	**Load (kN)**	**Defl. (mm)**
0.00	0.00	0.00	0.00	0.00	0.00	0.00	0.00	0.00	0.00
14.00	9.88	23.68	10.87	12.53	5.44	13.50	4.72	13.82	4.72
25.95	14.15	15.55	8.64	23.34	9.96	27.18	9.63	27.37	9.70
40.52	21.92	27.84	13.54	36.95	16.38	---	---	41.58	17.73
54.71	28.83	40.78	19.02	54.79	24.49	---	---	---	---